

AN ABSTRACT OF THE DISSERTATION OF

Neal C. Goebel for the degree of Doctor of Philosophy in Pharmacy presented on December 13, 2012.

Title: Biosynthesis and Modification of the Antibiotic Enduracidin

Abstract approved:

T. Mark Zabriskie

The continued propagation of antibiotic resistance requires the development of new therapeutics. The lipopeptide antibiotic enduracidin has demonstrated high activity against Gram-positive pathogens including methicillin-resistant *Staphylococcus aureus*. In addition to a lack of cross-resistance with existing antibiotic classes, enduracidin has no known transferrable resistance mechanism. The development of enduracidin as a human therapeutic is hampered by its poor solubility in plasma. Utilizing chemical and genetic techniques, analogs of enduracidin have been produced and evaluated for biological activity. Making use of the hydroxyphenylglycine (Hpg) biosynthetic pathway, fluorine was incorporated into enduracidin with minimal to no loss of bioactivity.

The semisynthetic chemical modification of enduracidin proved to be challenging. The chemical nitration of the Hpg residues was unsuccessful. Modifications to the lipid tail by cleavage at the C2-olefin with ozone and the use of Diels-Alder reagents to react with the lipid tail diene also proved unsuccessful. However, the reduction and dihydroxylation modifications of the lipid tail diene were successful. Introduction of polar hydroxyl groups onto the alkyl tail reduced bioactivity while reduction of the diene had no significant effect.

Analysis of the biosynthetic pathways involved in producing the lipid tail and the

unusual amino acid enduracididine yielded some insights into the formation of the antibiotic. Through complementation of mutants having disruptions in the biosynthetic gene cluster and crystallographic data, the function of EndR as a cyclase was established. Additionally, the use of 4-hydroxyarginine as an intermediate in enduracididine biosynthesis was demonstrated. The ability of EndQ to function as a transaminase on both 4-hydroxyarginine and 2-ketoenduracididine was also established. The specific functions of EndP and EndQ have not been determined. The introduction of the lipid tail diene by the three enzymes Orf39, Orf44 and Orf45 was confirmed. Orf45 functions as a CoA ligase and a dehydrogenase to introduce the C2 double bond. The functions of Orf39 and Orf44 appear to be the introduction of the C4 double bond and isomerization of the C2 olefin.

© Copyright by Neal C. Goebel

December 13, 2012

All Rights Reserved

Biosynthesis and Modification of the Antibiotic Enduracidin

by

Neal C. Goebel

A DISSERTATION

submitted to

Oregon State University

in partial fulfillment of

the requirements for the

degree of

Doctor of Philosophy

Presented December 13, 2012

Commencement June 2013

Doctor of Philosophy dissertation of Neal C. Goebel presented on December 13, 2012.

APPROVED:

Major Professor, representing Pharmacy

Dean of the College of Pharmacy

Dean of the Graduate School

I understand that my dissertation will become part of the permanent collection of Oregon State University libraries. My signature below authorizes release of my dissertation to any reader upon request.

Neal C. Goebel, Author

ACKNOWLEDGEMENTS

I would like to thank my wife, Kellee, for her support during this five year adventure. I want to thank my son, Jed, for his upbeat attitude and curiosity.

I am grateful for the advice, mentoring and guidance provided by my advisor Dr. Mark Zabriskie. He has provided me with the opportunity to explore, grow and discover my scientific interests.

Thank you to Drs. Joyce Loper, Taifo Mahmud, Phil Proteau and Kerry McPhail. It has been a privilege to have worked with you. The advice and help you have provided have been invaluable. I wish to acknowledge the members, past and present, of the Loper lab for the excellent chance to collaborate with them; the members of the Mahmud, McPhail and Proteau labs for the chance to work with and learn from you.

Lastly, I wish to acknowledge my committee for their teaching, aid and guidance through my doctoral studies.

CONTRIBUTION OF AUTHORS

Genetic manipulation of *Streptomyces fungicidicus* and most general microbiology were performed by Dr. Xihou Yin, Ying Cheng and Yang Wang (Oregon State University, Department of Pharmaceutical Sciences). Some preliminary work on the incorporation of 3-fluorotyrosine were performed by Dr. David Blanchard. Acquisition of NMR data for enduracidin isolated from the SF Δ orf39 strain (700 MHz, inverse cryogenic probe) was performed by Dr. Clemens Anklin (Bruker Biospin). Crystallographic data and analysis were performed by our collaborator Dr. Nicholas Silvaggi (University of Wisconsin-Milwaukee).

TABLE OF CONTENTS

	<u>Page</u>
1. Introduction	1
History of Antibiotics	2
Primary Antibiotic Modes of Action	4
Drug Resistance.....	6
Enduracidin, History and Potential.....	10
References	13
2. Mutasythetic Modification of Enduracidin	19
Introduction	20
Results and Discussion.....	22
Experimental Procedures	37
References	50
3. Biosynthesis of Enduracididine.....	53
Introduction	54
Results and Discussion.....	59
Experimental Procedures.....	74
References	82
4. Semisynthetic Modification of Enduracidin.....	87
Introduction	88
Results and Discussion.....	92
Experimental Procedures.....	113
References	126
5. General Conclusions	133
Biosynthetic Studies.....	134
Semisynthetic Studies	135
Mutasythetic Modification of Enduracidin	136
Potential of Enduracidin.....	137

LIST OF FIGURES

<u>Figure</u>	<u>Page</u>
Figure 1.1 A) Structure of penicillin G. B) Structure of Prontosil and sulfanilamide produced by reduction of the diazene bond.	2
Figure 1.2 Biosynthesis of dihydropteroate by dihydropteroate synthase.	3
Figure 1.3 Key steps in cell wall biosynthesis by Gram positive bacteria with the vancomycin recognition element, D-Ala-D-Ala, highlighted in green.	6
Figure 1.4 A Gram-negative membrane complex illustrating four drug efflux pumps: AcrAB-TolC, MacAB-TolC, NorM and Tet. Both NorM and Tet rely on passive transporters like the porin OmpF for removal of the drug from the periplasm. Figure from Alekshun et al.	7
Figure 1.5 A) Structure of vancomycin showing the five hydrogen bonds formed with the D-Ala-D-Ala terminus of Lipid II. B) The vancomycin resistance genes and their corresponding functions in producing D-Ala-D-Lac Lipid II. Figure from Wright.	8
Figure 1.6 Structures of A) Methicillin, B) Penicillin G and C) Clavulanic acid.	9
Figure 1.7 The structure of enduracidin A and B.	10
Figure 1.8 A) Peptidoglycan biosynthesis with the vancomycin (green) and enduracidin (purple) recognition elements highlighted. B) 3D NMR structure of enduracidin from Castiglione <i>et al.</i> C) Crystal structure of a ramoplanin dimer (yellow and purple) interfacing with detergent molecules (green), chloride ions (magenta) and ordered water molecules (red) figure is from Hamburger <i>et al.</i>	11
Figure 2.1 The structure of enduracidins A and B with the five hydroxyphenylglycines and one dichlorohydroxyphenylglycine labeled.	20
Figure 2.2 Biosynthesis of hydroxyphenylglycine in <i>S. fungicidicus</i> starting from prephenate.	21

LIST OF FIGURES (Continued)

<u>Figure</u>	<u>Page</u>
Figure 2.3 ESI positive mass spectrum showing the $[M+2H]^{2+}$ ions of polyfluorinated enduracidins produced from F-Tyr supplementation	22
Figure 2.4 Preparation of fluoro-Hpg from fluorobenzaldehyde. For n=1 fluorine is in the 2 or 3 position as specified. For n=2 fluorine is in the 2 and 5 positions.	23
Figure 2.5 MALDI mass spectrum of enduracidins isolated from SfWT supplemented with 3-F-Hpg showing the $[M+H]^+$ ions.....	24
Figure 2.6 I) Insertional disruption of <i>orf29</i> using the apramycin resistance gene <i>aac(3)IV</i> and Southern blot test confirming disruption. II) HPLC chromatogram of mycelia extracts from: A) <i>S. fungicidicus</i> , B) <i>Sforf29::Tn5AT</i> , C) <i>Sforf29::Tn5AT</i> + Hpg and D) <i>Sforf29::Tn5AT</i> + F-Hpg. Enduracidin A and B are indicated by red asterisks and 3'-F ₆ enduracidin A and B are indicated with blue asterisks.....	25
Figure 2.7 ESI positive MS of 3'-F ₆ enduracidins A and B showing the $[M+2H]^{2+}$ ions. The m/z peak groups at 1197.5 and 1204.5 correspond to deschloro species while the 1214.5 and 1221.5 peak groups are the monochloro species.....	26
Figure 2.8 A) Enduracidin A 1H-NMR spectrum B) 3'-F ₆ -Cl ₁ -End A 1H-NMR spectrum C) 19F-NMR spectrum of 3'-F ₆ -Cl ₁ End A D) Aromatic region of COSY spectrum of enduracidin A E) Aromatic region of 3'-F ₆ -Cl ₁ End A. Hpg correlations are indicated with asterisks.	27
Figure 2.9 Preparation of 3-nitro Hpg via aromatic nitration.	28
Figure 2.10 HPLC chromatogram showing A) Enduracidin standard, B) <i>Sforf29::Tn5AT</i> + 3-nitro Hpg, C) <i>Sforf29::Tn5AT</i> + 3-nitro Hpg and Hpg D) <i>Sforf29::Tn5AT</i> + 2,6-F ₂ Hpg, E) <i>Sforf29::Tn5AT</i> + 2,6-F ₂ Hpg and Hpg. Enduracidin A (left asterisk) merges with a common metabolite peak in chromatogram E. Enduracidin B (right asterisk) is also present in chromatogram E.	28

LIST OF FIGURES (Continued)

<u>Figure</u>	<u>Page</u>
<p>Figure 2.11 I) HPLC chromatogram of mycelial extract of <i>Sforf29::Tn5AT</i> supplemented with 2-F Hpg. Letters indicate the four enduracidin analogs present. II) ESI positive MS spectra showing $[M+2H]^{2+}$ ions for each of the peaks A) $m/z = 1214.5$, 2'-F₆-Cl₁ End A, B) $m/z = 1231.5$, 2'-F₆-Cl₂ End A, C) $m/z = 1221.5$, 2'-F₆-Cl₁ End B and D) $m/z = 1238.5$, 2'-F₆-Cl₂ End B.....</p>	29
<p>Figure 2.12 COSY spectra for A) 2'-F₆-Cl₁ End B and B) 2'-F₆-Cl₂ End B. Spectra showing the ¹⁹F NMR signals for C) 2'-F₆-Cl₁ End B and D) 2'-F₆-Cl₂ End B.....</p>	30
<p>Figure 2.13 Amino acid alignment of the flavin-dependent halogenases Orf30 from <i>S. fungicidicus</i> and CndH from <i>Chondromyces crocatus</i>. The sequences share 53% identity and 67% similarity. The residues designated in red, including lysine 76, are directly involved with reactivity. Those in blue designate key residues forming the binding pocket. The yellow sequence is a portion of the tunnel allowing hypochlorite to travel to the active site. The conserved GWxWxI sequence is used as a fingerprint to identify this class of halogenase.....</p>	31
<p>Figure 2.14 HOMO maps of the possible substrates for the halogenase Orf30. The values represent the calculated charge present on the potentially chlorinated carbon.....</p>	32
<p>Figure 2.15 ESI positive mass spectra of isolated unknown enduracidins from 3-F Hpg experiments showing 3'-F₆-Cl₂ enduracidin A ($m/z = 1231.5$) and B ($m/z = 1238.5$).....</p>	33
<p>Figure 2.16 A) Synthesis of hydroxypyridinylglycine starting from 3-hydroxy-6-methylpyridine to the aminonitrile. B) Degradation of hydrolyzed amino nitrile results in the production of N-benzyl-5-benzyloxypyridinyl-methylamine.....</p>	34
<p>Figure 2.17 Growth inhibition assay against <i>S. aureus</i> for A) enduracidins A, B and Ampicillin, B) 3'-F₆ enduracidins and C) 2'-F₆ enduracidins.....</p>	35
<p>Figure 3.1 The structure of enduracidin with amino acid labels.....</p>	54

LIST OF FIGURES (Continued)

<u>Figure</u>	<u>Page</u>
Figure 3.2 Natural products containing enduracididine and similar amino acid structures.	55
Figure 3.3 Biosynthesis of 3- <i>S</i> -L-capreomycinidene via non-heme iron α -ketoglutarate dependent oxygenase VioC and the pyridoxal phosphate dependent enzyme VioD from L-arginine.	56
Figure 3.4 Possible mechanisms for a pyridoxal phosphate catalyzed elimination cyclization reaction producing L-enduracididine from A) 3-OH arginine and B) 4-OH arginine.	57
Figure 3.5 Mechanism of action of acetoacetate decarboxylase from <i>Clostridium acetobutylicum</i>	58
Figure 3.6 Synthesis of 4-OH Arg from allylglycine via iodine mediated lactonization and using Mukaiyama's reagent and diBoc-thiourea for the guanylation reaction.	59
Figure 3.7 A) Preparation of the Tf-guan reagent from guanidine. B) Preparation of 4-OH Arg from the azidolactone 4 using the Tf-guan reagent.	60
Figure 3.8 ¹ H-NMR spectra of A) a mixture of <i>cis</i> and <i>trans</i> iodolactones 2 and 3 , B) crystallized <i>cis</i> iodolactone 2 , C) a mixture of <i>cis</i> and <i>trans</i> guanidinyllactone 7 and D) purified guanidinyllactone 6 having an absolute configuration of 2- <i>S</i> , 4- <i>S</i>	61
Figure 3.9 The preparation of enduracididine from the methyl ester of L-histidine.	62
Figure 3.10 ¹³ C-NMR of synthetic enduracididine showing the doubling of signals.	63
Figure 3.11 Diagram showing the disruptions introduced into <i>endP</i> , <i>endR</i> and <i>endQ</i>	64

LIST OF FIGURES (Continued)

<u>Figure</u>	<u>Page</u>
Figure 3.12 HPLC chromatograms of mycelial extracts of A) <i>SfendRΩAmR</i> + 3- <i>S</i> -OH Arg, B) <i>SfendRΩAmR</i> + 3- <i>R</i> -OH Arg, C) <i>SfendRΩAmR</i> , D) <i>SfΔendP</i> + 3- <i>S</i> -OH Arg, E) <i>SfΔendP</i> + 3- <i>R</i> -OH Arg, F) <i>SfΔendP</i> and G) <i>S. fungicidicus</i> wild-type. Enduracidin is indicated with asterisks. The peak marked with an X was determined by UV data to not be enduracidin.	64
Figure 3.13 HPLC chromatograms of mycelial extracts of A) <i>SfendQΩAmR</i> , B) <i>SfendQΩAmR</i> + End, and C) <i>S. fungicidicus</i> wild-type. Enduracidin is indicated with asterisks.	65
Figure 3.14 HPLC chromatograms of mycelial extracts of IA) <i>SfendRΩAmR</i> , IB) <i>SfendRΩAmR</i> + 4-OH Arg, IC) <i>SfendRΩAmR</i> + End, ID) <i>S. fungicidicus</i> wild-type, IIA) <i>SfΔendP</i> , IIB) <i>SfΔendP</i> + 4-OH Arg, IIC) <i>SfΔendP</i> + End and IID) <i>S. fungicidicus</i> wild-type. Enduracidin is indicated with asterisks.	66
Figure 3.15 Hypothetical biosynthesis of enduracididine based on complementation assay results showing possible non-enzyme bound intermediates.	67
Figure 3.16 A) The stereo view of the MppR binding pocket showing the electron density map of the bound HEPES molecule. B) illustration and distances (Å) of hydrogen bonding and coordinating interactions between the binding pocket and the HEPES molecule.	68
Figure 3.17 A) The stereo view of the MppR binding pocket showing the electron density map of the catalytic Lys forming a Schiff-base with pyruvate. B) Schematic of the binding pocket showing distances (Å) of possible coordinating interactions.	69
Figure 3.18 A) The stereo view of the MppR binding pocket showing the electron density map of the catalytic Lys forming a Schiff base with 2-keto-4- <i>R</i> -enduracididine. B) Schematic of the binding pocket showing distances (Å) of possible coordinating interactions.	70

LIST OF FIGURES (Continued)

<u>Figure</u>	<u>Page</u>
<p>Figure 3.19 The stereo view of the MppR binding pocket showing the electron density map of the catalytic Lys forming a Schiff base with (3<i>E</i>)-4-(1<i>H</i>-imidazol-5-yl)-2-oxobut-3-enoic acid. B) Schematic of the binding pocket showing distances (Å) of possible coordinating interactions. C) Proposed aldol reaction and dehydration reaction catalyzed by MppR.....</p>	71
<p>Figure 3.20 Nitroimidazole biosynthesis as proposed by Nakane et al. requires the oxidation of Arg followed by the formation of the 2-keto group. A retro aldol reaction is then catalyzed followed by cyclization and oxidation of the 2-amino group to form nitroimidazole.</p>	72
<p>Figure 4.1 A) Crystal structure of a ramoplanin dimer (yellow and purple) interfacing with detergent molecules (green), chloride ions (magenta) and ordered water molecules (red) figure is from Hamburger et al.2 B) The lipid tail structures of enduracidin (blue) and ramoplanin (cyan).</p>	88
<p>Figure 4.2 Possible methods for the introduction of the C2 and C4 double bonds and isomerization of the C2 alkene.</p>	89
<p>Figure 4.3 A) Removal of the lipid tail of ramoplanin as described by Ciabatti <i>et al.</i> starting with i) protection using Fmoc-OSu, ii) Ozonolysis with PPh₃ reductive work up, iii) reductive amination using NaBH₃CN and iv) Edman degradation. B) Proposed lipid tail replacements for enduracidin and tetrahydroxylation of the alkenes. C) Potential Diels-Alder reactions with the lipid tail alkenes.</p>	90
<p>Figure 4.4 A) Possible lipid tail configurations resulting from the disruption of <i>orf39</i>, <i>orf44</i> and <i>orf45</i>. i) enduracidin A, ii) 2-<i>trans</i> enduracidin A, iii) 2-<i>cis</i>-4,5-H₂-enduracidin A, iv) 2-<i>trans</i>-4,5-H₂-enduracidin A and v) H₄-enduracidin A. B) HPLC UV chromatogram (216 nm–blue, 254 nm–black) of the ambient temperature 30 min hydrogenation reaction.....</p>	92
<p>Figure 4.5 A) ESI (+) MS spectra showing the [M+2H]²⁺ ions of 1) Enduracidin A, 2) 2-<i>cis</i>-H₂-End A, 3) 2-<i>trans</i>-H₂-End A and 4) H₄-End A. B) ¹H NMR spectra for the corresponding compounds. The Lipid tail olefin protons are labelled indicating the carbon it is bound.</p>	93

LIST OF FIGURES (Continued)

<u>Figure</u>	<u>Page</u>
Figure 4.6 Mechanism for the Palladium-mediated isomerization of the <i>cis</i> olefin to the <i>trans</i> . A hydride addition forms the palladium enolate intermediate allowing for rotation around the C2-C3 bond.	94
Figure 4.7 Disk diffusion assay of enduracidin lipid tail reduction products against <i>S. aureus</i> A) Enduracidin A, B) H4-Enduracidin A, C) 2- <i>trans</i> -H2-End A and D) 2- <i>cis</i> -H2-End A.	94
Figure 4.8 A) HPLC chromatogram of extracts from wild-type <i>S. fungicidicus</i> (bottom) and <i>orf45</i> disruptant <i>Sf45dh::Tn5AT</i> (top). Enduracidin A and B are labelled with asterisks. New enduracidin compounds produced by the mutant strain are labelled with '#'. MALDI-TOF MS analysis of the 12 min peak, H4-End A (top) and 22 min peak, H4-End B (Bottom) showing the [M+H] ⁺ ion.	95
Figure 4.9 A) HPLC chromatogram of the <i>Sf44::Tn5AT</i> culture extract. The new compound is indicated with an asterisk. B) ESI (+) MS spectrum of the 9.6 min peak showing the [M+3H] ³⁺ ion. The neutral mass of 2356.8 Da corresponds with H4-End A.	96
Figure 4.10 Double quantum filtered COSY NMR spectra for A) Enduracidin A and B) the peptide isolated from <i>SfΔ39AmR</i> . The olefinic lipid tail correlations are labeled in each spectrum.	96
Figure 4.11 Mass spectra of Boc-End ozonolysis products under various conditions. A) 3:1 MeOH:DMF, DMS, 5 min, -78 °C; B) 3 Å MeOH, DMS, 5 min, -78 °C; C) 1:2 DCM:MeOH, DMS, 4 min, -78 °C; D) Close-up of the singly charged degradation products between 1150 and 1400 Da; E) 1:2 DCM:MeOH, DMS, 2 min, -78 °C; F) 1:2 DCM:MeOH, DMS, 1 min, -78 °C; G) 1:2 DCM:MeOH, TPP, 2 min, -78 °C; H) 1:2 DCM:MeOH, Pyr, 2 min, -78 °C.	99
Figure 4.12 Proposed mechanism for the reduction of carbonyl peroxides by pyridine N-oxide after the fragmentation of the primary ozonide.	100

LIST OF FIGURES (Continued)

<u>Figure</u>	<u>Page</u>
<p>Figure 4.13 A) HPLC chromatograms showing the analysis of the maleimide reaction with Boc-End under various conditions. Boc-End, a set of three peaks, is indicated with an asterisk. Enduracidins A and B are indicated with a '#'. B) ESI (+) MS analysis of representative of the whole reaction series.</p>	102
<p>Figure 4.14 A) ESI (+) MS analysis of the NO-Toluene MeOH, CuI reaction representative of the catalyzed reactions. B) HPLC chromatograms showing the analysis of the maleimide reaction with Boc-End under various conditions. Boc-End, a set of three peaks, is indicated with an asterisk. Enduracidins A and B are indicated with a '#'.</p>	103
<p>Figure 4.15 ESI (+) MS spectra showing the crude products from the A) first Boc-End Danishefsky's Diene reaction. B) A higher resolution spectra of the 1311.5 Da compound from the second reaction.</p>	104
<p>Figure 4.16 HPLC chromatograms showing the Boc-End/Danishefsky's diene reaction products from various conditions. Enduracidin is labelled with an '#' and Boc-End with an asterisk.</p>	105
<p>Figure 4.17 ESI (+) MS spectrum of the pooled HPLC fractions from four min. to 8 min. of the spectrum. Enduracidin A and B are present in the $[M+2H]^{2+}$ form at $m/z = 1177.5$ and 1185.5 respectively. The additional peaks are the sodium (+11) and potassium (+18) adducts of enduracidin A and B.</p>	106
<p>Figure 4.18 ESI (+) MS spectrum of the dihydroxylation reaction of enduracidin. The labeled signals are the +2 ions: A) $m/z=1194.5$, (OH)₂-End A; B) $m/z=1201.5$, (OH)₂-End B; C) $m/z=1205.5$, (OH)₂-End A Na⁺ adduct; D) $m/z=1211.5$, (OH)₄-End A; E) $m/z=1212.5$, (OH)₂-End B Na⁺ adduct; and F) $m/z=1222.5$, (OH)₄-End A Na⁺ adduct.</p>	106
<p>Figure 4.19 HPLC chromatogram showing the separation of hydroxyenduracidin species which were identified by ESI MS as A) (OH)₄-End A, B) (OH)₂-End A, C) (OH)₄-End B, D) (OH)₂-End B E) (OH)₂-End A and F) (OH)₂-End B. Unreacted enduracidin A and B are indicated with asterisks.</p>	107

LIST OF FIGURES (Continued)

<u>Figure</u>	<u>Page</u>
Figure 4.20 Proton NMR spectra comparing the hydroxylated enduracidins with End A. The lipid tail olefinic protons are indicated on each spectra with an asterisk. A) End A; B) Peak A, (OH) ₄ -End B; C) Peak B, (OH) ₂ -End A; and D) Peak F, (OH) ₂ -End A.	107
Figure 4.21 A) COSY spectrum of peak B showing the labelled correlations: a) H2-H3; and b) H3-H4. B) COSY spectrum of peak F showing the labelled correlations: a) H3-H4; b) H4-H5; and c) H5-H6. Lipid tail structures of each compound are shown to the right of their corresponding spectra.	108
Figure 4.22 Chart showing the percent growth inhibition of <i>S. aureus</i> by the various hydroxylated enduracidins compared with End A and ampicillin. Standard of deviation is shown.	109
Figure 4.23 Structures of FR901469 (left), mannopeptimycin (center) and Pneumocandin B0 (right).	110
Figure 4.24 HPLC chromatograms showing the A) TFA-KNO ₃ and B) AcOH-NaNO ₂ reactions.	110
Figure 4.25 ESI (+) MS spectra of pooled HPLC fractions from the A) TFA-KNO ₃ and B) AcOH-NaNO ₂ reactions.	111
Figure 4.26 HPLC chromatogram showing the product of the TNM-10 mM NH ₄ OAc buffer reaction. The peaks were identified as starting material.	111

CHAPTER ONE

INTRODUCTION

Neal Goebel

History of Antibiotics

The discoveries of Koch and Henle linking infectious disease to bacteria allowed for the modern development of antibiotics.¹ Research toward combating these pathogenic bacteria developed along two routes during the first half of the 20th century. The discovery of penicillin by Alexander Flemming in 1928 and its eventual purification and therapeutic development 12 years later by Florey *et al.* was the first example of an antibiotic discovered from natural sources.² Penicillin is a beta-lactam antibiotic produced by the fungus *Penicillium rubrum* and inhibits cell wall biosynthesis by covalently binding to the transpeptidase, carboxypeptidase and/or endopeptidase enzymes (Fig. 1.1A).³ The development of penicillin as a drug was spurred by the treatment of infections by the military during World War Two. During the first five months of 1943 400 million units of penicillin were produced. Two years later, in August 1945, advancements in technology led to the production of 650 billion units of penicillin monthly.⁴ An alternate approach to the development of antibacterial therapeutics was ongoing during the development of penicillin.

The discovery of Prontosil, the first of the ‘sulfa’ drugs, resulted from the intensive synthetic chemistry program run by Bayer.⁵ The compounds were found to be active against both Gram-negative and Gram-positive infections. The lack of *in vitro* activity by Prontosil led to the discovery that the compound served as a prodrug and was activated by reduction of the diazene linkage releasing the bioactive sulfanilamide (Fig. 1.1B).⁶ Sulfanilamide, developed 24 years prior by the dye

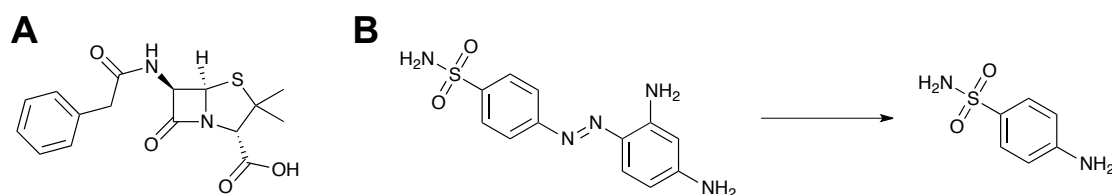


Figure 1.1 A) Structure of penicillin G. B) Structures of Prontosil and sulfanilamide produced by reduction of the diazene bond.

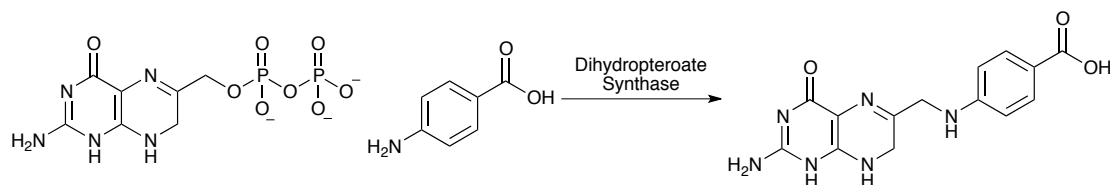


Figure 1.2 Biosynthesis of dihydropteroate by dihydropteroate synthase.

industry, was not protected under patent allowing for the rapid spread of sulfa drug production. Within a year of publication in 1935 the sulfonamides became the first medically used antibiotics.⁷ The sulfa drugs, *p*-aminobenzoic acid analogs, act as competitive inhibitors of dihydropteroate synthase during folate biosynthesis (Fig 1.2). The capability of producing kilotons of compound via synthesis led to the dominance of the sulfa drugs in clinical use until the mid 1950s. The sulfa drugs established that synthetic chemistry can yield new antibiotics.

The development of natural products chemistry in antibiotic research quickly gained dominance. Through the 50s and 60s pharmaceutical companies invested heavily on the acquisition and screening of bacterial strains for antibiotic production. The actinobacteria, specifically the genus *Streptomyces*, were found to be prodigious producers of bioactive compounds. The era became the golden age of antibiotics. In the 1970s the pace of drug discovery began to slow. New chemical classes of compounds began to be harder to find. Unique mechanisms of action were more difficult to discover. The discovery rate for antibiotics began to slow immensely. Natural product sources were no longer providing high returns for the discovery of new compounds. Efforts were focused on the semisynthetic modification of existing compounds through medicinal chemistry in an effort to overcome resistance and increase efficacy.⁸ During the past 15 years the exploration of combinatorial chemistry in target-directed drug discovery has yielded little success in providing new chemical scaffolds. The lack of profit margin in antibiotics coupled with the increasing cost and difficulty of FDA approval has decreased pharmaceutical industry interest in antibiotic discovery. The lack of funding in academic natural products chemistry research has

slowed the discovery of new chemical entities for use as antibiotics even further. It appears increased profits or an increase in the infectious disease mortality rate is needed to spur the funding of antibiotic discovery.

Primary Antibiotic Modes of Action

Antibiotics can be classified into five general modes of action: Inhibition of DNA functions; disruption of protein biosynthesis; interruption of vital metabolic pathways; disruption of cell membrane function; and blocking cell wall biosynthesis. Each mode has its own benefits and weaknesses. Different classes of bacteria are susceptible to certain antibiotics, i.e. glycopeptides are effective against Gram-positive bacteria while inherently inactive against Gram-negative bacteria due to the lipopolysaccharide (LPS) outer membrane.

The inhibition of DNA replication/transcription is demonstrated by the quinolones. The fluoroquinolone ciprofloxacin, for example, binds to DNA gyrase and topoisomerase blocking DNA replication and causing fracturing of the DNA.⁹ Rifampin, a strong inhibitor of RNA polymerase, blocks transcription and ultimately prevents protein biosynthesis.¹⁰ Antibiotics targeting DNA regulatory proteins are effective due to the structural differences between bacterial and mammalian proteins.

Inhibition of the bacterial ribosome is effective due to the significant differences from the mammalian ribosome. The translation of RNA to a protein is performed by the ribosome, having 30S and 50S portion in bacteria. Drugs such as chloramphenicol and erythromycin block protein synthesis by binding the the 50S portion of the ribosome. Phenicol antibiotics prevent peptide bond formation while macrolides block translocation of the ribosome along the RNA strand. The aminoglycosides bind to the ribosome complex in several areas causing misreading and early termination of protein synthesis.¹¹ The tetracyclines block tRNA from binding to the 30S portion of the ribosome.¹² The stalling of protein synthesis leads to bacteriostasis necessitating

immune response for elimination of bacterial infection. The misreading of RNA caused by some aminoglycosides is bactericidal.

The direct inhibition of vital metabolic pathways unique to bacteria is the last mode of intracellular antibiotic action. The sulfonamides and trimethoprim both inhibit the biosynthesis of tetrahydrofolate, a vital cofactor in metabolism. Sulfonamides, as mentioned earlier, inhibit dihydropteroate synthase. Trimethoprim inhibits dihydrofolate reductase.¹³ The two classes of drugs act synergistically by competitively inhibiting two steps in bacterial folate biosynthesis. The lack of folate in bacteria prevents them from making purine bases, blocking DNA synthesis and blocking the biosynthesis of methionine, which in turn inhibits most methyltransferase reactions and prevents protein biosynthesis. The effects of these drugs is bacteriostatic and rarely bactericidal.¹⁴

The last two modes of action involve the extracellular targets of the cell membrane and cell wall. The inhibition of membrane function prevents cells from working properly by disrupting ion gradients and causing leakage of cellular materials. Daptomycin binds to Ca^{2+} then penetrates the cellular membrane, forming pores. The resulting membrane depolarization disrupts cellular metabolism.¹⁵ Polymyxin, due to its positive charge, binds to phospholipids and lipopolysaccharide causing the disruption of both membranes of Gram-negative bacteria.¹⁶ The disruption of the bacterial membrane results in leakage of cellular components and possible lysis resulting in cell death. Antibiotics targeting the cellular membrane tend to have issues with toxicity to mammalian cells.

The disruption of cell wall biosynthesis has been a common target against Gram-positive bacteria. The penicillins block the transpeptidation reaction preventing the cross-linking of peptidoglycan and formation of the cell wall.³ Vancomycin blocks transglycosylation by binding to the D-Ala-D-Ala terminus of Lipid II and also inhibits the cross-linking of peptidoglycan strands by transpeptidases (Fig. 1.3).¹⁷ Fosfomycin, a phosphoenolpyruvate (PEP) mimetic, inhibits MurA (the first enzyme in

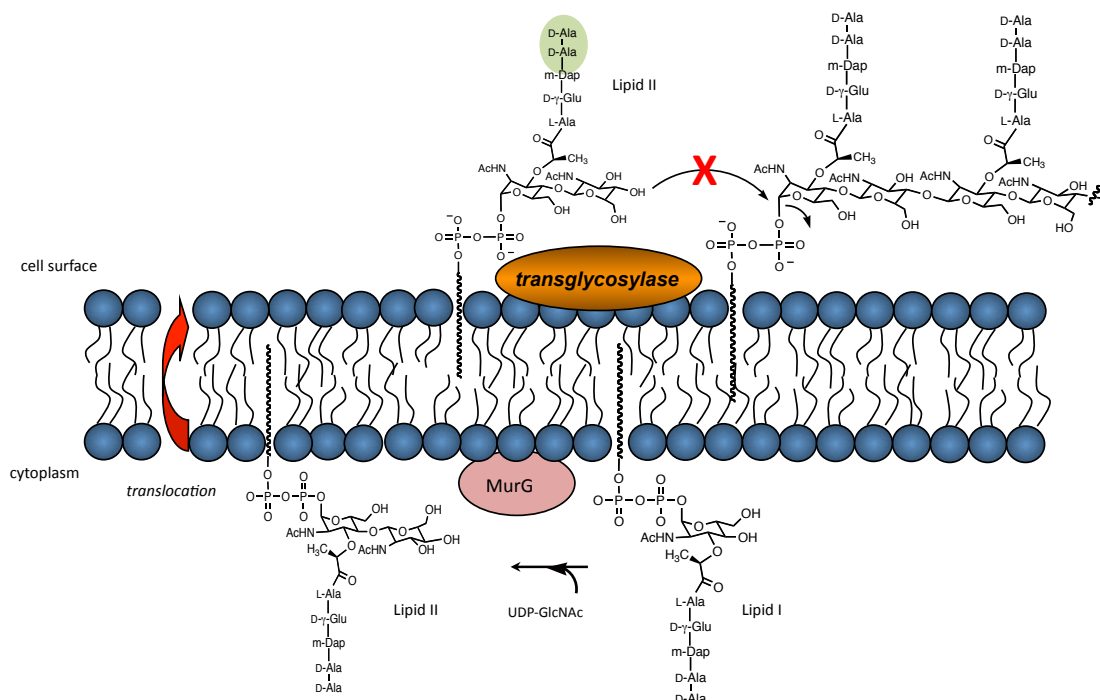


Figure 1.3 Key steps in cell wall biosynthesis by Gram positive bacteria with the vancomycin recognition element, D-Ala-D-Ala, highlighted in green.

peptidoglycan biosynthesis) by covalently binding the active site Cys, blocking the transfer of PEP to the 3'-hydroxyl group of UDP-N-Ac-glucosamine, the first committed step in peptidoglycan biosynthesis.¹⁸

Drug Resistance

For each of the modes of action, resistance mechanisms have evolved due to the inherent selective pressure of antibiotics. Beta-lactam antibiotics, as an example, induce, in resistant strains, the production of PBPs with lower beta-lactam affinity or beta-lactamases that degrade the antibiotic.¹⁹ It is important to note that penicillin resistance mechanisms evolved over millions of years not just the 6 years of therapeutic use required for ~40% of hospital *S. aureus* isolates to have acquired resistance.²⁰ The beta-lactamases are estimated to have evolved 2 billion years ago, prior to the divergence of Gram-negative and Gram-positive bacteria.²¹ Erythromycin

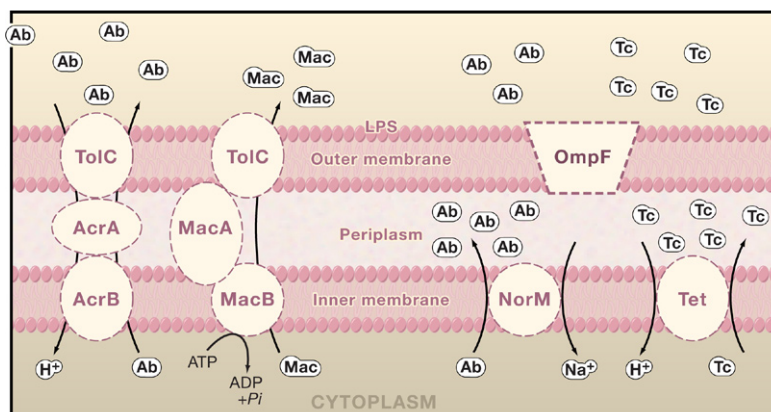


Figure 1.4 A Gram-negative membrane complex illustrating four drug efflux pumps: AcrAB-TolC, MacAB-TolC, NorM and Tet. Both NorM and Tet rely on passive transporters like the porin OmpF for removal of the drug from the periplasm. Figure from Aleksun *et al.*²⁴

resistance results from a post-transcriptional methylation of adenosine 2058 on 23S rRNA of the 50S ribosomal subunit causing a decrease in binding affinity.²² One general form of resistance is the development of drug efflux pumps by bacteria. Some efflux systems like AcrAB-TolC and NormM from *E. coli* can transport various antibiotics out of the cell using an ion gradient (Fig. 1.4). Others like MacAB only transport specific classes of compounds, i.e. macrolides, and require consumption of ATP.²³ The acquisition of drug efflux pumps can confer multi-drug resistance to pathogenic bacterial strains and is one down side to inhibiting intracellular targets.²⁴

Glycopeptide resistance is an instructive example when examining the acquisition of drug resistance genes. Clinical bacterial isolates resistant to vancomycin were not observed until nearly 40 years after its introduction.²⁰ Resistance arose from the alteration of the D-Ala-D-Ala terminus of Lipid II to D-Ala-D-Lactate causing a 1000-fold decrease in vancomycin binding affinity.²⁵ The strong selective pressure of vancomycin and other glycopeptides resulted in the acquisition of the *vanRSHAX* gene cluster encoding a two component regulatory system (VanR and VanS) and three enzymes used to install the new Lipid II peptide terminus (Fig. 1.5). The resistance gene cluster is found in numerous environmental bacteria and is likely the source of resistance genes found in pathogenic bacteria. Comparison of GC content of the resistance cluster from vancomycin resistant *Enterococci* (VRE), 40%, and

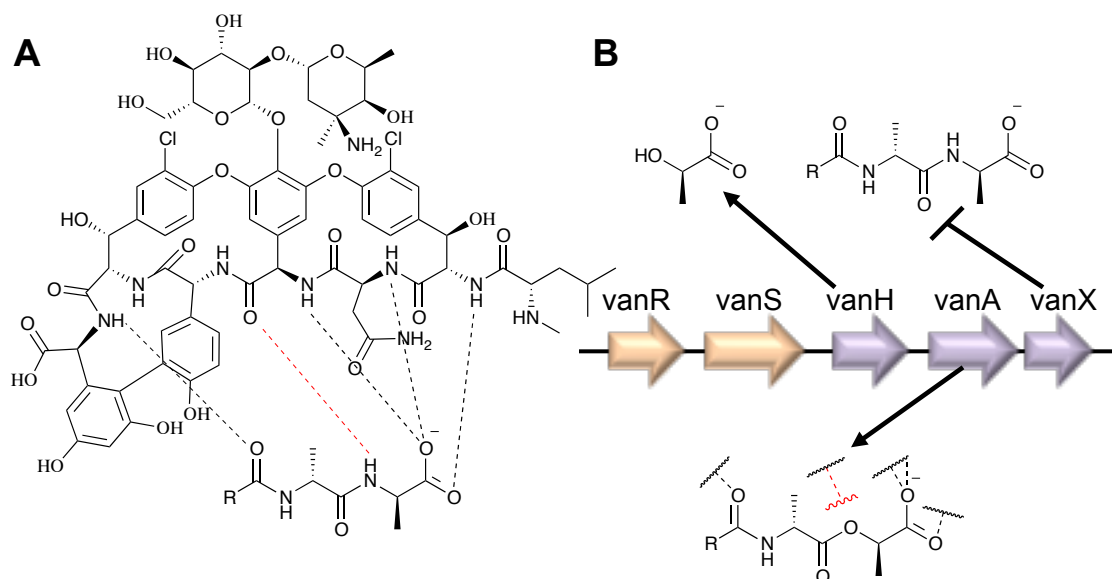


Figure 1.5 A) Structure of vancomycin showing the five hydrogen bonds formed with the D-Ala-D-Ala terminus of Lipid II. B) The vancomycin resistance genes and their corresponding functions in producing D-Ala-D-Lac Lipid II. Figure from Wright.⁴⁶

Streptomyces strains, 70%, indicates the gene cluster has had significant time for the drift of GC content. The gene cluster has been outside of the vancomycin-producing bacteria for a significant time since the evolution of vancomycin an estimated 240 million years ago. For many antibiotics the resistance mechanism already exists in non-pathogenic bacteria. The primary concern is the transfer of resistance genes into pathogenic strains.

The improper use of antibiotics causes selective pressures for pathogens to acquire resistance genes. Overprescription and patient noncompliance have resulted in extensive drug resistance in some pathogens.²⁶ The long patient compliance requirements for effective treatment of TB has aided in the propagation of multi-drug-resistant *Mycobacterium tuberculosis* (MDR-TB).²⁷ A survey of 58 geographical regions indicated 0-16% (1% median) of total new infections and 0-48% (9% median) of recurrent cases were MDR-TB. The highest incidence MDR-TB occur in the undeveloped regions of the survey due to incomplete treatment regimens.²⁸

Outside of the clinical setting, the use of antibiotics in the agricultural industry

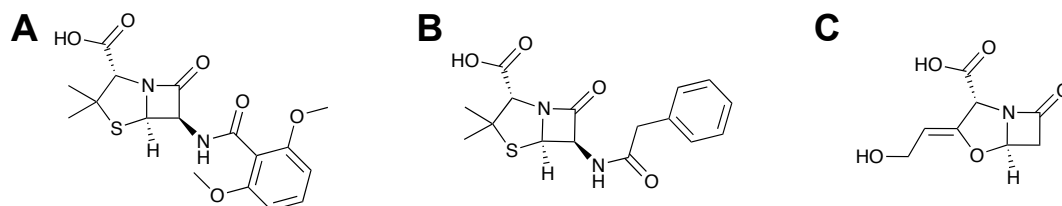


Figure 1.6 Structures of A) Methicillin, B) Penicillin G and C) Clavulanic acid.

has lead to further issues of drug resistance. *Chlamydia trachomatis* is an obligate intracellular Gram-negative pathogen. Human *chlamydial* infections have long been treated with tetracycline without the emergence of antibiotic resistance. However, a series of *Chlymadia suis* strains from pigs has been documented as having a transferrable genomic island containing tetracycline resistance genes.²⁹ The emergence of these resistant strains is attributed to the extensive use of tetracycline-containing feed additives in the U.S. and Europe.³⁰

To combat drug resistance, several approaches have been taken. The modification of existing drugs to avoid or adapt to the resistance mechanism is exemplified by the development of methicillin. Resistance to penicillin G through beta-lactamases led to the search for a beta-lactamase-resistant penicillin. From this semisynthetic discovery program came methicillin. Alternately, the use of beta-lactamase inhibitors such as clavulanic acid has been employed to retain sensitivity to beta-lactams by some penicillin-resistant pathogens (Fig. 1.6). The specter of antibiotic resistance has continually spurred the search for new antibiotic compounds. However, as the number of new chemical entities discovered has declined, the reevaluation and repurposing of previously discovered antibiotics has become more important. Compounds such as the aminoglycosides, omitted from use as first line antibiotics due to toxicity and physical properties, are finding increasing use combating drug resistant infections.³¹ Advances in bacterial genetics, biochemistry and synthetic chemistry bring the potential for the optimization of previously discovered antibiotic classes to combat drug resistance. Enduracidin has a high potential to fulfill this objective.

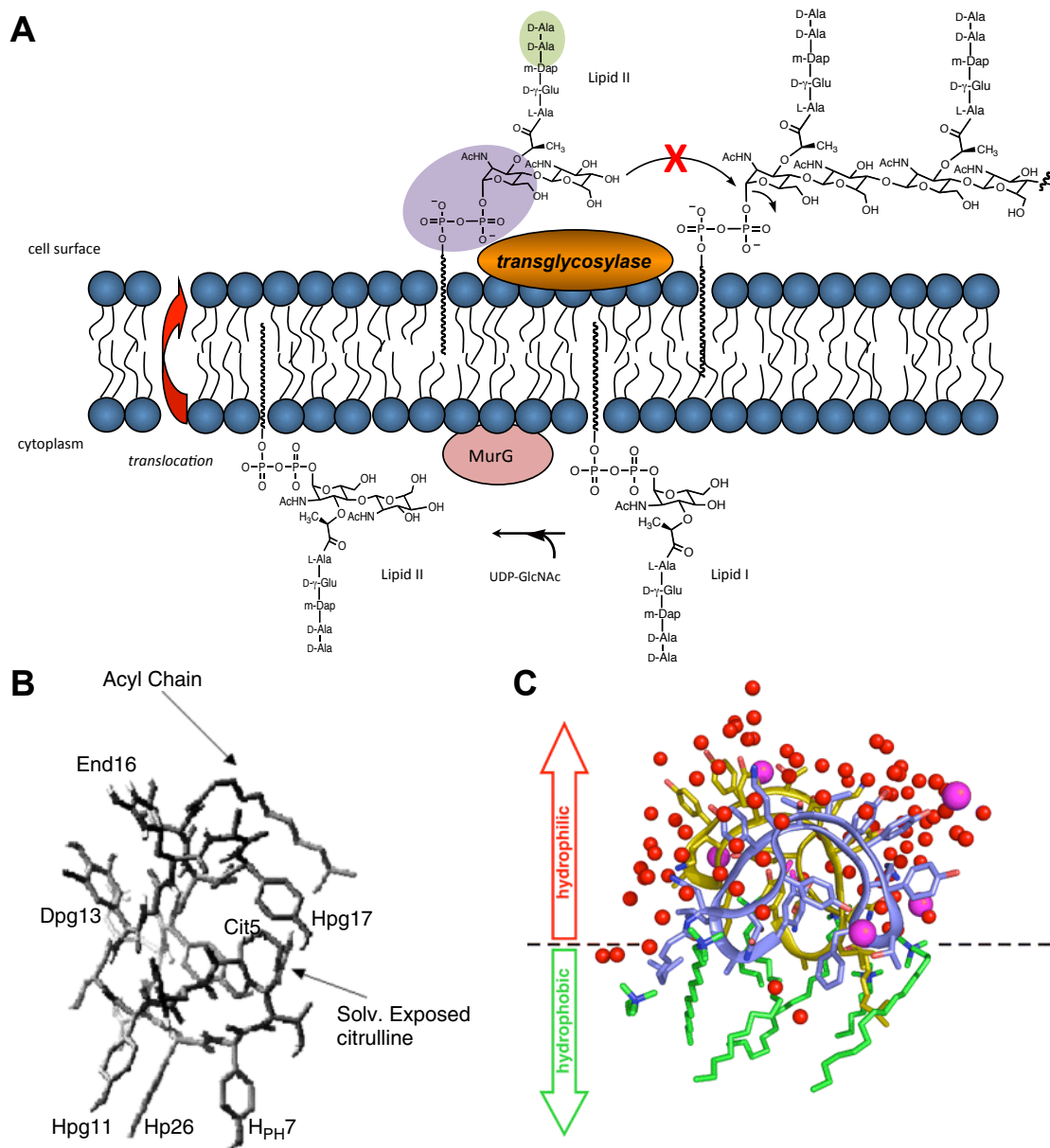


Figure 1.8 A) Peptidoglycan biosynthesis with the vancomycin (green) and enduracidin (purple) recognition elements highlighted. B) 3D NMR structure of enduracidin from Castiglione *et al.*^{38b} C) Crystal structure of a ramoplanin dimer (yellow and purple) interfacing with detergent molecules (green), chloride ions (magenta) and ordered water molecules (red) figure is from Hamburger *et al.*^{38c}

and ramoplanin are active against MRSA and VRE.^{37c, 41} Additionally there has been no observed transferrable resistance mechanism or cross resistance for enduracidin despite being used for over three decades as a poultry feed additive.^{17, 42}

Enduracidin was evaluated for use as a human therapeutic soon after its

discovery.⁴³ As a large peptide, enduracidin had no oral bioavailability so the use of enduracidin as an IV or intramuscularly (IM) injected drug was also evaluated.^{42, 44} The low solubility in blood plasma led to the testing of enduracidin for IM injection as a suspension in nonionic detergents. The results indicated an unacceptable accumulation effect was occurring, likely resulting from precipitation.⁴⁵ The insolubility of enduracidin resulted in it being allocated into use as a feed additive in the 1980s.

As the prevalence of antibiotic resistance continues to grow, new therapeutics are needed. The reevaluation of previously discovered antimicrobials provides a wealth of active compounds for development.³¹ Compounds put aside due to pharmacological properties or toxicity can now be modified using the advances in microbial genetics, biosynthesis and chemistry achieved in the past 20 years. Alteration of the pharmacological properties of enduracidin can potentially produce a superior antibiotic for the treatment of drug-resistant Gram-positive bacterial infections. The work of this thesis has focused on understanding the biosynthesis of enduracidin, then utilizing the biosynthetic pathways and chemical synthesis to alter the physical properties of enduracidin, improving solubility while maintaining bioactivity.

References

1. Evans, A. S., Causation and Disease: A Chronological Journey: The Thomas Parran Lecture. *Am. J. Epidemiol.* **1978**, *108* (4), 249-258.
2. (a) Chain, E.; Florey, H. W.; Gardner, A. D.; Heatley, N. G.; Jennings, M. A.; Orr-Ewing, J.; Sanders, A. G., Penicillin as a Chemotherapeutic Agent. *The Lancet* **1940**, *236* (6104), 226-228; (b) Flemming, A., On the Antibacterial Action of Cultures of a Penicillium, with Special Reference to their Use in the Isolation of B. influenzae. *Br. J. Exp. Pathol.* **1929**, *10* (3), 226-236.
3. (a) Nicola, G.; Tomberg, J.; Pratt, R. F.; Nicholas, R. A.; Davies, C., Crystal Structures of Covalent Complexes of β -Lactam Antibiotics with Escherichia coli Penicillin-Binding Protein 5: Toward an Understanding of Antibiotic Specificity. *Biochemistry (Mosc)*. **2010**, *49* (37), 8094-8104; (b) Waxman, D. J.; Strominger, J. L., Penicillin-Binding Proteins and the Mechanism of Action of Beta-Lactam Antibiotics. *Annu. Rev. Biochem* **1983**, *52* (1), 825-869.
4. Grossman, C. M., The First Use of Penicillin in the United States. *Ann. Intern. Med.* **2008**, *149* (2), 135-136.
5. Domagk, G., Chemotherapie der bakteriellen Infektionen. *Angew. Chem.* **1935**, *48* (42), 657-667.
6. Trefouel, J.; Trefouel, J.; Nitti, F.; Bovet, D., Activite du p-aminophenylsulfamide sur les infections streptococciques experimentales de la souris et du lapin. *C. R. Soc. Biol.* **1935**, *120*, 756-758.
7. Long, P. H.; Bliss, E. A., The Clinical use of Sulfanilamide and its Derivatives in the Treatment of Infectious Disease. *Ann. Intern. Med.* **1937**, *11* (4), 575-592.
8. Wright, G. D., The antibiotic resistome: the nexus of chemical and genetic diversity. *Nat Rev Micro* **2007**, *5* (3), 175-186.
9. Drlica, K.; Zhao, X., DNA Gyrase, Topoisomerase IV, and the 4-Quinolones.

Microbiol. Mol. Biol. Rev. **1997**, *61* (3), 377-392.

10. Campbell, E. A.; Korzheva, N.; Mustaev, A.; Murakami, K.; Nair, S.; Goldfarb, A.; Darst, S. A., Structural Mechanism for Rifampicin Inhibition of Bacterial RNA Polymerase. *Cell* **2001**, *104* (6), 901-912.

11. Davis, B. D., Mechanism of bactericidal action of aminoglycosides. *Microbiol. Rev.* **1987**, *51* (3), 341-350.

12. Brown, J. R.; Ireland, D. S., Structural Requirements for Tetracycline Activity. In *Adv. Pharmacol.*, Silvio Garattini, A. G. F. H. I. J. K.; Schnitzer, I. J., Eds. Academic Press: 1978; Vol. Volume 15, pp 161-202.

13. Gleckman, R.; Blagg, N.; Joubert, D. W., Trimethoprim: Mechanisms of Action, Antimicrobial Activity, Bacterial Resistance. *Pharmacotherapy* **1981**, *1* (1), 14-19.

14. Amyes, S. G., Bactericidal activity of trimethoprim alone and in combination with sulfamethoxazole on susceptible and resistant *Escherichia coli* K-12. *Antimicrob. Agents Chemother.* **1982**, *21* (2), 288-293.

15. Micklefield, J., Daptomycin Structure and Mechanism of Action Revealed. *Chem. Biol.* **2004**, *11* (7), 887-888.

16. (a) Daugelavicius, R.; Bakiene, E.; Bamford, D. H., Stages of Polymyxin B Interaction with the *Escherichia coli* Cell Envelope. *Antimicrob. Agents Chemother.* **2000**, *44* (11), 2969-2978; (b) Dixon, R. A.; Chopra, I., Polymyxin B and polymyxin B nonapeptide alter cytoplasmic membrane permeability in *Escherichia coli*. *J. Antimicrob. Chemother.* **1986**, *18* (5), 557-563.

17. Reynolds, P. E., Structure, Biochemistry and Mechanism of Action of Glycopeptide Antibiotics. *Eur. J. Clin. Microbiol. Infect. Dis.* **1989**, *8* (11), 943-950.

18. (a) Brown, E. D.; Vivas, E. I.; Walsh, C. T.; Kolter, R., MurA (MurZ), the Enzyme That Catalyzes the First Committed Step in Peptidoglycan Biosynthesis, is Essential in *Escherichia coli*. *J. Bacteriol.* **1995**, *177* (14), 4194-7; (b) Kahan, F. M.; Kahan, J. S.; Cassidy, P. J.; Kropp, H., The Mechanism of Action of Fosfomycin (Phosphonomycin). *Ann. N.Y. Acad. Sci.* **1974**, *235* (1), 364-386.

19. (a) Deurenberg, R. H.; Vink, C.; Kalenic, S.; Friedrich, A. W.; Bruggeman, C. A.; Stobberingh, E. E., The molecular evolution of methicillin-resistant *Staphylococcus aureus*. *Clin. Microbiol. Infect.* **2007**, *13* (3), 222-235; (b) Fisher, J. F.; Meroueh, S. O.; Mobashery, S., Bacterial Resistance to β -Lactam Antibiotics: Compelling Opportunism, Compelling Opportunity. *Chem. Rev.* **2005**, *105* (2), 395-424.
20. Chambers, H. F., The Changing Epidemiology of *Staphylococcus aureus*? *Emerging Infect. Dis.* **2001**, *7* (2), 178-182.
21. Hall, B. G.; Barlow, M., Evolution of the Serine β -lactamases: Past, Present and Future. *Drug Resist. Updat.* **2004**, *7* (2), 111-123.
22. Weisblum, B., Erythromycin resistance by ribosome modification. *Antimicrob. Agents Chemother.* **1995**, *39* (3), 577-85.
23. (a) Li, X. Z.; Nikaido, H., Efflux-mediated drug resistance in bacteria. *Drugs* **2004**, *64* (2), 159-204; (b) Murakami, S.; Yamaguchi, A., Multidrug-exporting secondary transporters. *Curr. Opin. Struct. Biol.* **2003**, *13* (4), 443-52.
24. Alekshun, M. N.; Levy, S. B., Molecular Mechanisms of Antibacterial Multidrug Resistance. *Cell* **2007**, *128* (6), 1037-1050.
25. Bugg, T. D. H.; Wright, G. D.; Dutka-Malen, S.; Arthur, M.; Courvalin, P.; Walsh, C. T., Molecular basis for vancomycin resistance in *Enterococcus faecium* BM4147: biosynthesis of a depsipeptide peptidoglycan precursor by vancomycin resistance proteins VanH and VanA. *Biochemistry* **1991**, *30* (43), 10408-10415.
26. (a) Kardas, P., Patient compliance with antibiotic treatment for respiratory tract infections. *J. Antimicrob. Chemother.* **2002**, *49* (6), 897-903; (b) Petersen, I.; Hayward, A. C., Antibacterial prescribing in primary care. *J. Antimicrob. Chemother.* **2007**, *60* (suppl 1), i43-i47.
27. Munro, S. A.; Lewin, S. A.; Smith, H. J.; Engel, M. E.; Fretheim, A.; Volmink, J., Patient Adherence to Tuberculosis Treatment: A Systematic Review of Qualitative Research. *PLoS Med* **2007**, *4* (7), e238.
28. Johnson, R.; Streicher, E. M.; Louw, G. E.; Warren, R. M.; van Helden, P. D.;

- Victor, T. C., Drug Resistance in *Mycobacterium tuberculosis*. *Curr. Issues Mol. Biol.* **2006**, 8 (2), 97-111.
29. Lenart, J.; Andersen, A. A.; Rockey, D. D., Growth and Development of Tetracycline-Resistant *Chlamydia suis*. *Antimicrob. Agents Chemother.* **2001**, 45 (8), 2198-2203.
30. Suchland, R. J.; Sandoz, K. M.; Jeffrey, B. M.; Stamm, W. E.; Rockey, D. D., Horizontal transfer of tetracycline resistance among *Chlamydia* spp. *in vitro*. *Antimicrob. Agents Chemother.* **2009**, 53 (11), 4604-11.
31. Falagas, M. E.; Grammatikos, A. P.; Michalopoulos, A., Potential of old-generation antibiotics to address current need for new antibiotics. *Expert Rev. Anti Infect. Ther.* **2008**, 6 (5), 593-600.
32. Higashide, E.; Hatano, K.; Shibata, M.; Nakazawa, K., Enduracidin, a new antibiotic. I. *Streptomyces fungicidicus* No. B5477, an enduracidin producing organism. *J. Antibiot.* **1968**, 21 (2), 126-37.
33. (a) Asai, M.; Muroi, M.; Sugita, N.; Kawashima, H.; Mizuno, K., Enduracidin, a new antibiotic. II. Isolation and characterization. *J. Antibiot.* **1968**, 21 (2), 138-46; (b) Goto, S.; Kuwahara, S.; Okubo, N.; Zenyoji, H., *In Vitro* and *in Vivo* Evaluation of Enduracidin, a New Peptide Antibiotic Substance. *J. Antibiot.* **1968**, 21 (2), 119-25; (c) Tsuchiya, K.; Kondo, M.; Oishi, T.; Yamazaki, I., Enduracidin, a New Antibiotic. III. *In vitro* and *in vivo* Antimicrobial Activity. *J. Antibiot.* **1968**, 21 (2), 147-53.
34. (a) Hori, M.; Iwasaki, H.; Horii, S.; Yoshida, I.; Hongo, T., Enduracidin, a New Antibiotic .VII. Primary Structure of the Peptide Moiety. *Chem. Pharm. Bull. (Tokyo)* **1973**, 21 (6), 1175-83; (b) Hori, M.; Sugita, N.; Miyazaki, M., Enduracidin, a New Antibiotic .VI. Separation and Determination of Enduracidins A and B by Column Chromatography. *Chem. Pharm. Bull. (Tokyo)* **1973**, 21 (6), 1171-74; (c) Iwasaki, H.; Horii, S.; Asai, M.; Mizuno, K.; Ueyanagi, J.; Miyake, A., Enduracidin, a new antibiotic .VIII. Structures of enduracidins A and B. *Chem. Pharm. Bull. (Tokyo)* **1973**, 21, 1184-1191.

35. (a) Tsuchiya, K.; Takeuchi, Y., Enduracidin, an Inhibitor of Cell Wall Synthesis. *J. Antibiot.* **1968**, *21* (6), 426-8; (b) Matsuhashi, M.; Ohara, I.; Yoshiyama, Y., Inhibition of Bacterial Cell Wall Synthesis *in vitro* by Enduracidin a New Polypeptide Antibiotic. *Agric. Biol. Chem.* **1969**, *33* (1), 134-137.
36. (a) Reynolds, P. E.; Somner, E. A., Comparison of the Target Sites and Mechanisms of Action of Glycopeptide and Lipoglycopeptide Antibiotics. *Drugs Exp. Clin. Res.* **1990**, *16* (8), 385-9; (b) Somner, E. A.; Reynolds, P. E., Inhibition of Peptidoglycan Biosynthesis by Ramoplanin. *Antimicrob. Agents Chemother.* **1990**, *34* (3), 413-419.
37. (a) Cudic, P.; Behenna, D. C.; Kranz, J. K.; Kruger, R. G.; Wand, A. J.; Veklich, Y. I.; Weisel, J. W.; McCafferty, D. G., Functional Analysis of the Lipoglycopeptide Antibiotic Ramoplanin. *Chem. Biol.* **2002**, *9* (8), 897-906; (b) Fang, X.; Tiyanont, K.; Zhang, Y.; Wanner, J.; Boger, D.; Walker, S., The Mechanism of Action of Ramoplanin and Enduracidin. *Mol. Biosyst.* **2006**, *2*, 69-76; (c) McCafferty, D. G.; Cudic, P.; Frankel, B. A.; Barkallah, S.; Kruger, R. G.; Li, W., Chemistry and biology of the ramoplanin family of peptide antibiotics. *Biopolymers* **2002**, *66* (4), 261-84.
38. (a) Hu, Y. N.; Helm, J. S.; Chen, L.; Ye, X. Y.; Walker, S., Ramoplanin inhibits bacterial transglycosylases by binding as a dimer to lipid II. *J. Am. Chem. Soc.* **2003**, *125* (29), 8736-8737; (b) Castiglione, F.; Marazzi, A.; Meli, M.; Colombo, G., Structure elucidation and 3D solution conformation of the antibiotic enduracidin determined by NMR spectroscopy and molecular dynamics. *Magn. Reson. Chem.* **2005**, *43* (8), 603-610; (c) Hamburger, J. B.; Hoertz, A. J.; Lee, A.; Senturia, R. J.; McCafferty, D. G.; Loll, P. J., A crystal structure of a dimer of the antibiotic ramoplanin illustrates membrane positioning and a potential lipid II docking interface. *Proc. Natl. Acad. Sci. U. S. A.* **2009**, *106* (33), 13759-13764.
39. Hsu, S.-T. D.; Breukink, E.; Tischenko, E.; Lutters, M. A. G.; de Kruijff, B.; Kaptein, R.; Bonvin, A. M. J. J.; van Nuland, N. A. J., The nisin-lipid II complex

reveals a pyrophosphate cage that provides a blueprint for novel antibiotics. *Nat. Struct. Mol. Biol.* **2004**, *11* (10), 963-967.

40. Hoffmann, A.; Pag, U.; Wiedemann, I.; Sahl, H.-G., Combination of antibiotic mechanisms in lantibiotics. *Il Farmaco* **2002**, *57* (8), 685-691.

41. Peromet, M.; Schoutens, E.; Yourassowsky, E., Clinical and Microbiological Study of Enduracidin in Infections Due to Methicillin-resistant Strains of *Staphylococcus aureus*. *Chemotherapy* **1973**, *19* (1), 53-61.

42. Matsuoka, T.; Takeda, K.; Goto, M.; Miyake, A. Feed Containing Enduracidin. 3697647, 1972.

43. (a) Tanayama, S.; Fugono, T.; Yamazaki, T., Enduracidin, a New Antibiotic. IV. The Fate of Enduracidin Administered Parenterally Into Rabbits. *J. Antibiot.* **1968**, *21* (5), 313-319; (b) Yokotani, H.; Ogiwara, S.; Nakaguchi, T.; Aomori, T.; Orita, S.; Aramaki, Y.; Usui, T.; Kawaji, H.; Nomura, M.; Kaziwara, K., Toxicological Study on Enduracidin in Mice, Rabbits, Dogs and Monkeys. *Takeda Kenkyusho Nenpo* **1969**, *28*, 76-95; (c) Kawakami, M.; Nagai, Y.; Fujii, T.; Mitsuhashi, S., Anti-microbial activities of enduracidin (enramycin) in vitro and in vivo. *J. Antibiot.* **1971**, *24* (9), 583-586.

44. Yourassowsky, E.; Monsieur, R., *In vitro* and *in vivo* Activity of Enduracidin on *Staphylococcus aureus*. *Chemotherapy* **1972**, *17*, 182-187.

45. Matsuzawa, T.; Fujisawa, H.; Aoki, K.; Mima, H., Effect of Some Non-ionic Surfactants on the Absorption of Enduracidin From the Muscles. *Chem. Pharm. Bull. (Tokyo)* **1969**, *17* (5), 999-1004.

46. Wright, G. D., The antibiotic resistome: the nexus of chemical and genetic diversity. *Nat. Rev. Microbiol.* **2007**, *5* (3), 175-186.

CHAPTER TWO

MUTASYNTHETIC MODIFICATION OF ENDURACIDIN

Neal Goebel

Introduction

Enduracidin contains five hydroxyphenylglycines (Hpg) and one dichlorohydroxyphenylglycine (Dpg) (Fig. 2.1). Structural studies of enduracidin have shown that the Hpg-3 hydroxyl group is involved in an intramolecular hydrogen bond important for conformation while Hpgs 6, 7, 11, 17 and Dpg-13 primarily interact with the solvent environment.¹ The number and distribution of Hpg residues throughout enduracidin make them a relevant target for modulating enduracidin's physical properties. The introduction of fluorine onto the phenol group of Hpg was selected to begin this study as it is metabolically stable and the minimal increase in steric bulk may reduce alterations in structural conformation, minimizing the reduction of bioactivity. Additionally, the electron-withdrawing nature of fluorine can reduce the pK_a of the phenolic hydroxyl proton.² A pK_a near biologically relevant ranges may improve solvation around the six Hpg-derived groups.

In *S. fungicidicus*, the enduracidin biosynthetic gene cluster contains the genes coding for the enzymes required to convert hydroxyphenylpyruvate and tyrosine into

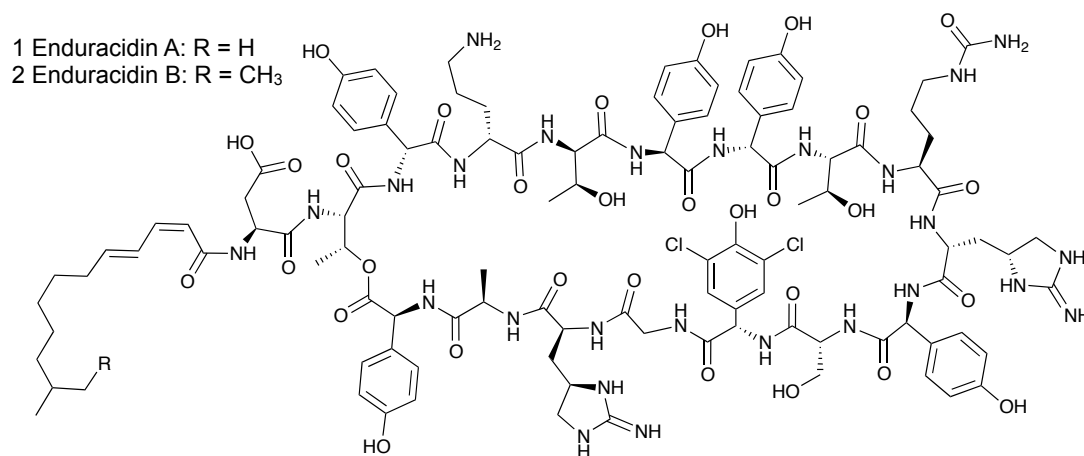


Figure 2.1 The structure of enduracidins A and B with the five hydroxyphenylglycines and one dichlorohydroxyphenylglycine labeled.

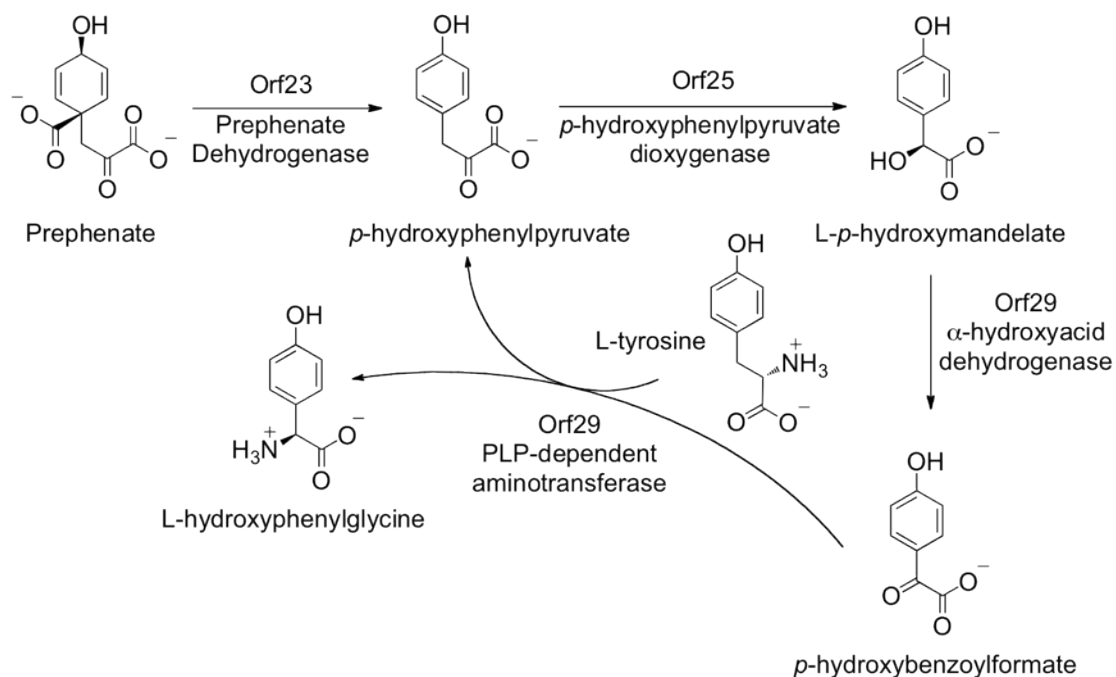


Figure 2.2 Biosynthesis of hydroxyphenylglycine in *S. fungicidicus* starting from prephenate.

Hpg (Fig. 2.2).³ The localization of Hpg biosynthetic genes in the enduracidin gene cluster suggests that Hpg production is not essential for other *S. fungicidicus* metabolites and is therefore an exploitable route for the alteration of enduracidin without disrupting other metabolic pathways. This work aims to demonstrate the ability to produce new enduracidin analogs with altered physical properties by manipulating the hydroxyphenylglycine biosynthetic pathway.

Results and Discussion

The phenol ring of tyrosine is not modified during its conversion to Hpg (Fig. 2.2) suggesting that 3-fluoro-hydroxyphenylglycine (3-F-Hpg) may be produced intracellularly if 3-fluoro-tyrosine (F-Tyr) could serve as a precursor via the Hpg biosynthetic enzymes. To demonstrate F-Hpg can be produced from F-Tyr and incorporated into enduracidin, cultures of *S. fungicidicus* were supplemented with a racemic mixture of DL-F-Tyr. The cultures produced a series of polyfluorinated enduracidins as evidenced by ESI-MS (Fig. 2.3). The fluorine incorporation produced a series of compounds ranging from difluoro-monochloro enduracidin A ($m/z=1178.5$) to 3'-hexafluoro-monochloro enduracidin A (3'-F₆-Cl₁ end A) ($m/z=1214.5$) as well as pentafluoro-dichloro enduracidin ($m/z=1222.5$). Interestingly, in this experiment the presence of fluorine did not inhibit the halogenase, resulting in the formation of a 3-chloro-5-fluoro-Hpg instead of 3-F-Hpg-13.⁴ The incorporation of fluorine into enduracidin demonstrated that the biosynthesis of Hpg was not disrupted by the presence of fluorine on the phenol moiety. Additionally, the production of hexafluoro-monochloro-enduracidin indicated the binding pockets of the Hpg adenylation

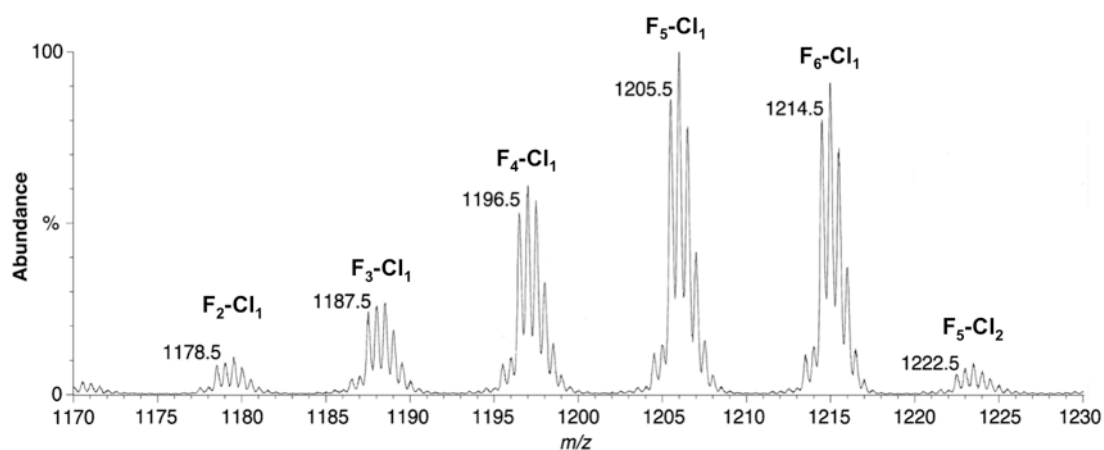


Figure 2.3 ESI positive mass spectrum showing the $[M+2H]^{2+}$ ions of polyfluorinated enduracidins produced from F-Tyr supplementation

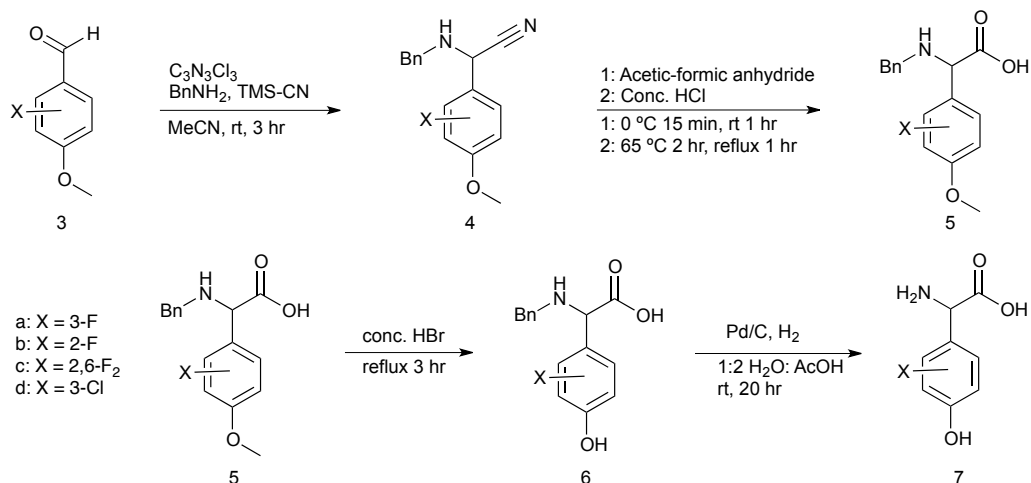


Figure 2.4 Preparation of fluoro-Hpg from fluorobenzaldehyde. For $n=1$ fluorine is in the 2 or 3 position as specified. For $n=2$ fluorine is in the 2 and 5 positions.

domains tolerate the altered electronegativity and steric bulk of fluorinated Hpg. The mixture of polyfluorinated enduracidins proved to be inseparable via chromatographic means, prohibiting studies on individual species.

In an attempt to reduce the number of fluorinated enduracidin species being produced we undertook the preparation of 3-F-Hpg (**7a**) starting from 3-fluoro-4-methoxybenzaldehyde (**3a**) (Fig. 2.4). A modified Strecker reaction utilizing, TMS-cyanide, benzylamine, and catalytic cyanuric chloride successfully yielded the *N*-benzyl aminonitrile (**4a**).⁵ To prevent degradation during hydrolysis of the nitrile, (**4a**) was first treated with formic-acetic anhydride, then heated in the presence of HCl to yield the *N*-benzyl amino acid (**5a**).⁶ Without further purification, the methoxyphenylglycine (**5a**) was converted to the hydroxyphenylglycine (**6a**) with concentrated HBr under refluxing conditions. Deprotection of the *N*-benzyl group via palladium-catalyzed transfer hydrogenation followed by crystallization from water afforded racemic DL-3-F-Hpg (**7a**) in 31% overall yield.

Supplementation of wild type cultures of *S. fungicidicus* with 3-F-Hpg produced a series of fluorinated enduracidins as observed via MALDI MS (Fig 2.5). The introduction of fluorine via F-Hpg, rather than F-Tyr, improved the production of the

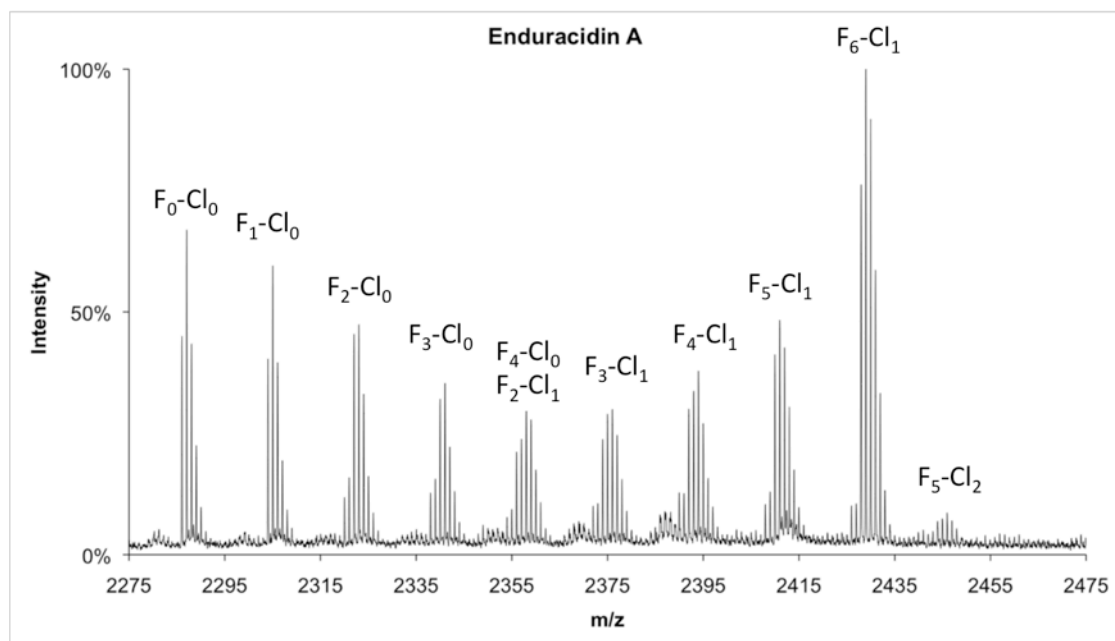


Figure 2.5 MALDI Mass spectrum of enduracidins isolated from SfWT supplemented with 3-F-Hpg showing the $[M+H]^+$ ions.

hexafluoro species. Interestingly, a series of deschloro fluorinated enduracidin species was also produced, as well as deschloro enduracin. The data showed that F-Hpg was readily incorporated into enduracidin. However, even at high levels of supplementation, a single hexafluoro enduracidin species was not produced.

To solely produce the 3'-hexafluoro enduracidin species we aimed to eliminate the endogenous production of Hpg and complement the deficiency with exogenous 3-F-Hpg. The gene product of *orf29* is predicted to be a fusion protein homologous to both the *p*-hydroxymandelate oxidase (HmO) and the aminotransferase (HpgT) from *S. coelicolor* and involved in Hpg biosynthesis (Fig. 2.2).^{3, 7} To prevent possible consumption of 3-F-Hpg via transamination, the aminotransferase portion of *orf29* was targeted for disruption. The gene disruption delivery fosmid pXYF148D3, containing the disruption cassette Tn5AT, was introduced into wild-type *S. fungicidicus* via conjugation (Fig. 2.6). Exconjugants demonstrating double crossover homologous recombination via retained apramycin resistance were verified for insertional disruption of *orf29* by Southern blot analysis of the chromosomal DNA. The disrupted

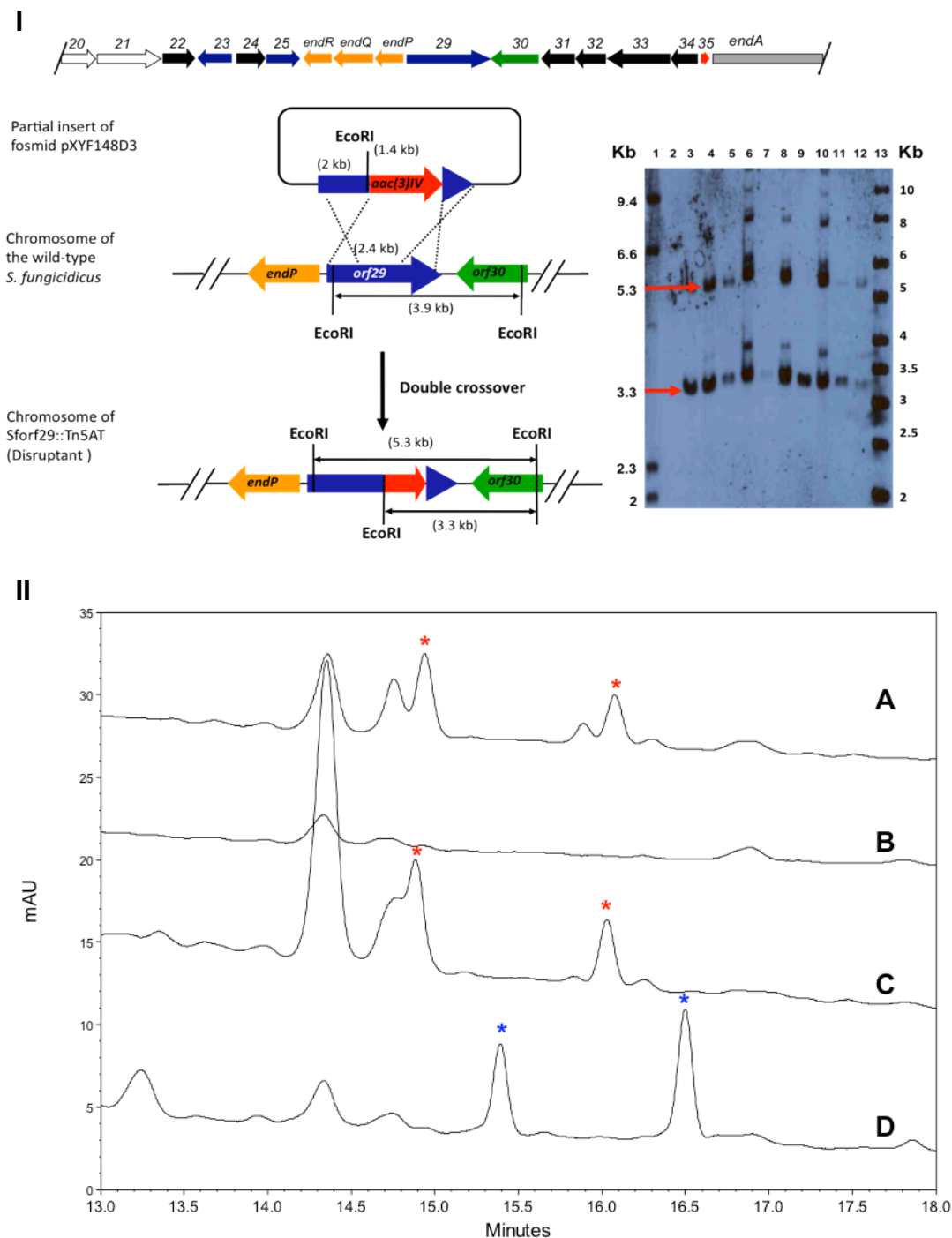


Figure 2.6 I) Insertional disruption of *orf29* using the apramycin resistance gene *aac(3)IV* and Southern blot test confirming disruption. II) HPLC chromatogram of mycelia extracts from: A) SfWT, B) Sfor29::Tn5AT, C) Sfor29::Tn5AT + Hpg and D) Sfor29::Tn5AT + F-Hpg. Enduracidin A and B are indicated by red asterisks and 3'-F₆ enduracidin A and B are indicated with blue asterisks.

strains were designated Sforf29::Tn5AT. HPLC analysis of Sforf29::Tn5AT mycelia extract indicated the *orf29* disruptant was unable to produce enduracidin (Fig. 2.6B). Furthermore, production was restored when cultures of the disruptant were supplemented with Hpg, demonstrating the gene disruption affected Hpg biosynthesis (Fig. 2.6C).

The Sforf29::Tn5AT strain, when supplemented with 3-F-Hpg, produced a new set of enduracidins having HPLC retention times of 15.4 and 16.5 min. (Fig. 2.6D). The isolated peaks, when analyzed via ESI-MS, showed molecular weights of 2427 and 2393 Da for the first peak (15.4 min) and 2407 and 2441 Da in the second peak (16.5 min) (Fig. 2.7). The compounds were likely the previously observed 3'-F₆-Cl₁ enduracidin A and B and the new set of 3'-hexafluoro-deschloroenduracidin A (3'-F₆-Cl₀ end A) and B. Further HPLC purification separated the deschloro and monochloro species allowing for characterization of each compound. NMR spectra for the 3'-hexafluoroenduracidin species show a high similarity to natural enduracidin A in the

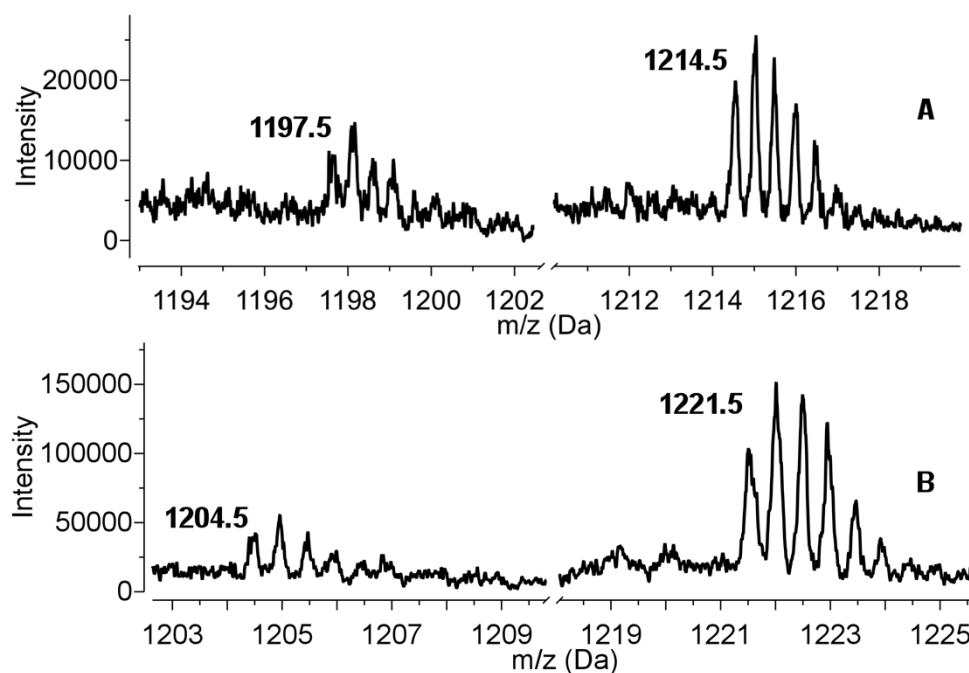


Figure 2.7 ESI positive MS of 3'-F₆ enduracidins A and B showing the [M+2H]²⁺ ions. The *m/z* peak groups at 1197.5 and 1204.5 correspond to deschloro species while the 1214.5 and 1221.5 peak groups are the monochloro species.

upfield region. The aromatic region, however, showed a significant difference in chemical shifts and splitting due to the presence of aryl-bound fluorine (Fig. 2.8A and B). These alterations are also observed in the ^1H - ^1H COSY spectra (Fig. 2.8D and E). The incorporation of six fluorine atoms bound to aryl rings was confirmed by ^{19}F -NMR. The spectrum shows four distinct resonances and two overlapping signals (Fig. 2.8C).

To further examine the ability to biosynthetically incorporate Hpg analogs into enduracidin, 2-F-Hpg and 2,6-F₂-Hpg were prepared using the previously described

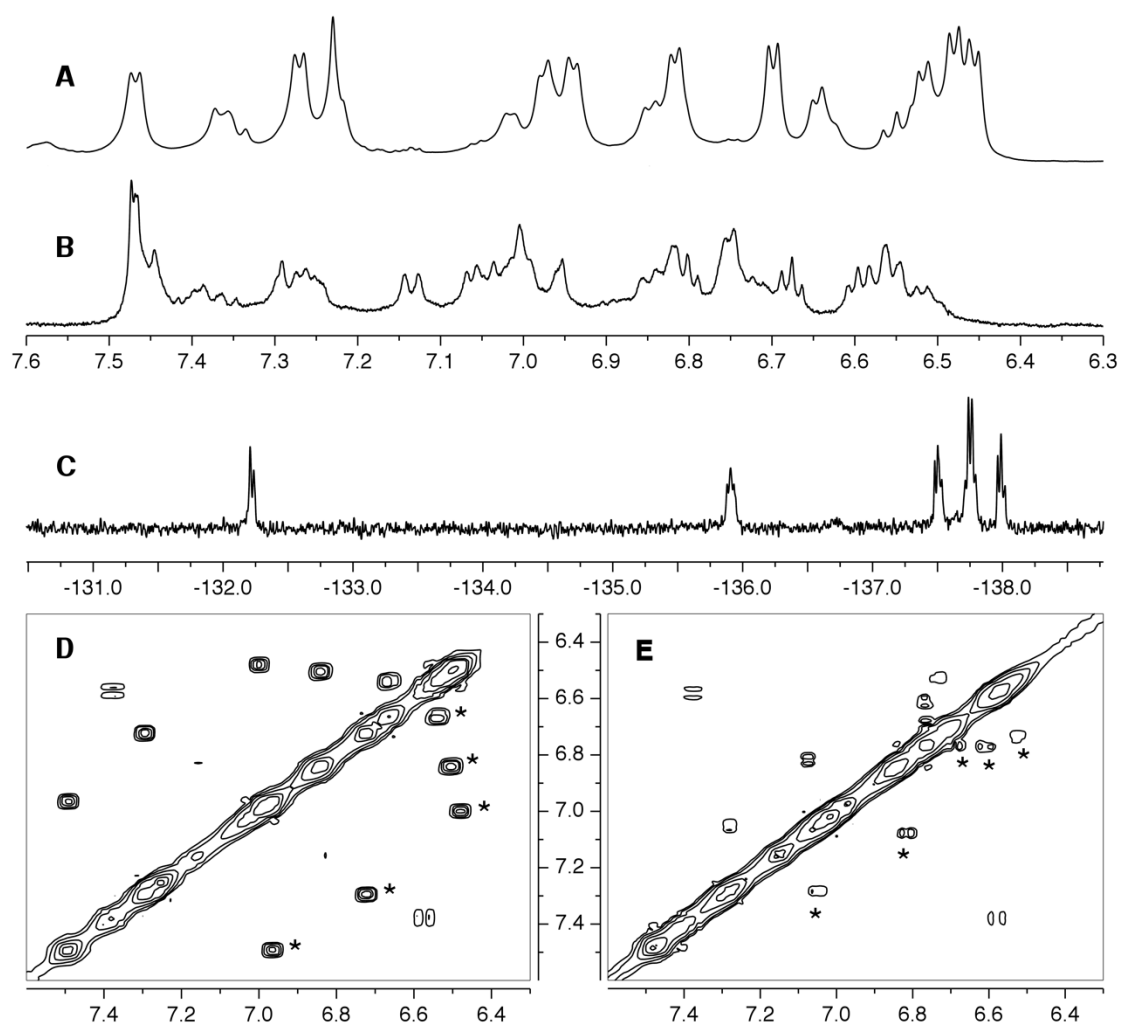


Figure 2.8 A) Enduracidin A ^1H -NMR spectrum B) 3'-F₆-Cl₁-End A ^1H -NMR spectrum C) ^{19}F -NMR spectrum of 3'-F₆-Cl₁ End A D) Aromatic region of COSY spectrum of enduracidin A E) Aromatic region of 3'-F₆-Cl₁ End A. Hpg correlations are indicated with asterisks.

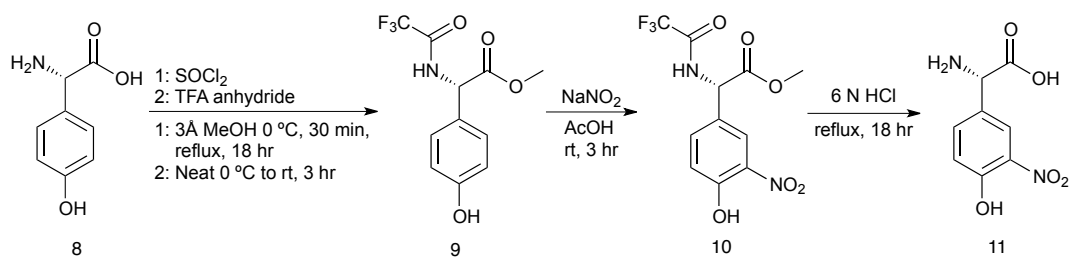


Figure 2.9 Preparation of 3-nitro Hpg via aromatic nitration.

procedure (Fig. 2.4). Additionally, L-3-nitro-Hpg was prepared from L-Hpg via nitration of the trifluoroacetamide protected Hpg methyl ester (9) using AcOH and NaNO_2 .⁸ Deprotection via acid hydrolysis afforded 3-nitro-Hpg in 56% overall yield (Fig. 2.9).

Analysis of mycelial extracts from cultures supplemented with 2,6- F_2 -Hpg and 3-nitro-Hpg indicated no new enduracidin species were produced (Fig. 2.10 B and D). Enduracidin production was restored when cultures were supplemented with both 2,6-

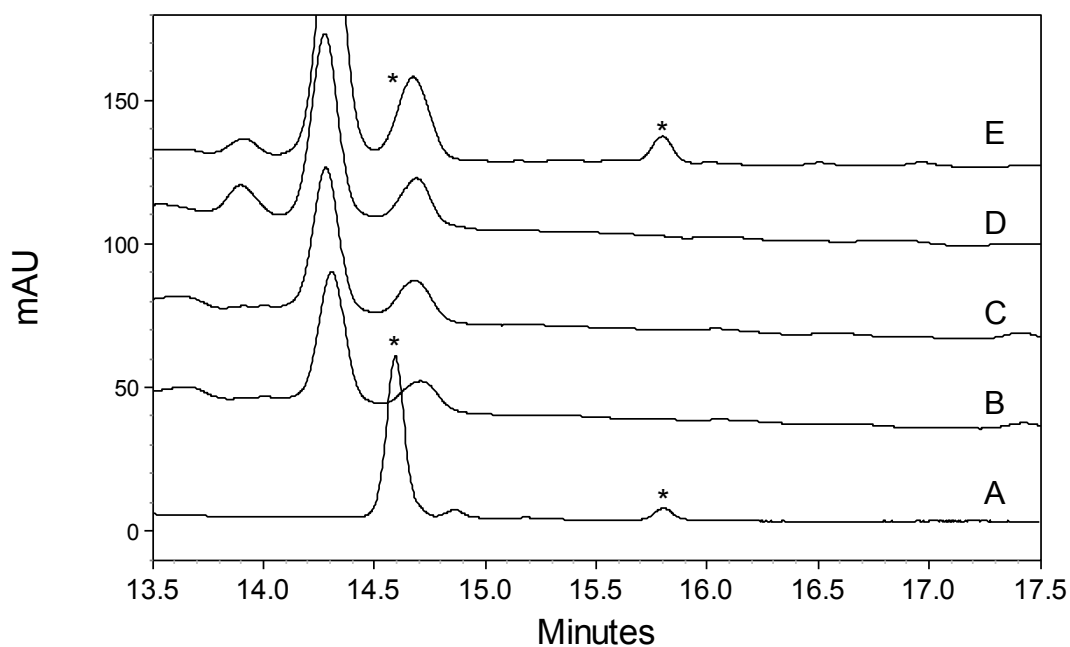
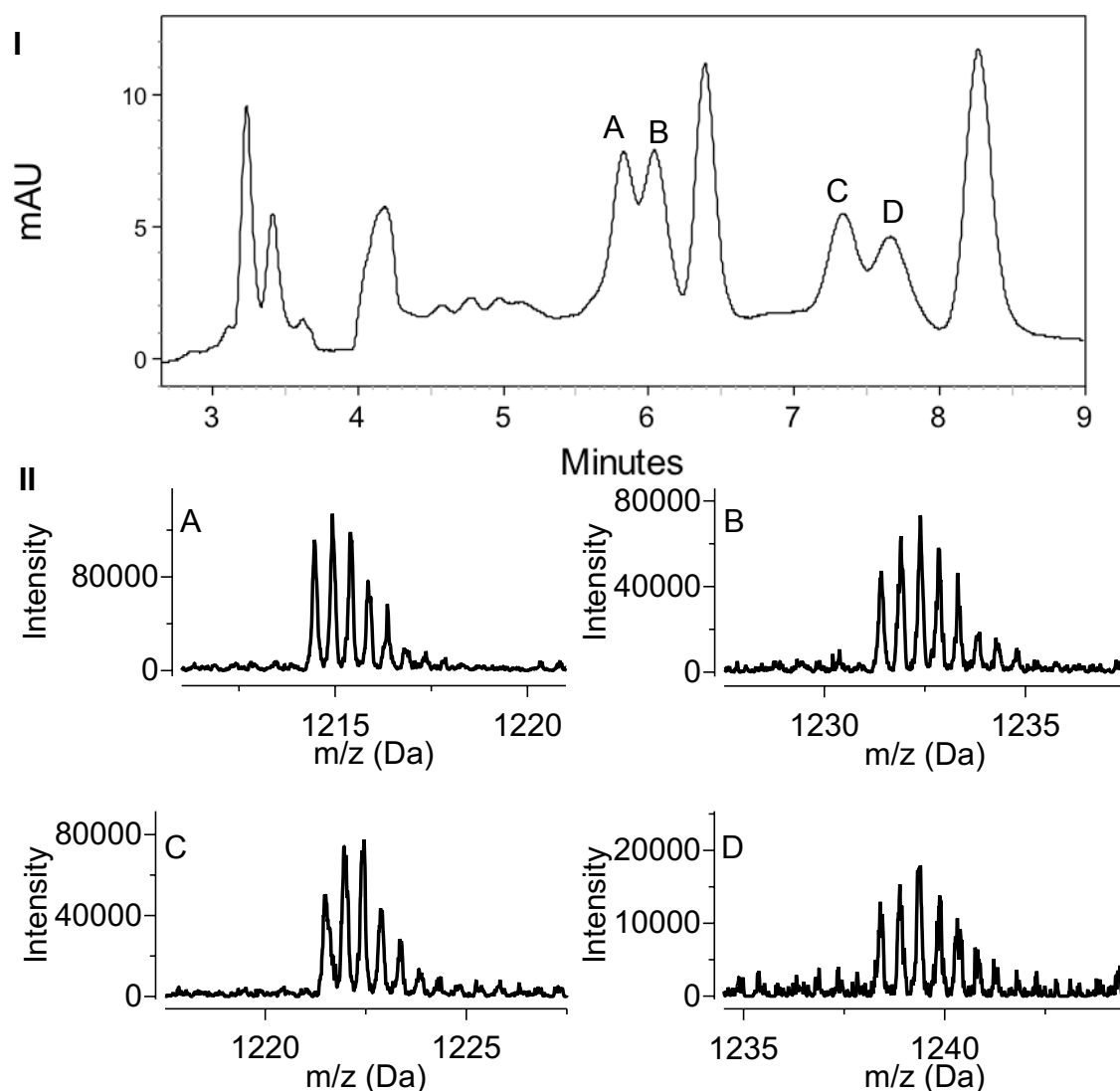


Figure 2.10 HPLC chromatogram showing A) Enduracidin standard, B) Sforf29::Tn5AT + 3-nitro Hpg, C) Sforf29::Tn5AT + 3-nitro Hpg and Hpg D) Sforf29::Tn5AT + 2,6- F_2 Hpg, E) Sforf29::Tn5AT + 2,6- F_2 Hpg and Hpg. Enduracidin A (left asterisk) merges with a common metabolite peak in chromatogram E. Enduracidin B (right asterisk) is also present in chromatogram E.

F₂ Hpg and L-Hpg. HPLC retention time indicated there was no fluorine incorporation. Cultures supplemented with 3-nitro Hpg and L-Hpg were unable to produce enduracidin (Figure 2.10 C). These data suggest that 3-nitro Hpg may be disrupting enduracidin production. However, Sforf29::Tn5AT cultures were observed to produce new enduracidin species when supplemented with 2-F-Hpg (Fig. 2.11 I).



Isolation and MS analysis of the peaks indicated the production of 2'-hexfluoromonochloro (2'-F₆-Cl₁ End) and 2'-hexafluorodichloro enduracidin (2'-F₆-Cl₂ End) analogs (Fig. 2.11 II). To deduce the chlorine position in 2'-F₆-Cl₁ enduracidin the ¹H-¹H COSY spectra of the mono and dichloro species were examined (Figure 2.12 A and B). Due to the overlap of signals the loss or shift of an individual signal corresponding to the addition of a chlorine was not observed. Examination of the ¹⁹F NMR spectra provided some evidence for the location of the chlorine on 2'-F₆-

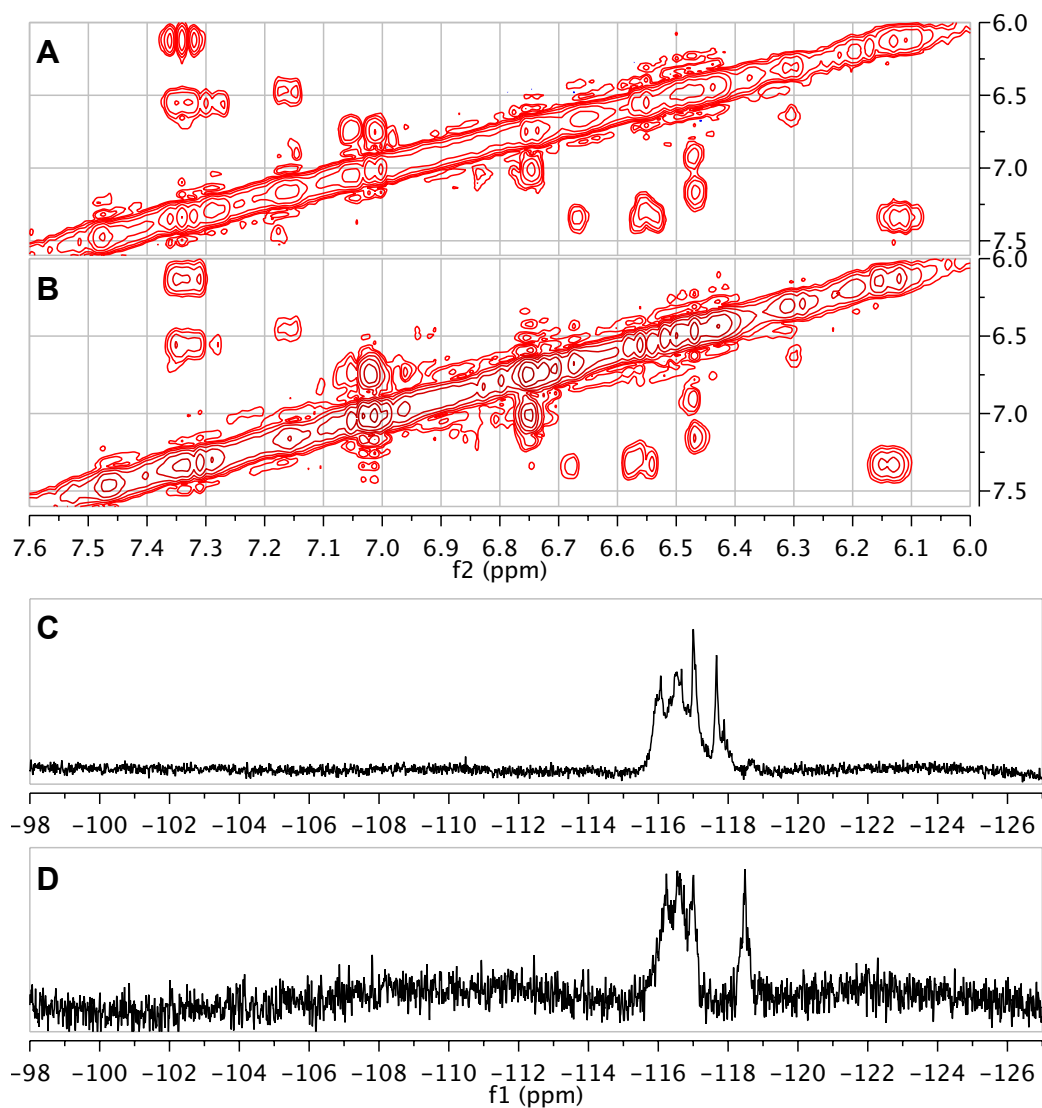


Figure 2.12 COSY spectra for A) 2'-F₆-Cl₁ End B and B) 2'-F₆-Cl₂ End B. Spectra showing the ¹⁹F NMR signals for C) 2'-F₆-Cl₁ End B and D) 2'-F₆-Cl₂ End B.

```

CndH      1 -----MST-RPEVFDLIVIGGGPGGSTLASFVAMRGHRVLLLEREAFPRHQIGESLLPAT 54
           MST + E FD++V+GGGP GSTL++ VAM+GH VLLLE+E FPR+QIGESLLP+T
Orf30     1 MPGGRMSTGQHEEFDVVVGGGPGSGSTLSTLVAMQGHVLLLEKETFPQIGESLLPST 60

CndH     55 VHGICAMLGLTDEMCRAGFPFKRGGTFRWGKEPEPWTFGFT--RHPDDPYGFAYQVERAR 112
           +HGIC +LG+TDE+ AGFP KRGGTFRWG P+PW F F+ P FAYQVER++
Orf30    61 IHGICHLGVTDELAAGFPFKRGGTFRWGA SPKPWNFSEFSVSSKVSQPTSFAFAYQVERSK 120

CndH     113 FDDMLLRNSERKGV D VRERHEVIDVLFEGE-RAVGVRYNTEGVELMAHARFIVDASGNR 171
           FD +LL N+ RKGV VR+ V DV+ + + RA G+RY + +G E AR++VDASGN
Orf30    121 FDKILLDNAARKGVVVRQDRTVTDVDDADGRARGLRYTDPDGT EHEVSARYVVDASGNT 180

CndH     172 TRVSQAVG-ERVYSRFFQNVALYGYFENGKRLPAPRQGNILSAAFQD GWFWYIPLS DTLT 230
           +R+ + VG R YS FF+++AL+GYFENGKR+PAP GNIL AF GWFWYIPLS TLT
Orf30    181 SRIHKRVGGSRTYSDFFKSLALFGYFENGKRPAPYAGNILCVAFGS GWFWYIPLSSTLT 240

CndH     231 SVGAVVSREAAEAIKDGHEAALLRYIDRCPIIKEYLAPATRVTTGDYGEIRIRKDYSCN 290
           SVGAVV RE A ++ E+AL ID CP+IKEYLA ATRVTTG YG++R+RKDYSY +
Orf30    241 SVGAVVRREDAAKVQGDPE SALRGLIDECPMIKEYLADATRVTTGQYQGLRVRKDYSYHH 300

CndH     291 TSFWKNGMALVGDAACFVDPV FSSGVHLATYSALLVARAINTCLAGEMSEQRCFEFERR 350
           T+FW+ GM LVGDAACFVDPV FSSGVHLATYSALL AR++N+ LAG + E+R F+EFE R
Orf30    301 TTFWRPGMVLVGDAACFVDPV FSSGVHLATYSALLAARSLNSVLAGRIDERRAFDEFEAR 360

CndH     351 YRREYGNFYQFLVAFYDMNQD TDSYFWSARKIINTEFRANEAFVRLIAGRNLDEPVFQS 410
           YRREYG FY+FL +FYDM+ D DSYFW+A+K+ + E+FV L+AG S+ D + S
Orf30    361 YRREYGVFEYFLTSEFYDMHVDEDSYFWTAKKVTRSS HAELESFVELVAGMSSTDFDL--S 418

CndH     411 VAKDFFTEREGFGAWFGGLVTSMAKGDGGGLMVGEGATDATESTGFAPENFMQGF TREIT 470
           A+ + A F V MA G + + F + +E +
Orf30    419 DAESSVLR LKQQA EFAFADAVDDMA-----GRQENMAPLFRSSAVSRAM-QEGS 466

CndH     471 ELQHLAMFGEDRGPETPLWSGGLVPSRDGLAWAVESGEDAAG 512
           ++Q A GE G + PL+ GGLV S D + W
Orf30    467 QVQTRAQLGEYAGEDVPLFDGGLVASSDSMFWEPPHS---- 504

```

Figure 2.13 Amino acid alignment of the flavin-dependent halogenases Orf30 from *S. fungicidicus* and CndH from *Chondromyces crocatus*. The sequences share 53% identity and 67% similarity. The residues highlighted in red, including lysine 76, are directly involved with reactivity. Those in blue designate key residues forming the binding pocket. The yellow sequence is a portion of the tunnel allowing hypochlorite to travel to the active site. The conserved GWxWxl sequence is used as a fingerprint to identify this class of halogenase.

Cl₁ End (Fig 2.12 C). Software calculations predict an approximate +7 ppm shift to approximately -109 ppm for the ¹⁹F signal of 2-F-3-Cl Hpg compared to the -116 ppm shift for 2-F-5-Cl-Hpg. With the spectroscopic data providing insufficient evidence, the position of chlorination was examined from a biosynthetic aspect. The enduracidin chlorinase (Orf30) is a flavin dependent halogenase.^{3, 9} Recent crystallization and biochemical work with the tyrosine chlorinase enzyme CndH (53% identity to Orf30) indicated the enzyme functions via hypochlorite formation using a FAD peroxide intermediate. The hypochlorite is then postulated to travel through a tunnel in the

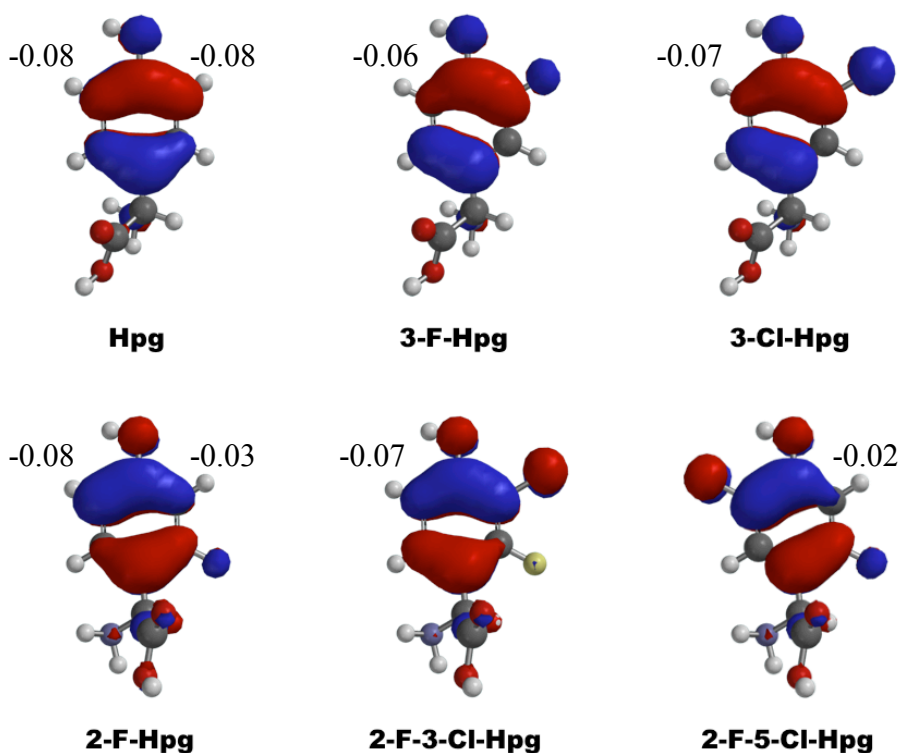


Figure 2.14 HOMO maps of the possible substrates for the halogenase Orf30. The values represent the calculated charge present on the potentially chlorinated carbon.

enzyme and form a chloramine intermediate with lysine 76 within the active site, a conserved feature of this family of enzymes.¹⁰ The key amino acid residues forming the active site, including lysine 76, are conserved in Orf30 (Fig. 2.13).¹¹

To begin understanding the influence of ring substitution on reactivity, charge localization calculations were made. Reduced partial negative charge was predicted on C-3 of 2-F-Hpg compared to C-5 of 3-F-Hpg and 3-Cl-Hpg (Fig. 2.14). The presence of fluorine in the three position of Hpg may prevent halogenation as evidenced by the reduced charge and production of 3-F₆-Cl₀ End. HOMO modeling of 2-F-Hpg and 2-F-5-Cl-Hpg showed that the reactive orbital is shifted away from C-3 in both cases. C-5 of 2-F-Hpg, however, is calculated to have a minimal reduction in partial negative charge and increased HOMO density. The reduced partial charge and HOMO density on the 3-carbon, coupled with the lack of ¹⁹F NMR shifts near -109 ppm for the

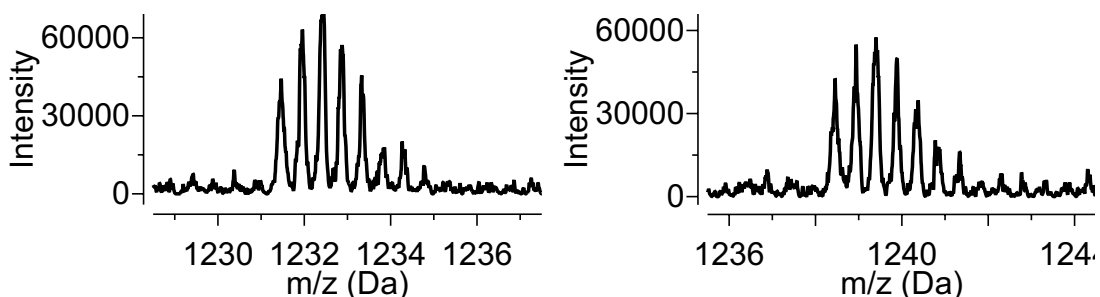


Figure 2.15 ESI positive mass spectra of isolated unknown enduracidins from 3-F Hpg experiments showing 3'-F₆-Cl₂ enduracidin A ($m/z = 1231.5$) and B ($m/z = 1238.5$).

isolated compound, suggests that chlorination occurs at the 5' position of residue-13. Interestingly, the ¹⁹F NMR spectrum for 2'-F₆-Cl₂-enduracidin also lacks a fluorine peak with a shift near the -109 ppm region (Fig 2.12D). MS/MS analysis of the dichloro species has been unsuccessful. From previous work enduracidin was successfully halogenated on Hpg-11.⁴ It is possible that the halogenation occurs on residue-13 and Hpg-11 both in the 5'-position. The ability of Orf30 to halogenate other Hpg residues was noted by the observation of a small amount of 3'-F₆-Cl₂ Enduracidins A and B by MS (Fig. 2.15).

Other Hpg analogs were pursued for investigation. After the successful incorporation of 3-F Hpg into enduracidin in the wild-type organism, the production of 3-Cl Hpg was undertaken using the same synthetic scheme (Fig. 2.4). The desired product was not obtained, however, due to the dehalogenation reaction which occurred during the reductive cleavage of the benzyl protecting group. To explore the incorporation of Cl-Hpg, cultures of *S. fungicidicus* were supplemented with 3-Cl Tyr, however the compound proved to be toxic. Further investigations with chlorine substitutions were not pursued.

The substitution of a pyr group for the phenyl group was undertaken starting from 2-Me, 5-OBn pyridine (Fig. 2.16 A). The production of the aldehyde and the aminonitrile proved successful using standard procedures.¹³ However, hydrolysis of the nitrile to the free carboxylic acid resulted in decarboxylation when exposed to neutral pH (Fig. 2.16 B). As the compound proved unstable and shifting the pyridinyl

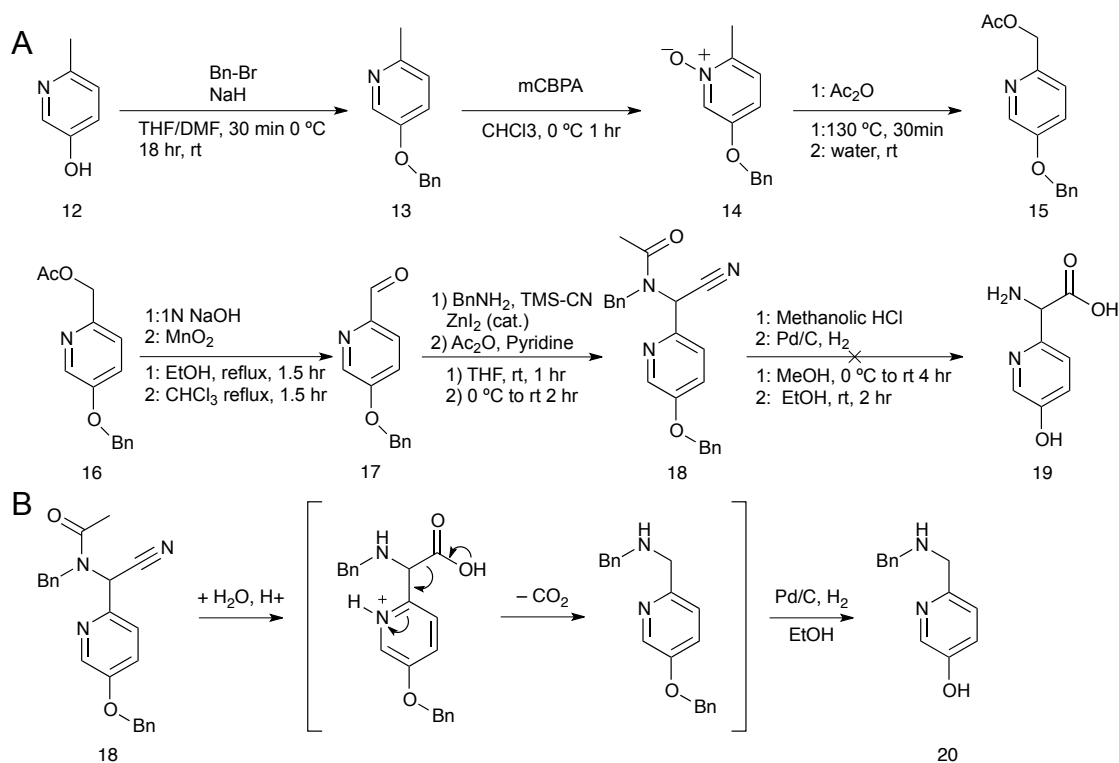


Figure 2.16 A) Synthesis of hydroxypyridinylglycine starting from 3-hydroxy-6-methylpyridine to the aminonitrile. B) Degradation of hydrolyzed amino nitrile results in the production of N-benzyl-5-benzyloxypyridinyl-methylamine.

nitrogen to the 3-position would potentially result in the formation of a reactive pyridinyl N-chloride species by the halogenase enzyme the concept was not pursued further.

As the structural alterations from the introduction of fluorine into enduracidin may affect its conformation and thereby its bioactivity, a bioassay against *S. aureus* was performed; comparing the hexafluoroenduracidins to enduracidins A, B and ampicillin (Fig 2.17 A). The 3'-F₆ enduracidins all exhibited MIC values of 0.4 μ M, equivalent to enduracidins A and B (Fig 2.17 B). The 2'-F₆ enduracidins, except 2'-F₆-Cl₁ End B (0.4 μ M), had a MIC of 0.8 μ M (Fig 2.17 C). The bioactivity was only reduced by two-fold in the 2'-F₆ analogs. Compared to the bioactivity of ampicillin (6.4 μ M) in the same assay the reduction of bioactivity is minimal. The data indicate that the potency of enduracidin is slightly negatively affected by fluorination on the 2'

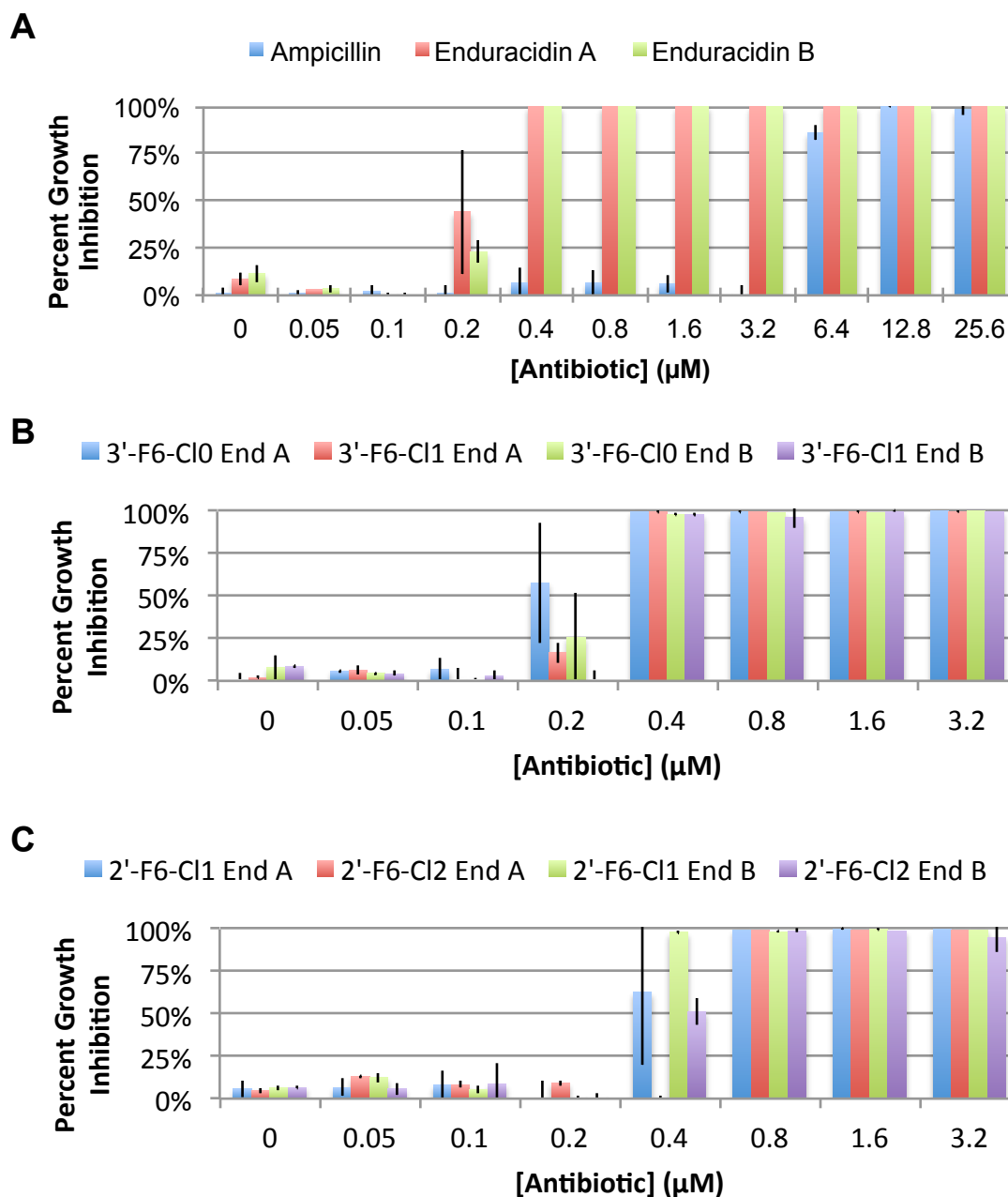


Figure 2.17 Growth inhibition assay against *S. aureus* for A) enduracidins A, B and Ampicillin, B) 3'-F₆ enduracidins and C) 2'-F₆ enduracidins.

carbon. The overall affect of fluorine on enduracidin appears to be minimal in terms of bioactivity. The size of the fluorine atom appears to minimally affect the conformation or binding to the bacterial target. Interestingly, placement in the 2' position affected bioactivity more. As fluorine at the 2' position has less effect on the pK_a of the

phenolic proton the reduction in activity is likely due to a hindered rotation/positioning of the Hpgs in the tertiary peptide structure. The effects of the decreased phenolic proton pK_a on the 3'-fluoro species appears to have had minimal or no effect on bioactivity. The intramolecular hydrogen bond of Hpg-3 also appears to have minimal effect in modifying the bioactive structure of enduracidin.

There are limitations to the mutasynthetic modification of enduracidin. Specifically, the 2,6-F₂-Hpg did not incorporate and the enduracidin production in the 2-F-Hpg supplemented cultures was highly reduced, to around 100 $\mu\text{g/L}$ total 2'-F₆ enduracidin, compared to a typical range of 5 to 50 mg/L of enduracidin production. The 3-F-Hpg supplementation led to better fluoroenduracidin production (1 mg/L). As production yields were low, sufficient quantities of fluoroenduracidin to analyze solubility or to test in live animal studies to evaluate the pharmacokinetics were not available. The results here, however, do indicate a that mutasynthetic approach to altering enduracidin is a viable means for producing new bioactive analogs.

Experimental Procedures

Bacterial Strains, media and culture conditions

The wild type *Streptomyces fungicidicus* strain (ATCC21013) and *S. aureus* (ATCC 29213) were purchased from ATCC. EPI300™-T1^R (Epicentre) was used as host for fosmids and *E. coli-Streptomyces* shuttle vectors. The plasmid pIJ773 was provided by Professor Keith Chater (JIC, Norwich, England). ISP2 (Difco), ISP4 (Difco) and tryptic soy broth (Difco) and other media components were purchased from VWR. For initial fluorine incorporation studies DL-3-F-tyrosine was purchased from Sigma. Media and culture conditions for *S. fungicidicus* were as previously described.¹²

Extraction method

Production cultures were centrifuged at $1500 \times g$ for 30 min. The supernatant was decanted and the pellet extracted with 70% *aq.* methanol overnight. Insoluble material was removed via centrifugation and the extract was decanted. The solvent was removed under reduced pressure and the solids were redissolved in minimal 70% *aq.* methanol for analysis or purification.

Construction of the Tn5AT cassette and fosmid pXYF148D3

Both *oriT* and *aaC3(IV)* (AT) were excised from plasmid pIJ773 as a *Xba*I fragment and then cloned into the transposon donor plasmid pMOD™-2(MCS) (Epicentre), previously linearized with *Xba*I. The resulting plasmids pXYTn5ATa and pXYTn5ATb only differ in the orientation of the *Xba*I fragment and were used to prepare the Tn5AT cassette by digestion with *Pvu*II. Transposon insertional mutation of fosmid pXYF148³ was performed at 37 °C for 2 hrs after mixing 10 μL (0.5 μg) fosmid template DNA, 2 μL (20 ng) Tn5AT cassette DNA, 2 μL 10 x reaction buffer, 1 μL Tn5 transposase and 5 μL sterile water. Transformation of *E. coli* competent cells EPI300™-T1^R (Epicentre) with the transposon reaction mixture was performed by

electroporation. Mutagenized fosmids were selected on LB agar plates supplemented with 100 µg/ml apramycin. Plates were incubated overnight at 37 °C and surviving colonies were randomly picked and grown in LB liquid culture with addition of apramycin (185 µM). The mutagenized fosmid DNA from these colonies and control fosmid pXYF148 were digested with *Hind*III and analyzed by electrophoresis on 1% agarose gels. Colonies carrying mutagenized fosmids with a single transposon insertion were randomly selected and grown in liquid culture to permit fosmid isolation and identification of the disrupted gene. Screening was conducted by sequence analysis using the primer (5'- AAGGAGAAGAGCCTTCAGAAGGAA-3'). Fosmid pXYF148D3 was found to have Tn5AT inserted into the *hpgT* homolog region of *orf29*, at nucleotide position 41407 (GenBank Accession No. DQ403252).

Disruption of *orf29* in *S. fungicidicus* ATCC21013

The fosmid pXYF148D3 was then introduced into wild-type *S. fungicidicus* by intergeneric conjugation.¹⁴ Exconjugants surviving apramycin selection were passed through two rounds of sporulation without antibiotic selection to produce the stable disruptant strain via double crossover homologous recombination. The resulting spores were diluted and plated on ISP2 plate supplemented with apramycin (92 µM) to obtain single colonies, which were used to inoculate the TSB cultures for preparation of the genomic DNA. The transposon insertional mutant *Sforf29::Tn5AT* was confirmed by Southern blot analysis of the chromosomal DNA and evidence of the abolishment of the enduracin production in mycelia extracts.

Southern blot analysis

Genomic DNA from wild type and disruptant strains was prepared as described previously.³ Restricted genomic DNA was separated by electrophoresis in 0.8% agarose gel and transferred onto positively charged nylon membrane (Roche). The DNA probe was prepared using digoxigenin-labeled dUTP and hybridization was revealed using a digoxigenin-DNA detection kit (Roche).

Complementation and Fluorine Incorporation Studies

Seed cultures (*S. fungicidicus* or Sforf29::Tn5AT) were incubated in 4 mL TSB broth in 15 mL culture tube (VWR) shaking at a 70° angle, 200 rpm for 24 hrs at 28 °C. Production cultures of complex media (60 mL) in Erlenmeyer flasks (250 mL) equipped with a spring baffle were inoculated with 2 mL of seed culture. After shaking at 220 rpm at 28 °C for 72 hrs. production cultures were supplemented with Hpg (24 mg in 2 mL water), F-Tyr (48 mg in 3 mL water) or substituted Hpg (48 mg in 3 mL water) three times at 24 hrs intervals. All supplementation samples required acidification with 0.1 N HCl to dissolve and were sterilized via syringe filtration (0.45 µm, VWR). Cultures were harvested after 11 days.

HPLC and MS analysis

HPLC analysis was performed using a Shimadzu (Kyoto, Japan) CBM-20A instrument equipped with an autosampler and a PDA detector scanning from 210 to 330 nm. All samples were filtered through a 0.45 µm syringe filter prior to injection. Analysis was performed using a Phenomenex Gemini C18 column (4.6 × 150 mm, 5 micron) with a 20 min. linear gradient from 10% acetonitrile in water with 0.1% TFA to 40% acetonitrile at a flow rate of 1.5 mL/min. Initial purification was performed using a Phenomenex Gemini C18 column (10 × 150 mm, 5 µm) with a 20 min. linear gradient from 10% acetonitrile in water with 0.1% TFA to 40% acetonitrile at a flow rate of 3 mL/min. Final purification was performed using a Phenomenex Polar-RP column (10 × 250 mm, 4 µm) with a linear gradient from 32% acetonitrile in water with 0.1% TFA to 40% acetonitrile over 17 min. at 3 mL/min. flow rate. Mass spectrometric analysis was performed using a Waters/MicroMass LCT Classic ESI spectrometer in positive ion mode, and a Thermo Finnigan LCQ Advantage instrument in ESI+ mode.

NMR analysis and computational chemistry

NMR spectra were recorded using a Bruker 300 MHz instrument for synthetic compounds (^1H -300 MHz, ^{13}C -75 MHz). Proton NMR experiments on enduracidin were performed using a Bruker Avance III 700 MHz instrument (^1H -700 MHz, ^{13}C -175 MHz). Enduracidin and fluorinated samples were dissolved in a mixture of 2:5 D_2O :Methanol- d_4 . The proton shifts are referenced to methanol- d_4 (3.31 ppm). Fluorine NMR spectra were recorded using a Bruker DPX-400 instrument (376 MHz) and a Bruker AvanceIII 500 instrument (471 MHz). Analysis of spectra was performed using Topspin ver. 1.3 and 3.1 (Bruker) and MestReNova ver. 8.0.2-11021 (Mestrelab Research).

Computational predictions and HOMO modeling was performed using Spartan 10 ver. 1.0.1 (Wavefunction, Inc. Irvine, CA USA). Charge calculations were performed using MarvinSketch ver. 5.10.3 (Chemaxon, Ltd. Cambridge, MA USA).

Amino acid sequence alignment and analysis was performed using Geneious Pro 5.6.5 (Biomatters, Ltd. Auckland, NZ).

Bioactivity assay

A culture of *S. aureus* was grown over night at 37 °C on tryptic soy agar. A single pure colony was used to inoculate a 5 mL TSB culture which was shaken at 150 rpm for 4 hrs at 37 °C. Antibiotic samples were prepared in 50% *aq.* MeOH and 20 μL of each dilution was loaded into wells on a 96-well Microtest plate (Falcon). To each test well was added 80 μL of sterile TSB followed by 100 μL of $\sim 5 \times 10^5$ cells per mL of *S. aureus* in TSB. Each antibiotic was tested concurrently three times at each concentration. Initial absorbance readings at 600 nm were recorded and the plates were then sealed with parafilm and incubated at 37 °C for 16 hrs. Final absorbance readings were taken and percent growth calculated using the untreated well values as the reference. The percent inhibition was then calculated (100% – percent growth), the average was taken and standard deviations were calculated. MICs were determined as the lowest antibiotic concentration that exhibited >95% growth inhibition.

Preparation of fluoro-hydroxyphenylglycines

Reagents were purchased from Sigma Aldrich or Alpha Aesar and used without further purification. Hydroxyphenolglycing was purchased as ACS grade in the L form at greater than 98% purity. All other reagents were purchased as ACS reagent grade products. Water was deionized (18 M Ω) using a Barnstead B-Pure filtration system. Acetonitrile and Methanol were purchased as HPLC grade solvents. Anhydrous methanol was purchased and stored under Ar. Triethylamine was purchased as ACS reagent grade and passed through a column of basic alumina (50-200 μ m) prior to use. Other solvents were purchased and used without further purification.

***N*-benzyl-3-fluoro-4-methoxy-1-aminonitrile-benzene (4a):** To a stirred solution of aldehyde **3a** (480 mg, 3.11 mmol) in acetonitrile (15 mL) was added benzylamine (410 μ L, 3.7 mmol, 1.2 eq.), TMS-cyanide (400 μ L, 3.11 mmol, 1 eq.) and cyanuric chloride (57 mg, 0.31 mmol, 0.1 eq.). The reaction was stirred for 5 hrs at ambient temperature and stopped by removing the solvent under reduced pressure. The solid was dissolved in EtOAc (100 mL) and washed with water (50 mL) and brine (50 mL). The organics were dried over anhydrous Na₂SO₄ and the solvent removed under reduced pressure. The resulting solid was purified using flash chromatography SiO₂ 1:3 EtOAc:Hexanes yielding **4a** (650 mg, 2.4 mmol, 77% yield) as a yellow amorphous solid. ¹H NMR (300 MHz, CDCl₃) δ 7.63 – 7.10 (m, 7H), 6.97 (t, *J* = 8.6 Hz, 1H), 4.69 (s, 1H), 4.18 – 3.61 (m, 5H), 1.86 (s, 1H); ¹³C NMR (75 MHz, CDCl₃) δ 152.40 (d, *J* = 247.6 Hz), 148.25 (d, *J* = 10.6 Hz), 138.00, 128.68, 128.39, 127.71, 127.61, 127.53, 123.14, 123.09, 118.49, 115.43, 115.16, 113.45, 113.42, 56.33, 52.55, 52.53, 51.14; LRMS ESI (+) *m/z* = 271.1 [M+H]⁺.

***N*-benzyl-2-fluoro-4-methoxy-1-aminonitrile-benzene (4b):** Yield: (772 mg, 3.24 mmol, 88%) as yellow amorphous solid. ¹H NMR (300 MHz, CDCl₃) δ 7.55 – 7.18

(m, 5H), 7.17 – 7.03 (m, 2H), 6.67 (dd, $J = 12.0, 2.5$ Hz, 1H), 4.85 (bs, 1H), 4.81 (s, 1H), 7.18, 4.00 (dd, $J = 37.7, 14.0$ Hz, 2H), 3.81 (s, 3H); ^{13}C NMR (75 MHz, CDCl_3) δ 161.73 (d, $J = 11.2$ Hz), 160.93 (d, $J = 249.0$ Hz), 139.09, 129.53 (d, $J = 5.0$ Hz), 128.61, 128.38, 127.65, 118.30, 114.49 (d, $J = 14.2$ Hz), 110.28 (d, $J = 3.2$ Hz), 102.29 (d, $J = 24.7$ Hz), 55.72, 51.44, 47.53 (d, $J = 3.0$ Hz); LRMS, ESI (+) $m/z = 271.1$ $[\text{M}+\text{H}]^+$.

***N*-benzyl-2,6-difluoro-4-methoxy-1-aminonitrile-benzene (4c):** Yield: (965 mg, 5.81 mmol, 58%) as yellow amorphous solid. ^1H NMR (300 MHz, CDCl_3) δ 7.54 – 7.18 (m, 5H), 6.50 (dd, $J = 9.7, 2.2$ Hz, 2H), 5.67 (s, 1H), 4.87 (s, 1H), 4.15 – 3.88 (m, 2H), 3.79 (s, 3H); ^{13}C NMR (75 MHz, CDCl_3) δ 161.88 (dd, $J = 14.3$ Hz), 161.25 (dd, $J = 248.5, 10.3$ Hz), 137.49, 128.69, 128.42, 127.79, 117.58, 103.95 (dd, $J = 18.6$ Hz), 98.55 (dd, $J = 26.3, 2.8$ Hz), 56.02, 51.67, 42.16 (dd, $J = 4.0$ Hz); LRMS, ESI (+) $m/z = 289.1$ $[\text{M}+\text{H}]^+$.

***N*-benzyl-3-chloro-4-methoxy-1-aminonitrile-benzene (4d):** Yield: (170 mg, 0.59 mmol, 51%) white amorphous solid. ^1H NMR (300 MHz, CDCl_3) δ 7.55 (d, $J = 2.4$ Hz, 1H), 7.49 – 7.22 (m, 6H), 6.93 (d, $J = 8.5$ Hz, 1H), 4.67 (s, 1H), 4.11 – 3.78 (m, 5H), 1.87 (s, 1H); ^{13}C NMR (75 MHz, CDCl_3) δ 155.47, 138.00, 129.18, 128.66, 128.38, 127.80, 127.68, 126.70, 122.98, 118.49, 112.10, 56.25, 52.42, 51.14; LRMS, ESI (+) $m/z = 287.1$.

***N*-benzyl-3-fluoro-4-methoxy-phenylglycine (5a):** A solution of 90% formic acid (410 μL , 9.8 mmol, 9.5 eq) and acetic anhydride (950 μL , 9.8 mmol, 9.5 eq) was stirred at 60 $^\circ\text{C}$ for 1 hr. The resultant solution of acetic-formic mixed anhydride was cooled in an ice bath and added to a cooled flask of aminonitrile **4a** (280 mg, 1.0 mmol). The reaction was stirred at 0 $^\circ\text{C}$ for 15 min. then at ambient temperature for 1 hr. To the reaction was added, slowly, concentrated HCl (2.5 mL). The reaction was

heated at 65 °C for 2 hrs then refluxed for 1 hr. The reaction was then allowed to cool and the solvent was removed under reduced pressure. The solid was triturated with DCM and the insolubles were collected by filtration as a white powder. The product was used in the next reaction without further purification. LRMS, ESI (+) m/z 290.1 [M+H]⁺.

***N*-benzyl-2-fluoro-4-methoxy-phenylglycine (5b)**: Grey powder; LRMS, ESI (+) m/z = 290.1.

***N*-benzyl-2,6-difluoro-4-methoxy-phenylglycine (5c)**: Grey powder; LRMS, ESI (+) m/z = 308.1.

***N*-benzyl-3-chloro-4-methoxy-phenylglycine (5d)**: Grey powder; LRMS, ESI (+) m/z = 306.1.

***N*-benzyl-3-fluoro-4-hydroxy-phenylglycine (6a)**: To a flask containing *N*-benzyl-3-fluoro-4-methoxy-phenylglycine **5a** (250 mg) was added conc. HBr (9 mL). The solution was refluxed for 3 hrs. The solvent was removed under reduced pressure. The solid product was dissolved in minimal 0.1 N HCl and the product was precipitated by adjusting the pH to 6.5 with 0.1 N NaOH. The solid was washed with MeOH and dried *in vacuo* yielding a white powder (200 mg, 0.73 mmol, 73% yield from **4a**). ¹H NMR (300 MHz, DMSO) δ 10.15 (bs, 1H), 8.90 (t, J = 13.6 Hz, 1H), 7.81 – 6.80 (m, 8H), 4.98 (m, 1H), 3.97 (dd, J = 51.8, 12.7 Hz, 2H); ¹³C NMR (75 MHz, DMSO) δ 170.00, 151.09 (d, J = 242.3 Hz), 151.01 (d, J = 241.9 Hz), 146.86 (d, J = 11.7 Hz), 146.38 (d, J = 11.0 Hz), 131.87, 130.81, 129.43, 128.93, 126.34 (d, J = 3.0 Hz), 125.20 (d, J = 2.8 Hz), 118.56 (d, J = 2.7 Hz), 118.40 (d, J = 3.1 Hz), 117.32 (d, J = 19.5 Hz), 116.57 (d, J = 19.7 Hz), 55.01, 49.21. LRMS, ESI (+) m/z = 276.1 [M+H]⁺.

***N*-benzyl-2-fluoro-4-hydroxy-phenylglycine (6b):** Yield: (450 mg, 1.7 mmol, 57% yield from **4b**). ^1H NMR (300 MHz, D_2O) δ 7.57 – 7.49 (m, 3H), 7.49 – 7.44 (m, 2H), 7.37 – 7.31 (m, 1H), 6.88 – 6.79 (m, 2H), 5.21 (d, $J = 1.1$ Hz, 1H), 4.40 – 4.20 (m, 2H); ^{13}C NMR (75 MHz, D_2O) δ 170.24, 161.45 (d, $J = 247.1$ Hz), 159.48 (d, $J = 11.9$ Hz), 131.43 (d, $J = 4.6$ Hz), 130.09, 129.89, 129.69, 129.20, 112.60, 109.16 (d, $J = 14.8$ Hz), 103.61 (d, $J = 24.2$ Hz), 57.19, 49.73. LRMS, ESI (+) $m/z = 276.1$ [$\text{M}+\text{H}$] $^+$.

***N*-benzyl-2,6-difluoro-4-hydroxy-phenylglycine (6c):** The difluoro compound could not be purified by the above method. Completion of the reaction was confirmed by LRMS with the appearance of ESI (+) $m/z = 294.1$ [$\text{M}+\text{H}$] $^+$ and disappearance of the $m/z = 308.1$ ion. The crude product was taken on to the next reaction.

***N*-benzyl-3-chloro-4-hydroxy-phenylglycine (6d):** Yield: (103 mg, 0.35 mmol, 59% yield from **4d**). ^1H NMR (300 MHz, $\text{DMSO}-d_6$) δ 10.86 (bs, 1H), 7.57 (d, $J = 2.0$ Hz, 1H), 7.54 – 7.36 (m, 6H), 7.33 (dd, $J = 8.6, 2.1$ Hz, 1H), 7.14 (d, $J = 8.3$ Hz, 1H), 5.00 (s, 1H), 4.36 – 3.67 (m, 2H); ^{13}C NMR (75 MHz, DMSO) δ 168.79, 154.45, 131.42, 130.51, 130.29, 128.99, 128.93, 128.45, 122.33, 119.90, 116.94, 61.28, 48.95; LRMS, ESI (+) $m/z = 292.1$ [$\text{M}+\text{H}$] $^+$.

3-fluoro-4-hydroxy-phenylglycine (7a): To a flask containing *N*-benzyl-3-F-4-hydroxyphenylglycine **6a** (200 mg, 0.73 mmol) dissolved in water (2 mL) and acetic acid (4 mL) was added Pd/C (15 mg, 0.01 mmol, 0.01 eq). The flask was flushed with H_2 three times and stirred overnight at ambient temperature. The reaction mixture was filtered through celite. The solvent of the collected filtrate was removed under reduced pressure. The crude product was crystallized from water heated and pH adjusted to 6.5 yielding **7a** as grey plates (75 mg, 71 μmol , 56% yield). ^1H NMR (300 MHz, D_2O) δ 7.48 – 7.36 (m, 1H), 7.29 (d, $J = 2.0$ Hz, 1H), 7.25 (d, $J = 8.4$ Hz, 1H), 5.22 (s, 1H); ^{13}C NMR (75 MHz, D_2O) δ 171.07, 151.42 (d, $J = 242.0$ Hz), 145.11 (d, $J = 12.7$ Hz),

125.07 (d, $J = 3.4$ Hz), 124.29, 124.21, 118.78 (d, $J = 3.0$ Hz), 116.28 (d, $J = 20.0$ Hz), 56.18; LRMS, ESI (+) $m/z = 186.0$ [M+H]⁺.

2-fluoro-4-hydroxy-phenylglycine (7b): Yield: (200 mg, 1.1 mmol, 62%). ¹H NMR (300 MHz, D₂O) δ 7.32 (t, $J = 8.8$ Hz, 1H), 6.95 – 6.57 (m, 2H), 5.27 (s, 1H); ¹³C NMR (75 MHz, D₂O) δ 170.73, 161.18 (d, $J = 246.7$ Hz), 159.17 (d, $J = 12.2$ Hz), 131.22 (d, $J = 4.7$ Hz), 112.41 (d, $J = 2.9$ Hz), 110.57 (d, $J = 14.8$ Hz), 103.57 (d, $J = 23.9$ Hz), 51.06 (d, $J = 2.5$ Hz); LRMS, EST (+) $m/z = 186.0$ [M+H]⁺.

2,6-difluoro-4-hydroxy-phenylglycine (7c): Yield: (427 mg, 2.1 mmol, 36% from 6c). ¹H NMR (300 MHz, D₂O) δ 6.25 (d, $J = 10.9$ Hz, 2H), 5.12 (s, 1H); ¹³C NMR (75 MHz, D₂O) δ 169.52, 161.17 (dd, $J = 247.5, 10.2$ Hz), 159.85 (dd, $J = 15.2$ Hz), 99.83 (dd, $J = 25.1, 2.4$ Hz), 99.26 (dd, $J = 19.0$ Hz), 45.67; LRMS, ESI (+) $m/z = 204.0$ [M+H]⁺.

3-chloro-4-hydroxy-phenylglycine (7d): The reaction was not successful. The reducing conditions caused the removal of the chlorine group and Hpg was the only observed product.

N-Trifluoroacetyl-4-hydroxy-phenylglycine-methyl ester (9): To a solution of L-Hpg **8** (3.0 g, 18 mmol) in anhydrous MeOH (150 mL) under Ar and cooled in an ice bath was added thionyl chloride (2.61 mL, 36 mmol, 2 eq.) over 20 min. The reaction was then refluxed overnight. The reaction was allowed to cool and the solvent removed *in vacuo*. The crude product was then cooled in an ice bath and treated with trifluoroacetic anhydride (15.1 mL, 110 mmol, 6 eq) and allowed to warm to ambient temperature. After stirring for 3 hrs the reaction was diluted with EtOAc (100 mL) and quenched with saturated NaHCO₃ (500 mL). The organic layer was separated and dried with Na₂SO₄ then removed *in vacuo* yielding **9** as a white amorphous solid (4.98

g, 18.0 mmol, quantitative). ^1H NMR (300 MHz, CDCl_3) δ 7.34 (d, $J = 7.0$ Hz, 1H), 7.22 (d, $J = 8.6$ Hz, 2H), 6.81 (d, $J = 8.6$ Hz, 2H), 5.48 (d, $J = 6.9$ Hz, 1H), 5.20 (s, 1H), 3.78 (s, 3H); ^{13}C NMR (75 MHz, CDCl_3) δ 170.35, 156.68 (q, $J = 38.5$ Hz), 156.35, 128.90, 126.86, 116.25, 118.36-112.41 (m), 56.17, 53.51; LRMS, ESI (-) $m/z = 276.0$ [M-H] $^-$.

***N*-Trifluoroacetyl-3-nitro-4-hydroxy-phenylglycine-methyl ester (10):** To a stirred solution of **9** (1.0 g, 3.6 mmol) in AcOH (100 mL) under Ar was added NaNO_2 (500 mg, 7.22 mmol, 2 eq.). The reaction stirred for 3 hrs. The solvent was removed under reduced pressure and the crude product was dissolved in MeOH and purified via HPLC; Phenomenex Polar RP column (10 x 250mm, 4 μm) 20 min. gradient from 10% to 70% MeOH in water with a flow rate of 3 mL/min. yielding **10** as a white amorphous solid (812 mg, 2.5 mmol, 70%). ^1H NMR (300 MHz, CDCl_3) δ 10.61 (s, 1H), 8.12 (d, $J = 1.8$ Hz, 1H), 7.59 (dd, $J = 8.8, 2.3$ Hz, 1H), 7.55 (bs, 1H), 7.21 (d, $J = 8.7$ Hz, 1H), 5.52 (d, $J = 6.5$ Hz, 1H), 3.81 (s, 3H); ^{13}C NMR (75 MHz, CDCl_3) δ 169.40, 156.72 (q, $J = 38.5$ Hz), 155.54, 136.20, 133.69, 127.34, 124.07, 121.31, 118.05 – 113.29 (m), 55.59, 53.93; LRMS, ESI (-) $m/z = 321.0$ [M-H] $^-$.

3-nitro-4-hydroxy-phenylglycine (11): A solution of **10** (500 mg, 1.6 mmol) in 6 N hydrochloric acid was refluxed under Ar for 18 hrs. The reaction was cooled and the solvent removed *in vacuo*. The resulting white powder (310 mg, 1.2 mmol, 80% yield as HCl salt) was shown to be pure via HPLC and was used without further purification. ^1H NMR (300 MHz, $\text{DMSO-}d_6$) δ 8.05 (s, 1H), 7.62 (d, $J = 8.2$ Hz, 1H), 7.28 (d, $J = 8.4$ Hz, 1H), 4.99 (s, 1H); ^{13}C NMR (75 MHz, DMSO) δ 169.09, 152.52, 136.50, 134.80, 125.03, 124.80, 119.41, 54.63, 39.52; LRMS, ESI (+) $m/z = 213.0$.

5-Benzyloxy-2-methyl-pyridine (13): To a suspension of NaH (2.0 g, 50 mmol) in distilled THF (100 mL) cooled in an ice bath was added 5-hydroxy-2-methylpyridine

12 (5.0 g, 46 mmol) dissolved in anhydrous DMF (50 mL) and stirred for 30 min. To the mixture was added benzylbromide (6.1 mL, 50 mmol) after which the reaction was removed from cooling and stirred at ambient temperature for 18 hrs. The reaction was quenched with saturated NaHCO₃ and extracted 3 times with EtOAc. The combined organics were washed with water and brine then dried over Na₂SO₄. The solvent was removed *in vacuo*. The crude product was purified via silica gel flash chromatography eluting with 1:2 EtOAc–hexanes affording the pure compound **13** (6.5 g, 33 mmol, 71% yield). ¹H NMR (300 MHz, CDCl₃) δ 8.27 (d, *J* = 3.0 Hz, 1H), 7.48 – 7.29 (m, 5H), 7.15 (dd, *J* = 8.5, 3.0 Hz, 1H), 7.04 (d, *J* = 8.5 Hz, 1H), 5.07 (s, 2H), 2.48 (s, 3H); ¹³C NMR (75 MHz, CDCl₃) δ 152.99, 150.78, 137.24, 136.51, 128.74, 128.27, 127.58, 123.38, 122.54, 70.58, 23.48; LRMS, ESI (+) *m/z* = 200.1.

5-Benzyloxy-2-acetatoxymethyl-pyridine (15): To a solution of protected methylpyridine **13** (700 mg, 3.5 mmol) in CHCl₃ (20 mL) cooled in an ice bath was added mCPBA (890 mg, 3.9 mmol) and stirred for 1 hr. The reaction was quenched with 5% *aqueous* Na₂CO₃ and extracted with EtOAc. The organics were washed with brine and dried over Na₂SO₄. The solvent was removed under reduced pressure yielding the crude N-oxide **14**. The crude product was then added to heated (80 °C) acetic anhydride (11.4 mL, 71 mmol) and then stirred at 130 °C for 30 min. The reaction was then poured into ice water (20 mL) and stirred for 2 hrs. The mixture was extracted with EtOAc. The extract was washed with saturated NaHCO₃, brine and then dried over Na₂SO₄. The solvent was removed *in vacuo* and the compound purified using silica gel flash chromatography (1:2 EtOAc–Hexanes) affording **15** (730 mg, 2.8 mmol, 80% yield) as a yellow oil. ¹H NMR (300 MHz, CDCl₃) δ 8.36 (d, *J* = 2.5 Hz, 1H), 7.46 – 7.14 (m, 8H), 5.15 (s, 2H), 5.11 (s, 2H), 2.12 (s, 3H); ¹³C NMR (75 MHz, CDCl₃) δ 170.85, 154.55, 147.99, 138.17, 136.13, 128.85, 128.45, 127.60, 123.14, 122.16, 70.61, 66.83, 21.07; LRMS, ESI (+) *m/z* = 257.1.

5-Benzyloxy-2-formyl-pyridine (16): To a solution of **15** (720 mg, 2.8 mmol) in ethanol (7 mL) was added 1 N NaOH (1.8 mL). The solution was refluxed for 1.5 hrs then allowed to cool and concentrated. The aqueous residue was extracted with CHCl₃. The extract was washed with water and dried over Na₂SO₄. The organics were then removed and the residue precipitated from EtOAc–Hexanes. The crude alcohol was dried under high vacuum overnight. The alcohol was dissolved in CHCl₃ (17 mL) and MnO₂ (1.7 g, 19.5 mmol) was added and the mixture was refluxed for 30 min. The reaction mixture was filtered through celite and the solvent removed under reduced pressure. The crude product was purified using silica gel flash chromatography (1:4 EtOAc–Hexanes) to yield aldehyde **16** (320 mg, 1.5 mmol, 52% yield) as white crystals. ¹H NMR (300 MHz, CDCl₃) δ 9.92 (s, 1H), 8.43 (d, *J* = 2.8 Hz, 1H), 7.85 (d, *J* = 8.6 Hz, 1H), 7.42 – 7.22 (m, 6H), 5.11 (s, 2H); ¹³C NMR (75 MHz, CDCl₃) δ 191.72, 157.94, 146.27, 138.93, 135.09, 128.67, 128.44, 127.40, 123.15, 120.81, 70.49; LRMS, ESI (+) *m/z* = 214.1.

5-Benzyloxy-2-(N-Bn-NAc-aminonitrile)-pyridine (17): To a solution of aldehyde **16** (100 mg, 0.47 mmol) and benzylamine (51 μL, 0.47 mmol) in THF (0.5 mL) under Ar was added ZnI₂ (74 mg, 0.23 mmol). The reaction was stirred for 10 min. then TMS- cyanide (66 μL, 0.52 mmol) was added. The reaction was stirred for 1 hr then cooled and acetic anhydride (180 μL, 1.7 mmol) and pyridine (190 μL, 2.3 mmol) were added. The reaction was allowed to come to ambient temperature over 2 hrs. The reaction was poured into water and extracted with EtOAc. The organics were washed with saturated NaHCO₃, water, brine and dried over Na₂SO₄. The solvent was removed under reduced pressure and the crude product was purified via silica gel flash chromatography (1:4 EtOAc–hexanes) yielding aminonitrile **17** (50 mg, 0.13 mmol, 28% yield) as colorless amorphous solid. ¹H NMR (300 MHz, CDCl₃) δ 8.37 (d, *J* = 2.9 Hz, 1H), 7.48 – 7.22 (m, 12H), 5.12 (s, 2H), 4.75 (s, 1H), 4.25 – 3.88 (m, 2H), 2.04 (s, 3H); ¹³C NMR (75 MHz, CDCl₃) δ 171.23, 154.87, 143.81, 138.09, 135.86,

135.55, 128.60, 128.55, 128.27, 127.37, 127.32, 126.03, 123.38, 122.06, 116.36, 70.30, 60.18, 50.22, 21.68; LRMS, ESI (+) $m/z = 372.5$.

5-Benzyloxy-2-(N-Bn-methylamine)-pyridine (20): Aminonitrile **17** (13 mg, 35 μmol) was dissolved in anhydrous MeOH (500 μL) at 0 °C and treated with 3 M HCl in MeOH (200 μL). The reaction was stirred for three hrs. and allowed to come to ambient temperature over four hrs. The solvent was removed under reduced pressure and the product was dissolved in EtOH (2 mL) and Pd/C (2 mg, 0.8 μmol) was added and stirred under H₂ atmosphere for 4 hrs. The reaction was filtered through celite and the solvent removed. NMR and MS results indicated a decarboxylation reaction or loss of cyanide had occurred producing amine **19** instead of hydroxypyridinylglycate **18**. ¹H NMR (300 MHz, D₂O) δ 7.85 (d, $J = 2.6$ Hz, 1H), 7.72 – 7.38 (m, 2H), 7.12 – 6.78 (m, 5H), 4.15 (s, 2H), 3.90 (s, 2H); ¹³C NMR (75 MHz, D₂O) δ 156.21, 134.47, 133.10, 130.71, 129.80, 129.73, 129.61, 129.36, 129.03, 51.27, 45.58; LRMS ESI (+) $m/z = 215.1$.

References

1. Castiglione, F.; Marazzi, A.; Meli, M.; Colombo, G., Structure elucidation and 3D solution conformation of the antibiotic enduracidin determined by NMR spectroscopy and molecular dynamics. *Magn. Reson. Chem.* **2005**, *43* (8), 603-10.
2. Han, J.; Tao, F.-M., Correlations and Predictions of pKa Values of Fluorophenols and Bromophenols Using Hydrogen-Bonded Complexes with Ammonia. *J. Phys. Chem. A* **2005**, *110* (1), 257-263.
3. Yin, X.; Zabriskie, T. M., The enduracidin biosynthetic gene cluster from *Streptomyces fungicidicus*. *Microbiology* **2006**, *152* (10), 2969-83.
4. Yin, X.; Chen, Y.; Zhang, L.; Wang, Y.; Zabriskie, T. M., Enduracidin Analogues with Altered Halogenation Patterns Produced by Genetically Engineered Strains of *Streptomyces fungicidicus*. *J. Nat. Prod.* **2010**, *73* (4), 583-589.
5. Das, B.; Kumar, R. A.; Thirupathi, P., One-Pot Three-Component Synthesis of α -Amino Nitriles Catalyzed by 2,4,6-Trichloro-1,3,5-triazine (Cyanuric Acid). *Helv. Chim. Acta* **2007**, *90* (6), 1206-1210.
6. (a) Gómez-Gallego, M.; Sierra, M. A.; Alcázar, R.; Ramírez, P.; Piñar, C.; Mancheño, M. J.; García-Marco, S.; Yunta, F.; Lucena, J. J., Synthesis of o,p-EDDHA and Its Detection as the Main Impurity in o,o-EDDHA Commercial Iron Chelates. *J. Agric. Food. Chem.* **2002**, *50* (22), 6395-6399; (b) Zuend, S. J.; Coughlin, M. P.; Lalonde, M. P.; Jacobsen, E. N., Scaleable catalytic asymmetric Strecker syntheses of unnatural α -amino acids. *Nature* **2009**, *461* (7266), 968-970.
7. Hojati, Z.; Milne, C.; Harvey, B.; Gordon, L.; Borg, M.; Flett, F.; Wilkinson, B.; Sidebottom, P. J.; Rudd, B. A. M.; Hayes, M. A.; Smith, C. P.; Micklefield, J.,

Structure, Biosynthetic Origin, and Engineered Biosynthesis of Calcium-Dependent Antibiotics from *Streptomyces coelicolor*. *Chem. Biol.* **2002**, *9* (11), 1175-1187.

8. Black, R. M.; Balkovec, J. M.; Nollstadt, K. M.; Dreikorn, S.; Bartizal, K. F.; Abruzzo, G. K., Synthesis and structure-activity relationships of novel 3-Hty-substituted pneumocandins. *Bioorg. Med. Chem. Lett.* **1997**, *7* (22), 2879-2884.

9. (a) van Pée, K. H.; Patallo, E., Flavin-dependent halogenases involved in secondary metabolism in bacteria. *Appl. Microbiol. Biotechnol.* **2006**, *70* (6), 631-641; (b) Puk, O.; Huber, P.; Bischoff, D.; Recktenwald, J.; Jung, G.; Sussmuth, R. D.; van Pee, K. H.; Wohlleben, W.; Pelzer, S., Glycopeptide Biosynthesis in *Amycolatopsis mediterranei* DSM5908: Function of a Halogenase and a Haloperoxidase/Perhydrolase. *Chem. Biol.* **2002**, *9* (2), 225-235.

10. (a) Yeh, E.; Blasiak, L. C.; Koglin, A.; Drennan, C. L.; Walsh, C. T., Chlorination by a Long-Lived Intermediate in the Mechanism of Flavin-Dependent Halogenases. *Biochemistry.* **2007**, *46* (5), 1284-1292; (b) Dong, C.; Flecks, S.; Unversucht, S.; Haupt, C.; van Pee, K. H.; Naismith, J. H., Tryptophan 7-Halogenase (PrnA) Structure Suggests a Mechanism for Regioselective Chlorination. *Science* **2005**, *309* (5744), 2216-2219.

11. Buedenbender, S.; Rachid, S.; Müller, R.; Schulz, G. E., Structure and Action of the Myxobacterial Chondrochloren Halogenase CndH: A New Variant of FAD-dependent Halogenases. *J. Mol. Biol.* **2009**, *385* (2), 520-530.

12. (a) Takeda, Y.; Uoto, K.; Chiba, J.; Horiuchi, T.; Iwahana, M.; Atsumi, R.; Ono, C.; Terasawa, H.; Soga, T., New highly active taxoids from 9 β -Dihydrobaccatin-9,10-acetals. Part 4. *Bioorg. Med. Chem.* **2003**, *11* (20), 4431-4447; (b) Wang, J.; Masui, Y.; Onaka, M., Synthesis of α -Amino Nitriles from Carbonyl Compounds, Amines, and Trimethylsilyl Cyanide: Comparison between Catalyst-Free Conditions and the

Presence of Tin Ion-Exchanged Montmorillonite. *Eur. J. Org. Chem.* **2010**, 2010 (9), 1763-1771.

13. Higashide, E.; Hatano, K.; Shibata, M.; Nakazawa, K., Enduracidin, a new antibiotic. I. *Streptomyces fungicidicus* No. B5477, an enduracidin producing organism. *J. Antibiot.* **1968**, 21 (2), 126-37.

14. Mazodier, P.; Petter, R.; Thompson, C., Intergeneric conjugation between *Escherichia coli* and *Streptomyces* species. *J. Bacteriol.* **1989**, 171 (6), 3583-3585.

CHAPTER THREE

BIOSYNTHESIS OF ENDURACIDIDINE

Neal Goebel

Introduction

Enduracidin contains 17 amino acid residues. Four are proteinogenic residues and 13 are nonproteinogenic, with seven having the D configuration. One of these residues, enduracididine (End), found in both the D and L configurations, contains a 2-amino-2-imidazoline moiety; an uncommon amino acid structure (Fig. 3.1). Structurally similar amino acids include: capreomycin and viomycin from the tuberactinomycins¹ (including viomycin² and capreomycin), muraymycin³ and chymostatin⁴; stendomycin from stendomycin⁵; 3-hydroxyenduracididine from mannopeptimycin⁶; and tetrahydrolathyrine⁷ a derivative of lathyrine.⁸ Enduracididine and *N*-(6-bromo-1H-indolyl-3-carbonyl)-L-enduracididine were isolated from the ascidian *Leptoclinides dubius*.⁹ The seeds from *Lonchocarpus sericeus* were found to contain enduracididine as well.¹⁰ The aminocyclitol minosaminomycin is the only other structurally complex bioactive natural product reported that contains enduracididine.¹¹ While the aminoimidazoline structure is found in a variety of natural products with deduced biosynthetic pathways, the mechanism of enduracididine biosynthesis remains unknown.¹²

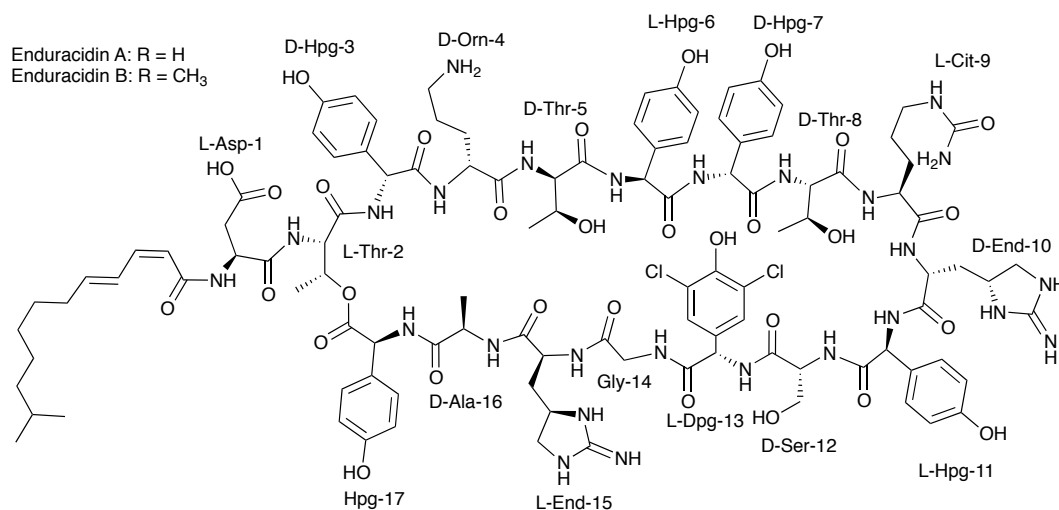


Figure 3.1 The structure of enduracidin with amino acid labels.

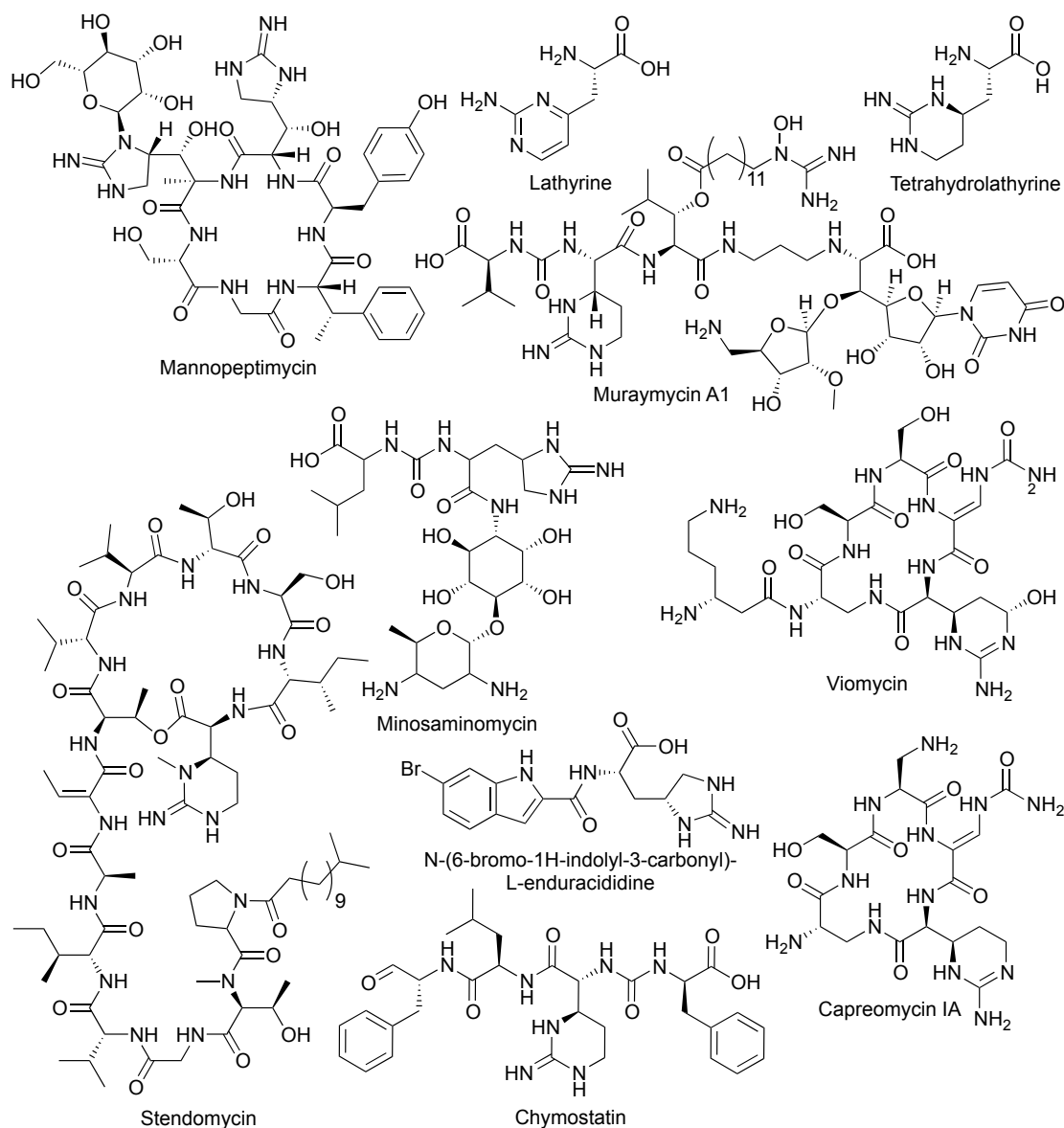


Figure 3.2 Natural products containing enduracididine and similar amino acid structures.

Initial studies into the biosynthetic origin of enduracidin found through ^{14}C radiolabeling studies that enduracididine was likely produced from arginine (Arg).¹³ Work on the capreomycin biosynthetic pathway found that a hydroxyl group was introduced on the 3-carbon of Arg by the 2-ketoglutarate-dependent monooxygenase VioC.¹⁴ The resulting 3-hydroxy-Arg (3-OH-Arg) was cyclized using an elimination-cyclization reaction catalyzed by the PLP-dependent enzyme VioD (Fig. 3.3).¹⁵

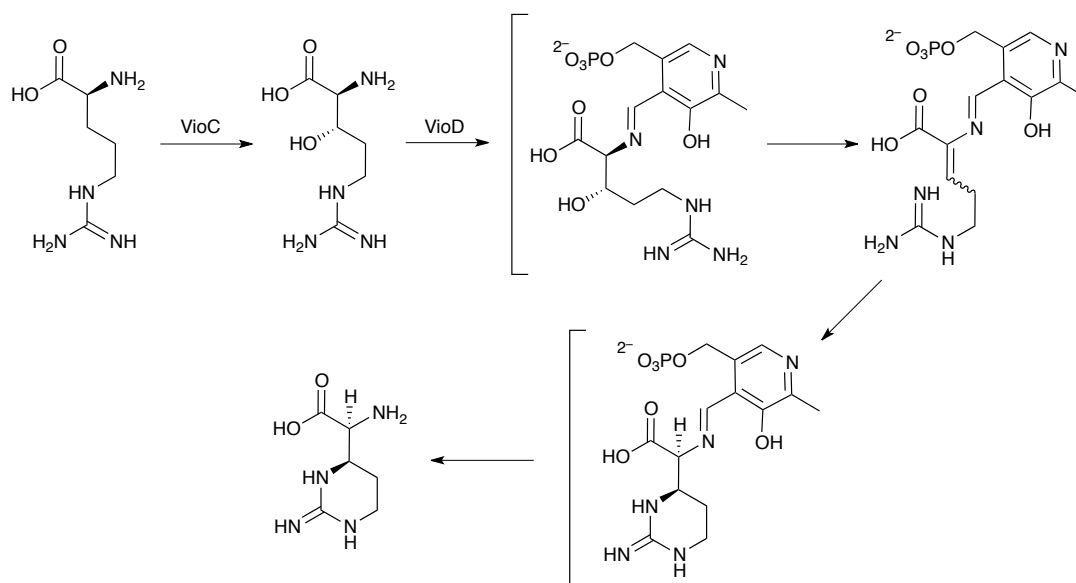


Figure 3.3 Biosynthesis of 3-S-L-capreomycin via non-heme iron α -ketoglutarate dependent oxygenase VioC and the pyridoxal phosphate dependent enzyme VioD from L-arginine.

Bioinformatic analysis of the enduracidin biosynthetic pathway identified three open reading frames (orfs) that were postulated to be involved in enduracididine biosynthesis: *endP*, *endQ* and *endR*.¹⁶ Comparison to the mannopeptimycin biosynthetic pathway revealed a highly similar operon containing four orfs: *mppO*, *mppP*, *mppQ* and *mppR*.¹⁷ A series of experiments involving recombinant MppO, an oxygenase similar to VioC, indicated that it was responsible for the introduction of the 3-hydroxyl group on End and did not accept Arg as a substrate.¹⁸ End is the only unusual amino acid common between the two peptides and as *endPQR* and *mppPQR* share high sequence similarity, the gene products are likely responsible for End biosynthesis. Bioinformatic analysis classified the gene products into two groups: EndP and EndQ are predicted to be PLP-dependent enzymes, while EndR is loosely related to the acetoacetate decarboxylase (ADC) family of enzymes.¹⁶ Interestingly, none of the enzymes shared similarity with an oxygenase enzyme.

The presence of the PLP-dependent enzyme suggests an elimination–cyclization reaction is used in the formation of enduracididine. These types of reactions require the introduction of a leaving group, often a hydroxyl group, which then is eliminated

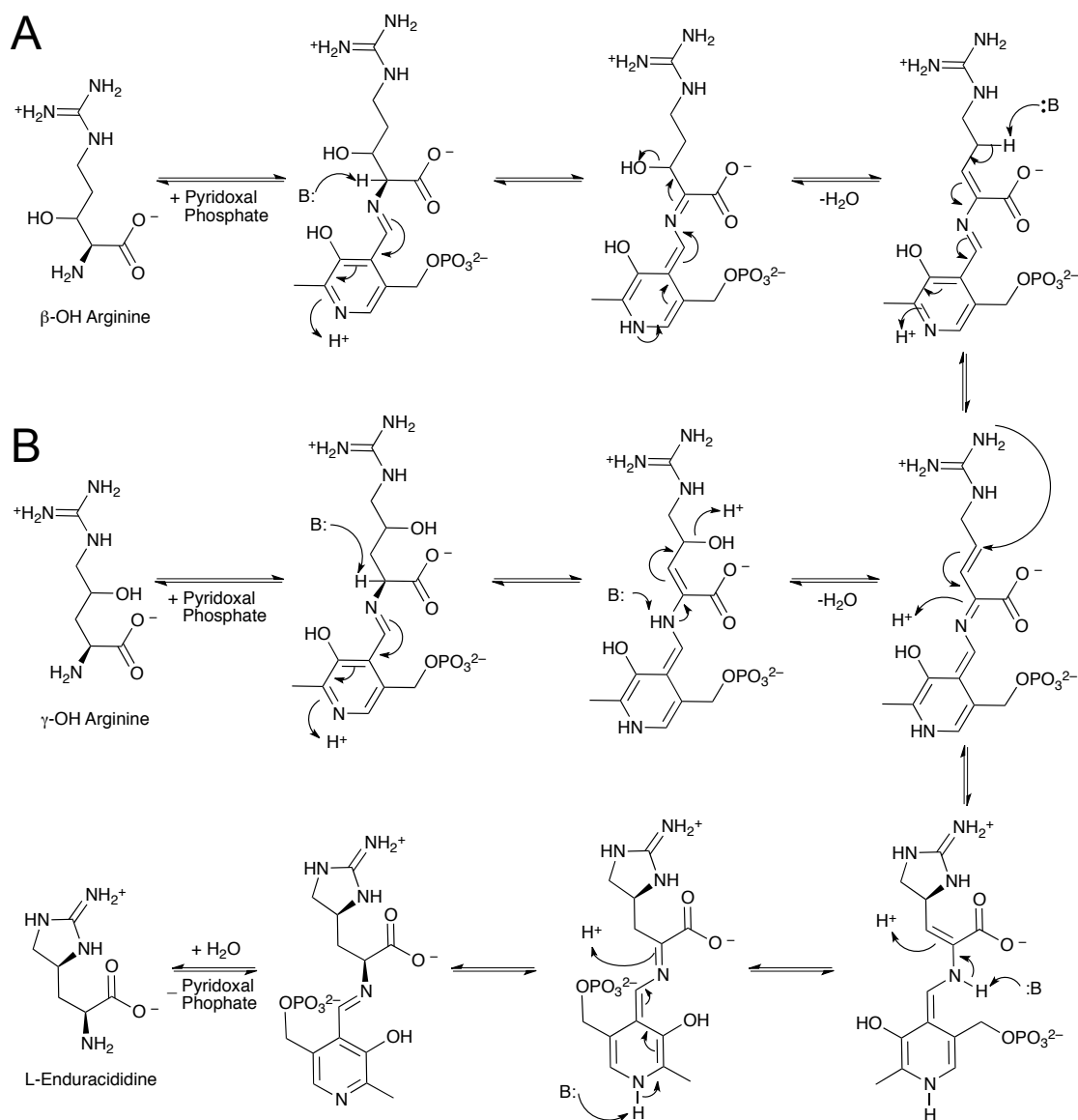


Figure 3.4 Possible mechanisms for a pyridoxal phosphate catalyzed elimination cyclization reaction producing L-enduracididine from A) 3-OH arginine and B) 4-OH arginine.

via conjugation to the PLP cofactor. Mechanisms involving either a 3-OH or 4-OH Arg as a precursor are possible (Fig. 3.4). Michael-type reactions have been shown to be involved in the formation of naturally occurring aminoimidazoles. The guanidinomines, noted for their inhibition of type III secretion, contain a terminal aminoimidazole ring originating from guanidinoacetate. After formation of the PKS-bound 4-guanidino-but(2-ene)oate intermediate the guanidine cyclizes onto C3

forming the aminoimidazoline moiety.¹⁹ A series of three similar Michael-type reactions are involved in the biosynthesis of the cyanobacterial cytotoxin cylindrospermopsin suggesting the formation of the aminoimidazoline ring of End by Michael-type reaction is probable.^{12b}

The function of EndR is unknown. As no other enzymes are predicted to have oxidative/hydroxylation activity, EndR may be an unknown form of a hydroxylase. The ADC family of enzymes utilize a Lys residue to form an imine with 3-keto acids and catalyze the decarboxylation reaction, as illustrated by the ADC from *Clostridium acetobutylicum* (Fig. 3.5).²⁰ Given the limited bioinformatic data on the enzyme experimentation is the only means to gain further understanding of its role in End biosynthesis.

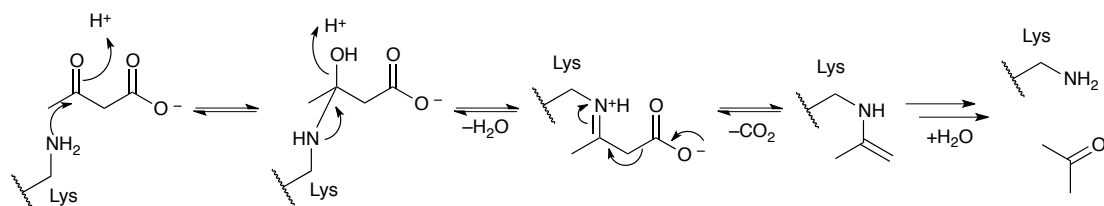


Figure 3.5 Mechanism of action of acetoacetate decarboxylase from *Clostridium acetobutylicum*.

Previous work on this biosynthetic problem had focused around the overexpression and isolation of the proteins EndP EndQ and EndR for *in vitro* testing of the proposed biosynthetic intermediates Arg, 3-OH Arg and 4-OH Arg and possible cofactors. Though significant work was performed, poor solubility of the proteins proved an insurmountable obstacle. To overcome this limitation, *in vivo* complementation experiments were approached. As the work moved forward on the complementation experiments we began a collaboration with Dr. Nicholas Silvaggi (University of Wisconsin-Milwaukee), a structural biologist. Dr. Silvaggi's work has focused on the mannopeptimycin biosynthetic proteins MppP, MppQ and MppR. From these two complementary approaches important details have been uncovered concerning the biosynthesis of enduracididine.

Results and Discussion

To perform the complementation studies, the preparation of biosynthetic intermediates as well as enduracididine was undertaken. Previous work with the Gould lab provided a source of L-3-OH arginine in both L-3-*R* and L-3-*S* configurations.^{15, 21} Additionally, a method for preparing 4-OH Arg had previously been accomplished in our lab (Fig 3.6). Briefly, Boc protected allyl-glycine (**1**) is subjected to an iodine-mediated cyclization reaction under basic conditions. The resulting iodo-lactones (**2** and **3**) are converted to the azide (**4**) and subsequently reduced to the amine (**5**). The amine is then converted to the diBoc-protected guanidine (**6**) using Mukaiyama's reagent (**8**) and *N,N'*-diBoc thiourea.²² The lactone is then hydrolyzed under basic conditions and the Boc groups are removed under acidic conditions, yielding 4-OH Arg (**7**).²³

Though reported to give high yields and being used in many examples in the literature, the use of Mukaiyama's reagent for the guanylation reaction gave poor yields and side products proved difficult to separate.²⁴ Other reactions involving Hg catalysts had proved to be unsuccessful in the past work on this reaction.^{23, 25} The

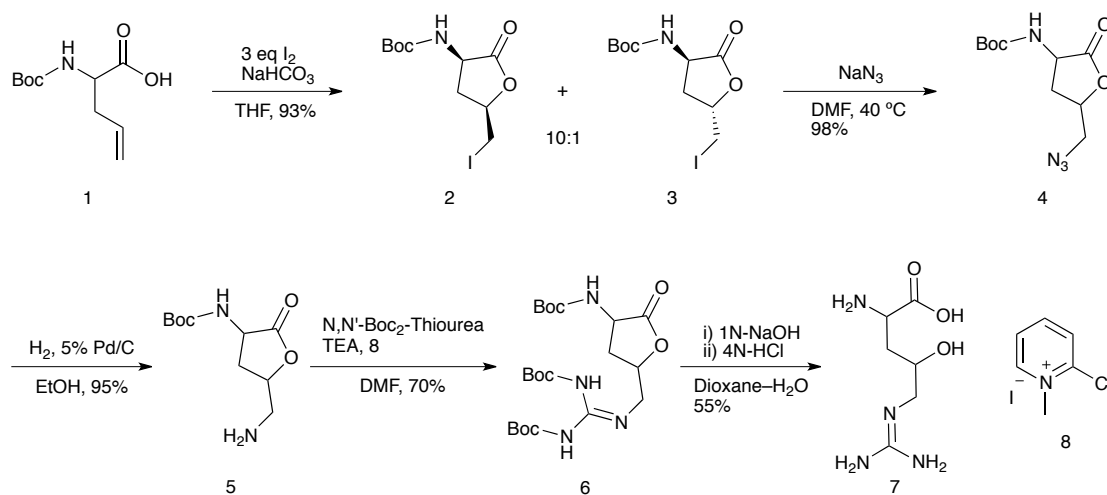


Figure 3.6 Synthesis of 4-OH Arg from allylglycine via iodine-mediated lactonization and using Mukaiyama's reagent and diBoc-thiourea for the guanylation reaction.

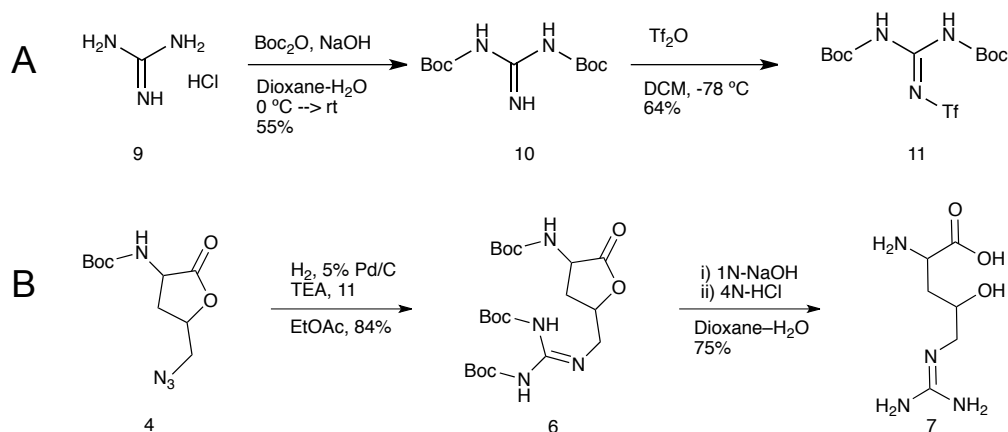


Figure 3.7 A) Preparation of the Tf-guan reagent from guanidinium chloride. B) Preparation of 4-OH Arg from the azidolactone 4 using the Tf-guan reagent.

larger scale production of 4-OH Arg called for a new guanylation reagent. Additionally, a reaction where exposure of the lactone to the free amine (5) was limited, preventing lactam formation or polymerization, was desirable. The work by Goodman *et al.* appeared to provide a viable solution to the problem.²⁶ The N-Tf-N',N''-diBoc-guanidine (Tf-guan) (11) reagent is readily produced in good yields from guanidinium chloride (9) on a large scale (Fig. 3.7A). The product is stable and proved to be highly effective in the production of 4-OH Arg. The yields were increased from ~20% with difficult isolation using Mukaiyama's reagent to 84% of readily purified compound using Tf-guan (Figure 3.7B). The reaction could also run under reducing conditions, allowing the combination of the azide reduction and the guanylation reaction in a one pot reaction. The increased yield, facile isolation, one-pot reaction setup and the ability to run gram-scale reactions made Tf-guan an ideal reagent for preparing 4-OH Arg.

The ability to selectively produce single diastereomers of 4-OH Arg was of interest. Crystallization of the crude iodolactone product from EtOAc-Hexanes selectively yielded the *cis* product (Fig 3.8A and B). The initial complementation work primarily aimed to utilize a racemic mixture of the four diastereomers of 4-OH Arg for testing. Further investigation would require the production of single diastereomers. To

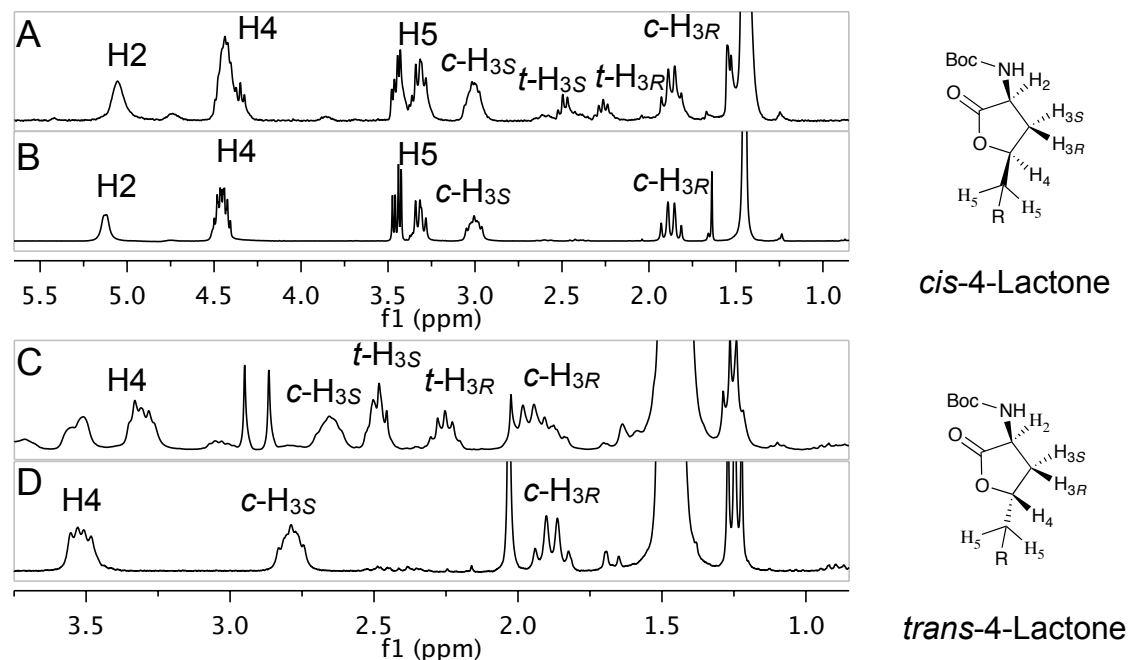


Figure 3.8 $^1\text{H-NMR}$ spectra of A) a mixture of *cis* and *trans* iodolactones **2** and **3**, B) crystallized *cis* iodolactone **2**, C) a mixture of *cis* and *trans* guanidinyllactone **7** and D) purified guanidinyllactone **6** having an absolute configuration of 2-S, 4-S.

produce the 4-*S* isomer, L-allylglycine was selected as the starting material. Successful production of 4-*S*-OH-L-Arg was observed in the $^1\text{H NMR}$ spectra of racemic and enriched guanidinyllactone (**6**) (Fig. 3.8 C and D). Attempts to isolate the *trans* configured iodolactone through repeated crystallization proved unsuccessful.

Large quantities of End were needed to establish a complementation protocol, demonstrate the ability to chemically complement *endPQR* mutant strains and serve as a positive control during the experiments. Previous preparations of End have been accomplished.²⁷ Recently work by Dodd's group produced protected enduracididine in a stereo specific manner. Unfortunately, the methodology involved several low yield conversions and required HPLC purification for several steps. The strategy devised by Tsuji *et al.* appeared to be promising, however the experience of others in the lab indicated the process was unreliable and gave yields too low to be practical for the supplementation experiments.

In evaluating the preparation of End from His, several examples were found for

generating 2,4,5-triamidopent(4-ene)ate from L-His (a Bamberger cleavage), including industrial applications.^{27b, 28} The reduction of the diamido-alkene had been previously demonstrated by Altman *et al.* and could be circumvented via hydrolysis of one enamide to form the ketone.^{28b} The triamine could easily be produced via acidic hydrolysis. The selective formation of cyclic guanidine between vicinal amines in the presence of other amines had been previously accomplished in the synthesis of streptolidine by utilizing cyanogen bromide under basic conditions.²⁹ Requiring only 4 steps from readily available L-His methyl ester and just one chromatography step during preparation, this synthetic route was chosen for investigation before other,

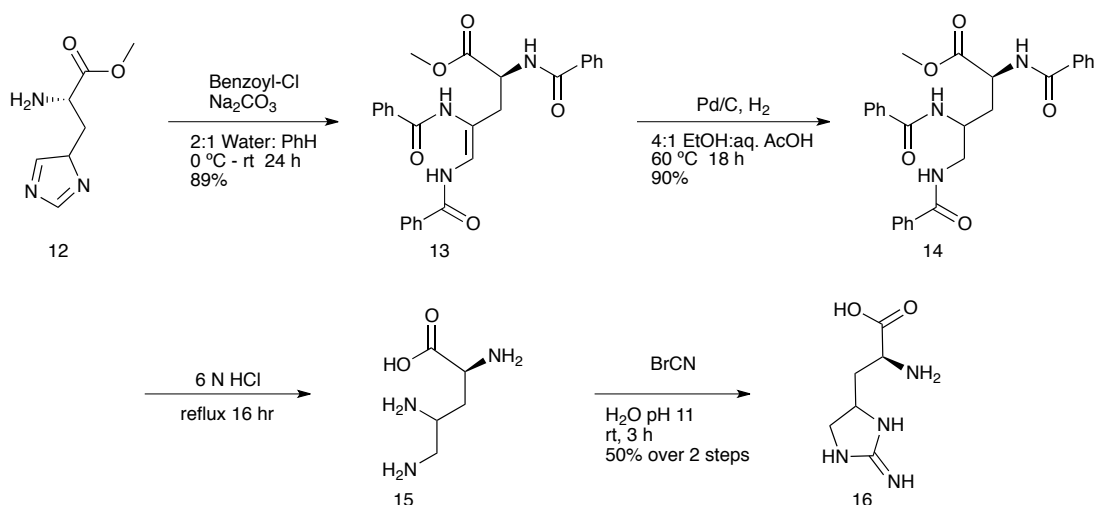


Figure 3.9 The preparation of enduracididine from the methyl ester of L-histidine.

more complex, routes were explored.

The imidazole ring of His was successfully opened using Bamberger cleavage conditions affording the 2,4,5 N-benzamido-pent-4-eneoate methylester (**13**) in good yield (Fig. 3.9). The reduction of (**13**) to produce the unsaturated product triamidopentanoate (**14**) required acidic conditions and heating, but proved a viable method. Acidic hydrolysis of the benzoyl groups with 6 N HCl yielded the triaminopentanoic acid (**15**). The introduction of the amino-imidazoline ring was accomplished using cyanogen bromide. When pH was controlled using tribasic sodium phosphate buffer the yields were significantly lower, ~30% yield. It was

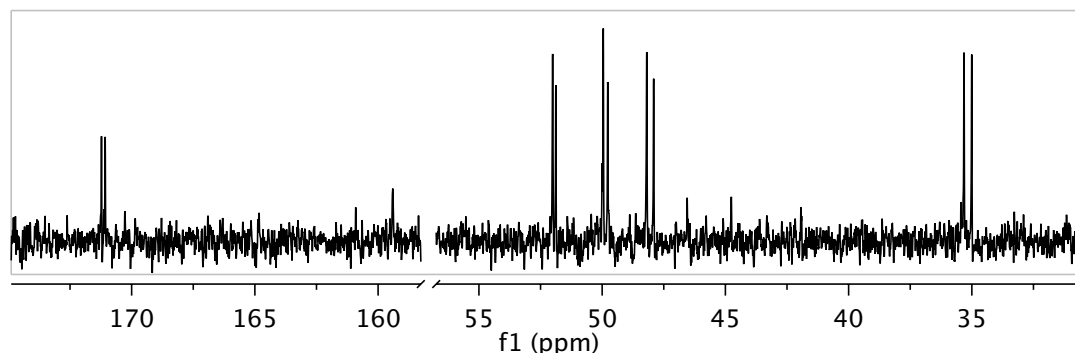


Figure 3.10 ^{13}C NMR (75 MHz, D_2O) of synthetic enduracididine (**16**) showing the doubling of signals.

observed that the buffer was insufficient to maintain the pH above 10 for the duration of the reaction. Alternately, continuous monitoring of the reaction pH and adjustment using 1 N NaOH to maintain \sim pH 10.5 over the duration of the reaction resulted in a significant increase in yield (72%) over 2 steps starting from 6 g of triamide (**14**). The product was easily isolated via ion exchange chromatography. This short preparation of enduracididine afforded large quantities with an efficiency not previously reported.

NMR analysis of the product showed a doubling of the ^{13}C NMR signals suggesting that both diastereomers were formed (Fig. 3.10). The C2 and C1 signals were shifted by 21.4 and 11.3 Hz respectively. The greatest signal shift observed was for C3 at 23.6 Hz. The resonances of C4 and C5, being in the rigid aminoimidazoline ring showed the smallest signal shifts at 9.8 and 13.7 Hz respectively. The shifts may result from rigid structures formed due to intramolecular hydrogen bonding unique for each of the diastereomers produced. HMBC experiments showed no correlations from the C2 and C3 protons to the guanidinyll carbon. The results support the assignment of the ring structure as that of End.

For the complementation studies, a series of genetic mutations were introduced by Dr. Yin, disrupting *endP*, *endQ* and *endR* using methods previously described.^{16, 30} An in-frame deletion was used to remove *endP* from the wild-type strain of *S. Fungicidicus*, creating the strain denoted Sf Δ endP. Strains with *endQ* and *endR* disrupted via insertion of the apramycin resistance gene *aac(3)IV* were denoted as

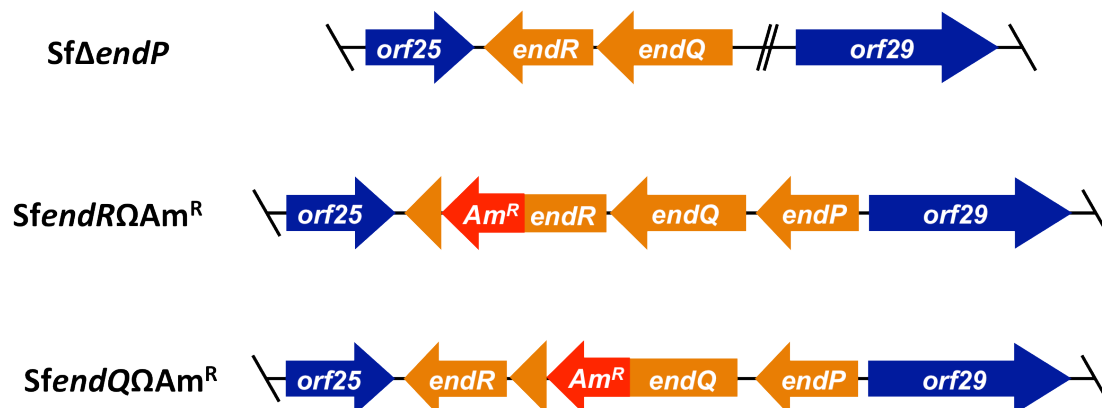


Figure 3.11 Diagram showing the disruptions introduced into *endP*, *endR* and *endQ* of *S. fungicidicus*.

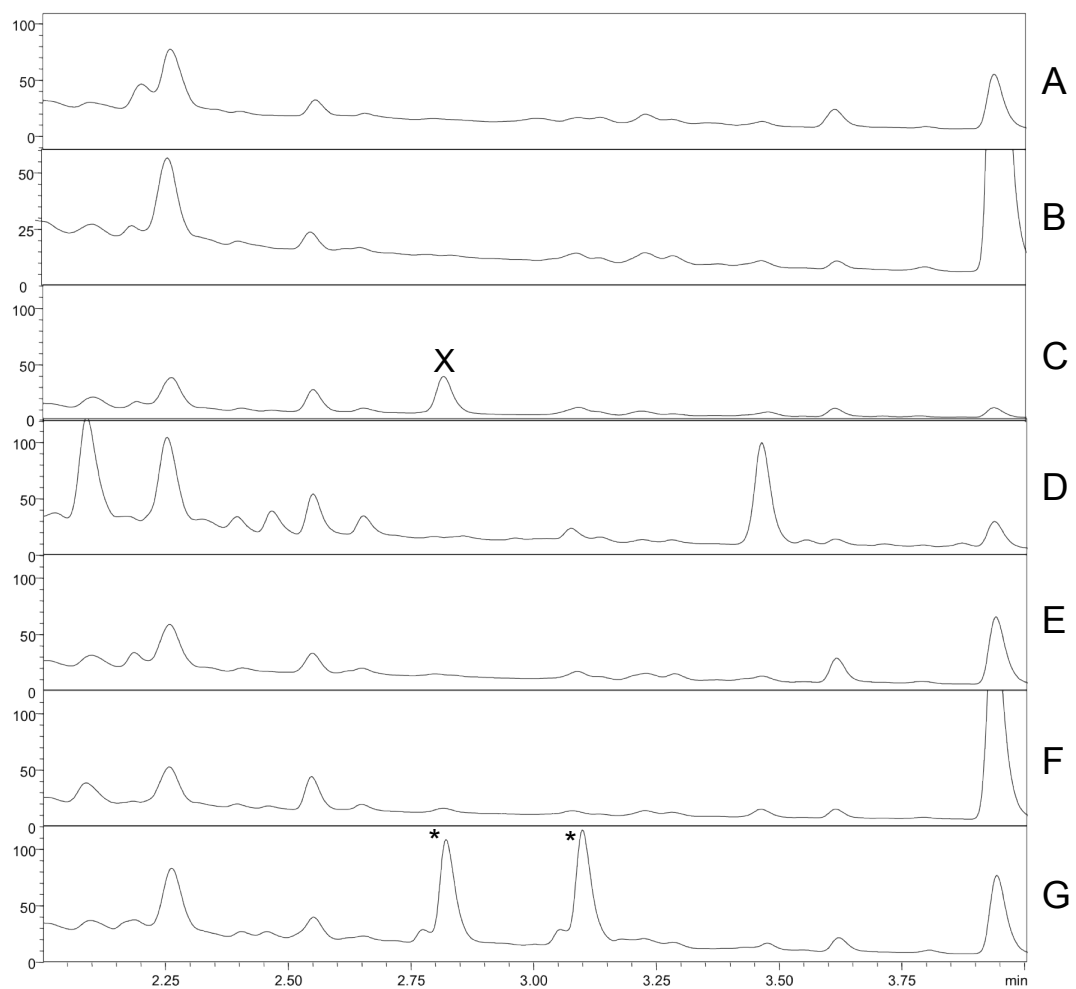


Figure 3.12 HPLC chromatograms of mycelial extracts of A) SfendR Ω Am^R + 3-S-OH Arg, B) SfendR Ω Am^R + 3-R-OH Arg, C) SfendR Ω Am^R, D) Sf Δ endP + 3-S-OH Arg, E) Sf Δ endP + 3-R-OH Arg, F) Sf Δ endP and G) *S. fungicidicus* wild type. Enduracidin is indicated with asterisks. The peak marked with an X was determined not to be enduracidin from UV data.

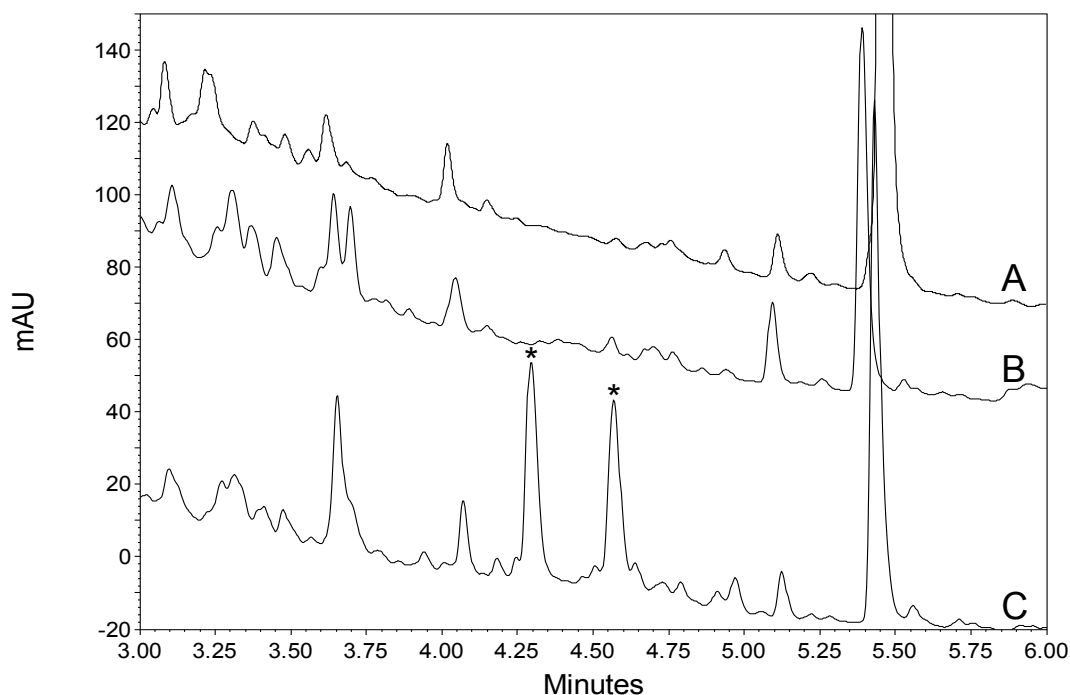


Figure 3.13 HPLC chromatograms of mycelial extracts of A) SfendQΩAm^R, B) SfendQΩAm^R + End, and C) *S. fungicidicus* wild type. Enduracidin is indicated with asterisks.

SfendRΩAm^R and SfendQΩAm^R respectively (Fig. 3.11). The genetic modifications were confirmed by Southern blot hybridization. The resulting mutants were then screened for enduracidin production. Each showed an inability to produce enduracidin. Each of the mutants was then supplemented with 3-*S*-OH-L-Arg, 3-*R*-OH-L-Arg or racemic 4-OH Arg. A culture of each group was also supplemented with synthetic enduracididine to serve as a control (data not shown for all experiments). The results for the 3-OH Arg experiments indicated that supplementation failed to restore enduracidin production in any of the mutant strains (Fig. 3.12). Only the SfendQΩAm^R strain was not complemented by the addition of enduracididine (Fig. 3.13). In the 4-OH Arg experiments, both the SfΔendP and SfendRΩAm^R strains were complemented and enduracidin production was restored. This complementation of both the *endP* and *endR* mutants suggested that EndP and EndR were responsible for the production of 4-OH Arg. To further test this result, 4-*S*-OH-L-Arg was supplemented to cultures of the SfΔendP and SfendRΩAm^R strains. The results again

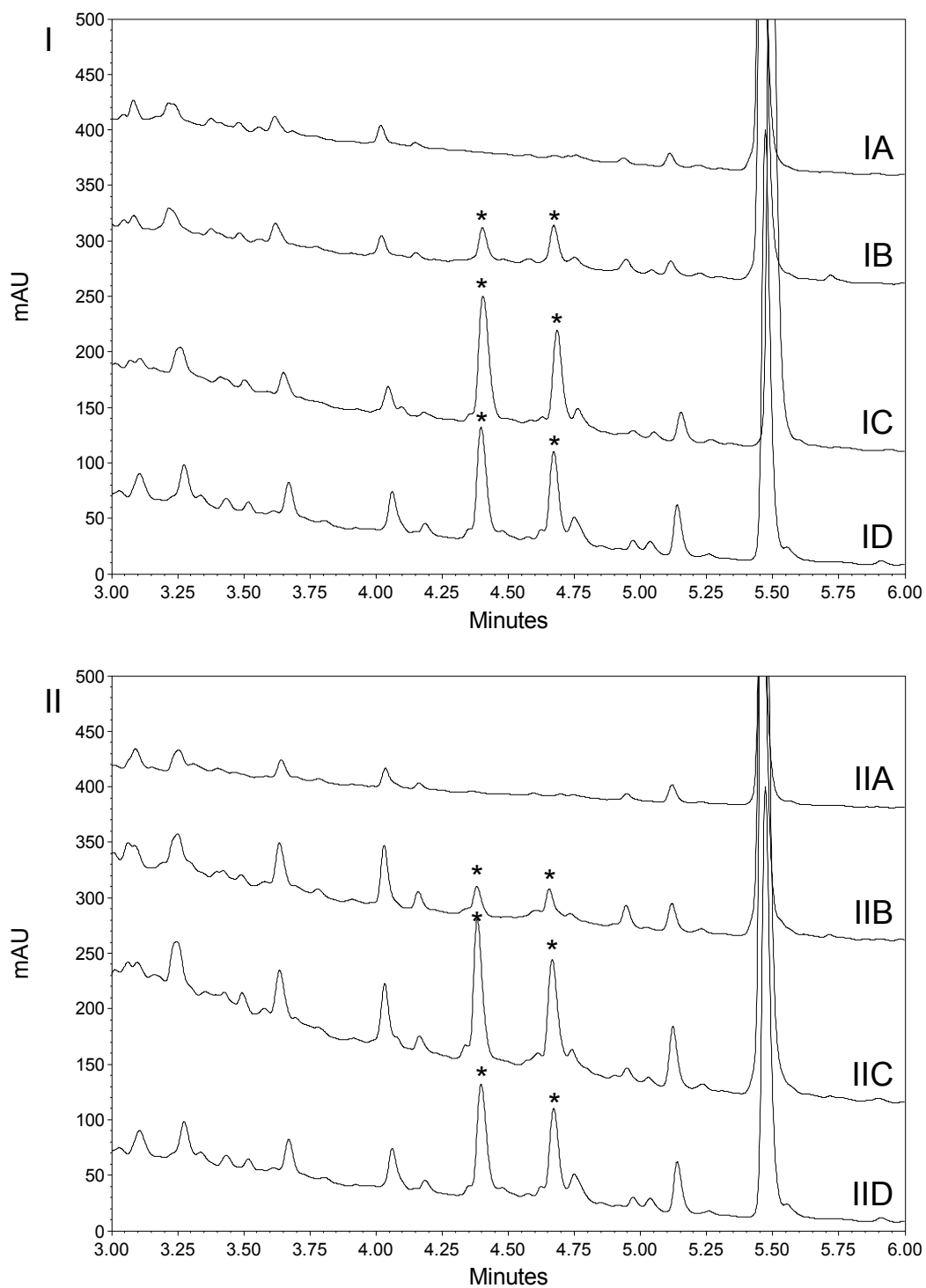


Figure 3.14 HPLC chromatograms of mycelial extracts of IA) SfendRQAm^R, IB) SfendRQAm^R + 4-OH Arg, IC) SfendRQAm^R + End, ID) *S. fungicidus* wild type, IIA) SfΔendP, IIB) SfΔendP + 4-OH Arg, IIC) SfΔendP + End and IID) *S. fungicidus* wild type. Enduracidin is indicated with asterisks.

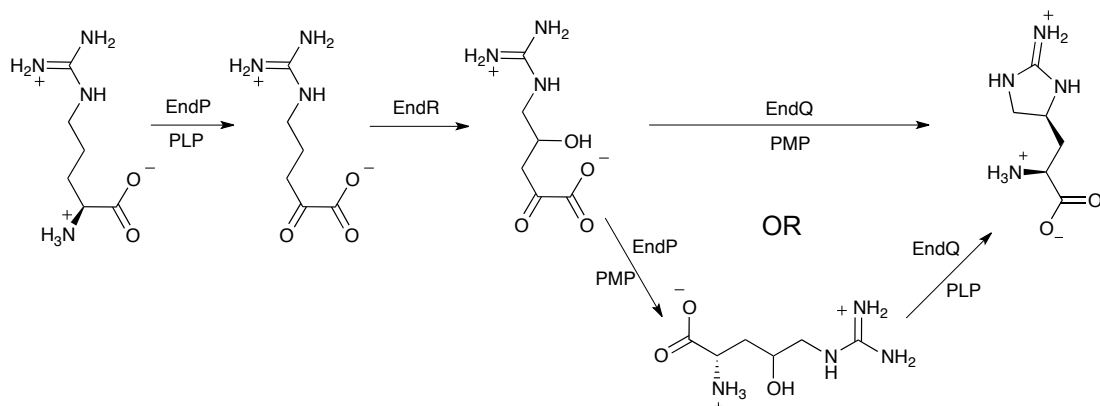


Figure 3.15 Hypothetical biosynthesis of enduracididine based on complementation assay results showing possible non-enzyme bound intermediates.

showed the restoration of enduracidin production (Fig. 3.14). The production of enduracidin was confirmed by LCMS which showed masses at $m/z = 1177.2$ and 1184.3 Da, corresponding with $[M+2H]^{2+}$ for enduracidins A and B respectively.

The complementation results led to a hypothetical biosynthetic route where EndP and EndR are responsible for the production of 4-OH Arginine or 2-keto-4-OH arginate and EndQ is responsible for the cyclization reaction and releasing enduracididine. Using the bioinformatic data as a guide, EndP would function as a transaminase forming 2-keto-arginate which is then oxidized by EndR to yield 2-keto-4-OH arginate. This species could then be transformed to 4-OH Arg by EndP or used directly by EndQ. EndQ could theoretically cyclize either product, only requiring a change from pyridoxal phosphate to pyridoxamine as a cofactor. It seemed likely from the complementation data that EndQ formed the aminoimidazoline moiety and released enduracididine.

All attempts to produce an EndQ mutant that could be complemented with enduracididine were unsuccessful. Further, some strains with *endQ* disruptions were found to produce enduracidin. As such the role of EndQ could not be determined experimentally using a complementation assay. Bioinformatic analysis of *endQ* provided possible insight into these results. EndQ shows greater than 50% similarity to several proteins belonging to the GntR family of transcriptional regulators

suggesting EndQ may play a role in regulating enduracidin production in addition to acting as a cyclase. Disruption of the regulatory properties of EndQ could explain why the disruptants were unable to be complemented, while disruption of the aminotransferase activity could be overcome, though at significantly lower production levels, by EndP filling the role of EndQ.

The bioinformatic analysis of *endP*, *endQ* and *endR* showed no known metal or cofactor binding sites besides the PLP binding sites in *endP* and *endQ*.^{16, 18} The introduction of the hydroxyl group on arginine presented a difficult biosynthetic question given the three enzymes possibly responsible.

Our collaborator, Dr. Silvaggi, sought an alternate route for the analysis of this biosynthetic pathway. As EndR and MppR are 73% identical, the results obtained from the crystallography on MppR should translate directly to EndR. From isolated recombinant MppR protein a full crystal structure (2.2 Å resolution) was obtained using the single-wavelength anomalous diffraction (SAD) method. MppR required an active site-bound ligand in order to crystallize. The active site of MppR with a HEPES molecule was shown to be similar to the acetoacetate family of enzymes. The key features of the binding site are Lys156, Arg148 and Glu283 surrounded by a hydrophobic pocket (Fig. 3.16). Arg148 coordinates the carboxyl group of the

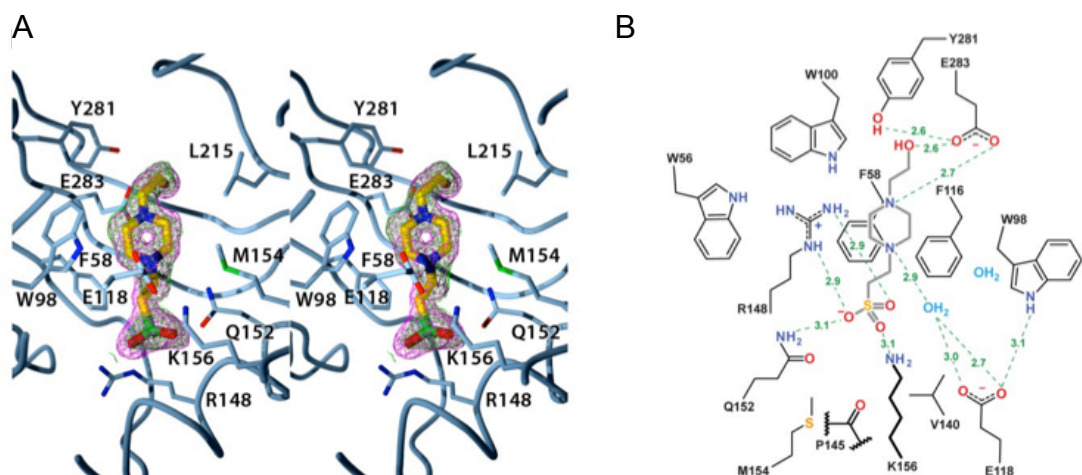


Figure 3.16 A) The stereo view of the MppR binding pocket showing the electron density map of the bound HEPES molecule. B) illustration and distances (Å) of hydrogen bonding and coordinating interactions between the binding pocket and the HEPES molecule.

substrate or, in this case, the sulphonate of HEPES and assists in the alignment of the substrate with Lys156 to form a Schiff base with the keto group. The negatively charged Glu283 hydrogen bonds with the piperazine ring of HEPES and is positioned to hydrogen bond with an arginic guanidine. The alignment suggests that MppR favors 2-keto acids rather than the 3-keto acids of typical acetoacetate decarboxylases. These data were confirmed when pyruvate, not acetoacetate, was observed bound in the active site (Fig. 3.17). Interestingly, when MppR crystals were soaked in a solution of 2-keto-4-OH arginate a 2-keto-enduracididine was observed bound to Lys156 in the active site. The reaction presumably occurred via spontaneous dehydration and cyclization of 2-keto-4-OH arginate in solution since both enantiomers were observed LC-MS and NMR analysis of the supernatant. However, the crystal structure of 2-keto enduracididine bound to MppR showed that only the correct 2-keto-4-*R* End was bound, suggesting that MppR is responsible for the cyclization reaction (Fig. 3.18).

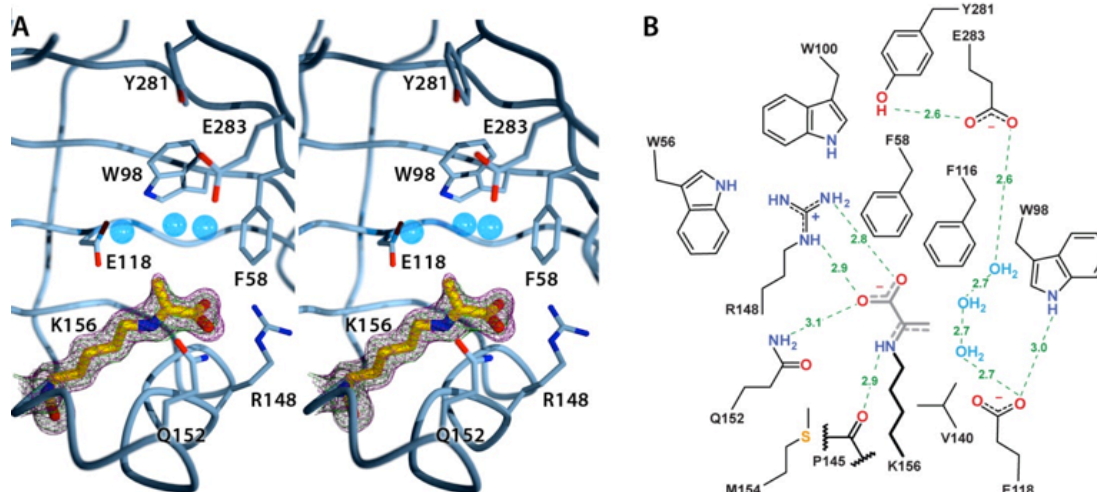


Figure 3.17 A) The stereo view of the MppR binding pocket showing the electron density map of the catalytic Lys forming a Schiff base with pyruvate. B) Schematic of the binding pocket showing distances (Å) of possible coordinating interactions.

The crystallographic data for MppR prompted a reassessment of the roles of the enzymes in enduracididine biosynthesis and reevaluation of the complementation assay results. For simplicity in discussion EndR/MppR will be referred to as EndR, EndP/MppP as EndP and EndQ/MppQ as EndQ. The crystallographic data suggest

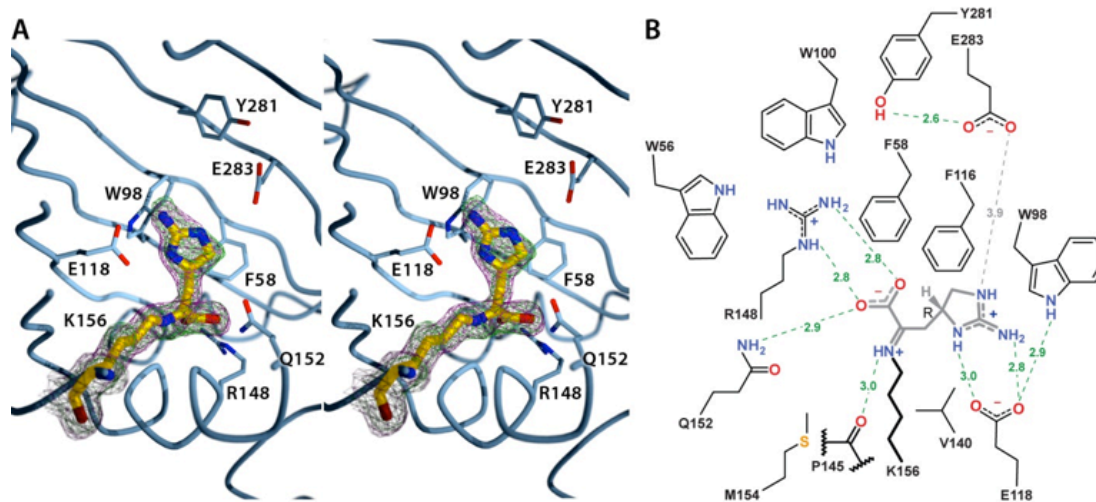


Figure 3.18 A) The stereo view of the MppR binding pocket showing the electron density map of the catalytic Lys forming a Schiff base with 2-keto-4-*R*-enduracididine. B) Schematic of the binding pocket showing distances (Å) of possible coordinating interactions.

EndQ most likely functions as a transaminase and EndR as a cyclase. EndP is proposed to function as a transaminase affording the 2-keto species to be used by EndR, as evidenced by the complementation studies. Assuming no other enzymes are involved in enduracididine biosynthesis, if EndP reacts with Arg then it must also function as an oxidase given that EndR shows no signs of having oxidase functionality and appears to function as a cyclase. If the substrate of EndR is derived directly from arginine then an oxidation must occur.

The possible spontaneous cyclization of 2-keto-4-OH arginate decreases the certainty of the previously hypothesized biosynthesis based on results from the feeding studies (Fig. 3.15). A conclusion that can be reached is that EndQ, assuming it is the only transaminase functioning in the pathway, can perform a transamination reaction with both 2-keto enduracididine and 4-OH Arg based on the complementation of the *endP* mutant and the need for the 2-keto group to facilitate the spontaneous elimination cyclization reaction. Either EndP or EndQ may be responsible for the oxidation, however the oxidative agent is unknown or bound to the protein in a manner not previously described in the bioinformatic databases.

An alternate pathway for enduracididine formation was proposed by Dr. Silvaggi based on an observed reaction that occurred during experiments with pyruvate-bound MppR. Soaking MppR in a solution containing pyruvate and 4-formylimidazole produced a new chemical species bound to the active site identified as (3*E*)-4-(1*H*-imidazol-5-yl)-2-oxobut-3-enoic acid (Fig. 3.19). This product is proposed to result from an aldol reaction followed by dehydration (Fig. 3.19C). From this observed product it is proposed that pyruvate and 2-guanidinoethaldehyde, produced from Arg, could undergo an aldol reaction followed by a dehydration cyclization reaction while bound to EndR/MppR. The species was found to be bound tightly to the enzyme preventing sufficient turnover to analyze the reaction kinetics. It is possible that EndP/MppP or EndQ/MppQ could act as a transaminase on alanine yielding pyruvate specifically for this reaction. The possible source of 2-guanidinoethaldehyde is

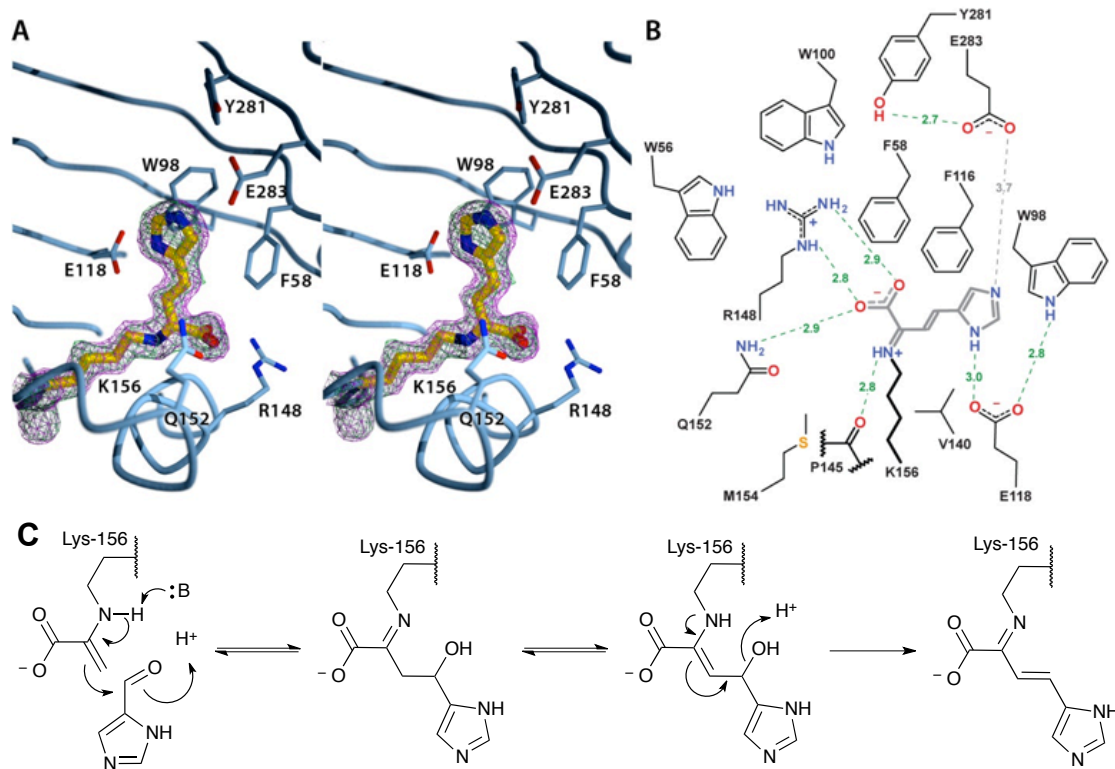


Figure 3.19 The stereo view of the MppR binding pocket showing the electron density map of the catalytic Lys forming a Schiff base with (3*E*)-4-(1*H*-imidazol-5-yl)-2-oxobut-3-enoic acid. B) Schematic of the binding pocket showing distances (Å) of possible coordinating interactions. C) Proposed aldol reaction and dehydration reaction catalyzed by MppR.

unknown, however, work done on the biosynthesis of nitroimidazole suggested that 4-OH Arg serves as a precursor for the production of 2-guanidinoethaldehyde via retro-aldol reaction. The aldehyde intermediate is then cyclized, possibly spontaneously, to form the aminoimidazole intermediate which is then oxidized to form the final 2-nitroimidazole product (Fig. 3.20). The production of 4-OH Arg requires oxygen and suggests that a flavin or transition metal-based oxygenase is responsible for the hydroxylation of Arg in *Streptomyces eurocidicus*.³¹ Additionally the possibility of a dehydrogenase forming the 2-keto-3-ene-arginate, a possible PLP-bound intermediate (Fig. 3.4), from 2-keto arginate remains plausible biosynthetic route yet to be explored.

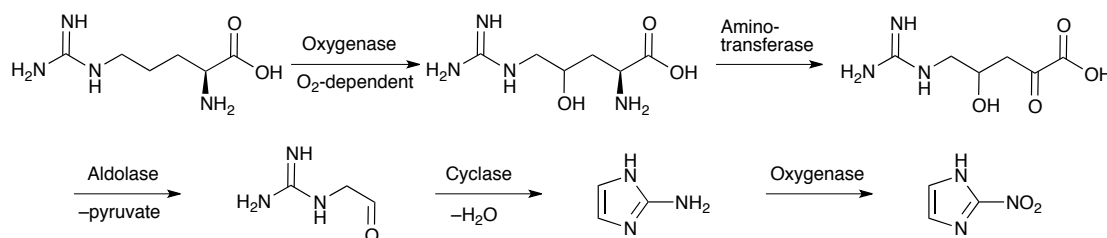


Figure 3.20 Nitroimidazole biosynthesis as proposed by Nakane *et al.* requires the oxidation of Arg followed by the formation of the 2-keto group. A retro aldol reaction is then catalyzed followed by cyclization and oxidation of the 2-amino group to form nitroimidazole.

As previously noted, the enduracidin biosynthetic gene cluster appears to contain only three genes for the production of 4-OH Arg and enduracididine. The further characterization of EndP and EndQ will determine whether 4-OH-2-ketoarginate is produced by EndP and then cyclized on EndR or if EndR performs an aldol reaction followed by cyclization. The experimental data suggests that enduracididine biosynthesis goes through 4-OH Arg or a related intermediate (*i.e.* 3,4-didehydro Arg) and that 4-OH Arg can serve as a biosynthetic intermediate to rescue enduracidin production in *endP* and *endR* mutants. From the crystallization data, it appears the spontaneous dehydration-cyclization of 2-keto-4-OH arginate, to form 2-keto enduracididine, complements the *endR* mutant in the supplementation studies. The complementation of the *endP* deletion mutant with 4-OH Arg indicates that EndQ can

act as an aminotransferase for both 2-ketoenduracididine and 4-OH Arg. The lack of a monooxygenase in the *end* biosynthetic gene cluster suggests 4-OH Arg precursors may be produced by gene products coded for elsewhere on the chromosome. Complete analysis of the *S. fungicidicus* and *Amycolatopsis hygrosopicus* genomes may provide insight into the possible origin of these precursors. The final steps of cyclization and amine formation in enduracididine biosynthesis have been determined, however, the formation of 4-OH Arg and its possible precursors require further experimentation to determine.

Experimental Procedures

Bacterial Strains, media and culture conditions

The wild type *Streptomyces fungicidicus* strain (ATCC21013) and *S. aureus* (ATCC 29213) were purchased from ATCC. EPI300TM-T1^R (Epicentre) was used as host for fosmids and *E. coli-Streptomyces* shuttle vectors. The plasmid pIJ773 was provided by Professor Keith Chater (JIC, Norwich, England). ISP2 (Difco), ISP4 (Difco) and tryptic soy broth (Difco) and other media components were purchased from VWR. For initial fluorine incorporation studies DL-3-F-tyrosine was purchased from Sigma. Media and culture conditions for *S. fungicidicus* were as previously described.¹⁶

Disruption of *endP*, *endQ* and *endR* genes

Three gene disruption plasmids were constructed using the methods previously described³⁰: pXY300 Δ endP for in-frame-deletion of *endP* on the chromosome, pXY148-endQ Ω Am^R for insertional disruption of *endQ* and pXY17R Ω Am^R for insertional disruption of *endR*. After completion of the gene disruption procedures in the enduracin-producing wild-type strain of *S. fungicidicus*, we obtained the desired mutant strains Sf Δ endP, SfendQ Ω Am^R and SfendR Ω Am^R. All these mutant strains were confirmed by Southern blot analysis.

Southern blot analysis

Genomic DNA from wild type and disruptant strains was prepared as described previously.³⁰ Restricted genomic DNA was separated by electrophoresis in 0.8% agarose gel and transferred onto positively charged nylon membrane (Roche). The DNA probe was prepared using digoxigenin-labeled dUTP and hybridization was revealed using a digoxigenin-DNA detection kit (Roche).

Complementation studies

Seed cultures for each strain (wild-type strain was used as a control) were inoculated and grown in TSB broth (5 mL) in sterile 20 mL culture tubes for 24 hr. Sterile production media (25 mL in 125 erlenmeyer flasks containing a spring) was inoculated using 1 mL of seed culture and incubated at 29 °C and shaking at 200 rpm. Solutions of enduracididine and hydroxyarginine (100 mg/mL in DI water) were sterilized by syringe filtration (0.2 µm). Cultures were supplemented with 30 mg of compound on day 4, 20 mg on day 5, and 10 mg on day 6. After 11 days the culture mycelia were pelleted by centrifugation at 3000 rpm for 30 min. The pellets were extracted using 70% *aq.* methanol overnight, concentrated *in vacuo* and analyzed via HPLC.

HPLC and mass spectroscopic analysis

HPLC analysis was performed using a Shimadzu CBM-20 instrument equipped with an SPD-20 diode array detector monitoring 230, 254 and 270 nm wavelengths. A Phenomenex 4.6 x 100 mm Kinetex 2.6 µm XB-C18 column was used with a linear gradient from 10% MeCN in water + 0.1% TFA to 100% MeCN over 13 min. to analyze the samples. Mass spectrometric analysis was performed using a Thermo Finnigan LCQ Advantage instrument in ESI+ mode. LCMS analysis was performed on a ABSciex 3200 Triple Quadrupole spectrometer with a Shimadzu CBM-20 instrument using a gradient from 10% MeCN in 50 mM ammonium formate buffer to 50% MeCN over 30 min with a flow rate of 0.5 mL/min using the Kinetex column.

NMR analysis

NMR spectra were recorded using a Bruker DRX 300 MHz instrument (¹H-300 MHz, ¹³C-75 MHz). Data were processed and analyzed using Topspin ver 1.3 (Bruker) and MestReNova ver. 8.0.2-11021 (Mestrelab Research).

Solvents and reagents

All reagents were purchased from Sigma Aldrich or Alpha Aesar. Allylglycine was

purchased as a racemic mixture of 95% purity and as L-allylglycine at greater than 99% purity. Histidine was purchased as the L form as biological grade. All other reagents were purchased as ACS reagent grade products. Water was deionized (18 MΩ) using a Barnstead B-Pure filtration system. THF was distilled under Ar from a sodium-benzophenone solvent still using unstabilized anhydrous solvent. Triethylamine was purchased as ACS reagent grade and passed through a column of basic alumina (50-200 μm) prior to use. Other solvents were purchased and used without further purification.

***tert*-Butyl 5-(iodomethyl)-2-oxo-tetrahydrofuran-3-ylcarbamate (2,3):** A solution of iodine (26.45 g, 104 mmol) in THF (160 mL) was added dropwise at 0 °C to a solution of **1** (7.48 g, 34 mmol) in THF (120 mL) and 1M sodium bicarbonate (350 mL). The reaction mixture was stirred in an ice bath for 5 hrs then quenched with saturated sodium sulfite (160 mL). The mixture was extracted with EtOAc and the combined organics were washed with water and brine, then dried over sodium sulfate. The solvent was removed under reduced pressure yielding an off-white solid. The *cis* isomers were separated by crystallization from EtOAc and hexanes precipitation of the mother liquor produced a mixture of the *cis* and *trans* isomers. *Cis* isomers **2** (9.81 g, 28.7 mmol, 84%), ¹H-NMR (300 MHz, CDCl₃) δ (ppm): 1.46 (s, 9H), 1.87 (dd, *J*₁ = 12.3 Hz, *J*₂ = 10.5 Hz, 1H), 3.02 (m, 1H), 3.32 (dd, *J*₁ = 10.5 Hz, *J*₂ = 7.2 Hz, 1H), 3.45 (dd, *J*₁ = 10.5 Hz, *J*₂ = 4.8 Hz, 1H), 4.45 (m, 2H), 5.07 (bs, 1H). *Trans* isomers **3** (0.98 g, 2.9 mmol, 9%) ¹H-NMR (300 MHz, CDCl₃) δ (ppm): 1.46 (s, 9H), 2.41 (dd, *J*₁ = 12.3 Hz, *J*₂ = 10.5 Hz, 1H), 2.62 (m, 1H), 3.36 (m, 2H), 4.36 (m, 1H), 4.75 (m, 1H), 5.06 (bs, 1H). LRMS, ESI (+) *m/z* = 342.0.

***Cis t*-Butyl 5-(azidomethyl)-2-oxo-tetrahydrofuran-3-ylcarbamate (4):** To a solution of the iodides **2** and **3** (for 4-*S*-OH-L-Arg only **2** was used) (0.5 g, 1.47 mmol) in anhydrous *N,N*-dimethylformamide (8 mL) sodium azide (0.476 g, 7.3 mmol) was

added and the mixture was stirred at 40 °C for 17 hrs. After cooling to room temperature, the reaction mixture was poured into ice and extracted with ethyl acetate. The combined organic extracts were washed with water as well as brine, dried and evaporated *in vacuo* to give an oil that was purified by flash chromatography (ethyl acetate: hexane = 3:7) to afford **4** (368 mg, 1.43 mmol, 98%) as a clear solid. ¹H-NMR (300 MHz, CDCl₃) δ (ppm): 1.46 (s, 9H), 1.87 (q, *J* = 11.4 Hz, 1H), 2.77 (m, 1H), 3.50 (dd, *J*₁ = 13.5 Hz, *J*₂ = 5.4 Hz, 1H), 3.64 (dd, *J*₁ = 13.5 Hz, *J*₂ = 3.6 Hz, 1H), 4.48 (m, 1H), 4.57 (m, 1H), 5.09 (bs, 1H); ¹³C-NMR (75 MHz, CDCl₃) δ (ppm): 28.63, 33.04, 50.98, 53.29, 75.65, 80.80, 155.31, 173.83. LRMS, ESI (+) *m/z* = 257.1.

4-Hydroxylarginine HCl salt (7): To a solution of **6** (0.60 g, 1.26 mmol) in dioxane (11 mL) was added 1N-NaOH (15 mL) and the mixture was stirred at room temperature for 18 hrs. After being cooled to 0 °C, 4N-HCl (15 mL) was added slowly and the mixture was stirred at room temperature for 4 hrs. Then the solvents were evaporated to give a white solid. The product was chromatographed on a Dowex 50W X 8 (hydrogen form, 200 mesh) column and eluted using a gradient, with water and 4N-HCl yielding **7** (250 mg, 95 mmol, 75% yield) as a foamy solid. ¹H-NMR (300 MHz, D₂O) δ (ppm): 2.09 (q, *J* = 12 Hz, 1H), 2.81 (m, 1H), 3.43 (dt, *J*₁ = 15.3 Hz, *J*₂ = 5.4 Hz, 1H), 3.66 (d, *J*₁ = 15.3 Hz, 1H), 4.50 (dd, *J*₁ = 12 Hz, *J*₂ = 9 Hz, 1H), 4.78 (m, 1H); ¹³C-NMR (75 MHz, D₂O) δ (ppm): 172.85, 157.26, 77.60, 49.24, 43.35, 29.23; LRMS ESI (+) *m/z* = 190.1.

***N',N''*-Di-Boc-guanidine (10):** To a solution of **9** (2.4 g, 25 mmol) in H₂O (25 mL) was added NaOH (4.1 g, 100 mmol) and dioxane (50 mL). The solution was cooled in an ice bath and Boc₂O (12.26 g, 55 mmol) was added and allowed to come to ambient temperature over 20 hrs. The reaction was concentrated to one third volume under reduced pressure, diluted with water and extracted with EtOAc. The combined organics were washed with 10% citric acid, water and brine then dried over Na₂SO₄

and the solvent removed *in vacuo*. The crude product was purified via flash chromatography (silica gel, 1:4 EtOAc:Hexanes) yielding **10** (3.6 g, 13.9 mmol, 55% yield) as a white amorphous solid. ¹H-NMR (300 MHz, CDCl₃) δ (ppm): 10.42 (br s, 1 H), 8.44 (br s, 2H), 1.38 (s, 18H) ¹³C NMR (75 MHz, CDCl₃) δ 158.43, 152.41, 80.99, 27.88. LRMS, ESI (+) *m/z* = 260.2.

N-Tf, N',N''-di-Boc-guanidine (11): To a solution of **8** (2.5 g, 9.6 mmol) and triethylamine (1.4 mL, 9.6 mmol) in distilled DCM (50 mL) at -78 °C trifluoromethanesulfonic anhydride (1.7 mL, 9.6 mmol) was added dropwise maintaining temperature below -65 °C. The reaction was allowed to warm to 10 °C over 5 hrs. The reaction was quenched with 1M potassium bisulfate and then washed with water. The organics were dried over Na₂SO₄ and the solvent removed *in vacuo*. The crude product was purified via flash chromatography (silica gel, DCM) yielding **11** (2.4 g, 6.13 mmol, 64% yield) as a white crystalline solid. ¹H-NMR (300 MHz, CDCl₃) δ (ppm): 10.04 (br s, 2 H), 1.5 (s, 18H). ¹³C NMR (75 MHz, CDCl₃) δ 151.44, 148.89, 119.26 (q, *J*=320.1 Hz), 85.90, 27.70. LRMS, ESI (+) *m/z* = 391.1.

L-Histidine methyl ester (12): To a stirred mixture of L-His (3 g, 19.34 mmol) and MeOH (180 mL) in an ice bath was added thionylchloride (2.81 mL, 38.67 mmol) over 1 hr. The insoluble His dissolved after half of the thionyl chloride was added. The flask was removed from the ice bath and equipped with a reflux condenser and refluxed 18 hrs. The reaction was then cooled and the solvent was removed under reduced pressure. The product was crystallized from MeOH–ether yielding **12** (4.28 g, 17.7 mmol, 91% yield) as white crystals. ¹H NMR (300 MHz, methanol-*d*₄) δ 8.67 (d, *J* = 1.4 Hz, 1H), 7.41 (d, *J* = 1.1 Hz, 1H), 4.47 (t, *J* = 6.8 Hz, 1H), 3.81 (s, 3H), 3.53 – 3.29 (m, 2H); ¹³C NMR (75 MHz, methanol-*d*₄) δ 167.94, 134.57, 126.92, 118.49, 52.88, 51.66, 25.09; LRMS ESI (+) *m/z* = 170.1.

(S,Z) 2,4,5-tris(benzamido)pent-4-enoate methyl ester (13): To a stirred solution of **12** (500 mg, 2.07 mmol) in water (17 mL) in an icebath was added concurrently benzoyl chloride (1.44 mL, 12.4 mmol) in benzene (10 mL) with Na₂CO₃ (2.85 g, 26.9 mmol) over 1 hr. The reaction was stirred at ambient temperature for 24 hrs. EtOAc (40 mL) was then added and the organic layer was isolated and the solvent removed under reduced pressure. The product was dissolved in 3:2 THF:1M NaHCO₃ (30 mL) and stirred for 24 hours. The precipitate was removed by filtration and washed with water. The solid was dissolved in MeOH and precipitated affording **13** (871 mg, 1.84 mmol, 89% yield) as a white solid. ¹H NMR (300 MHz, DMSO-*d*₆) δ 9.80 (d, *J* = 9.3 Hz, 1H), 9.54 (s, 1H), 8.75 (d, *J* = 7.9 Hz, 1H), 7.98 – 7.72 (m, 6H), 7.65 – 7.36 (m, 9H), 6.84 – 6.57 (m, 1H), 4.70 (bs, 1H), 3.62 (s, 3H), 3.20 (td, *J* = 12.6, 11.0, 5.1 Hz, 1H), 2.81 (dd, *J* = 14.3, 10.2 Hz, 1H); ¹³C NMR (75 MHz, DMSO-*d*₆) δ 172.28, 166.63, 166.00, 163.38, 134.46, 133.96, 133.46, 131.92, 131.66, 131.50, 128.62, 128.32, 128.00, 127.47, 127.32, 117.28, 115.32, 52.05, 51.12, 33.89. LRMS, ESI (+) *m/z* = 472.2.

(S,Z) 2,4,5-tris(benzamido)pentanoate methyl ester (14): To a solution of **13** (400 mg, 0.85 mmol) dissolved in EtOH (60 mL) and 2:1 AcOH:H₂O (10 mL) was added Pd/C (542 mg, 0.25 mmol). The reaction was purged with H₂ gas 4 times and then heated to 60°C. After stirring for 18 hrs the reaction was cooled and filtered through a pad of celite. The solvent was then removed under reduced pressure. The product was dissolved in EtOH with heating, allowed to cool to ambient temperature and then precipitated with the addition of Et₂O affording **14** (359 mg, 0.77 mmol, 90% yield). ¹H NMR (300 MHz, DMSO-*d*₆) δ 8.80 (dd, *J* = 10.0, 7.7 Hz, 1H), 8.61 (t, *J* = 5.9 Hz, 0.5H), 8.52 (t, *J* = 6.2 Hz, 0.5H), 8.39 (dd, *J* = 11.4, 8.6 Hz, 1H), 7.94 – 7.73 (m, 6H), 7.63 – 7.36 (m, 9H), 4.68 (q, *J* = 7.1 Hz, 0.5H), 4.59 – 4.47 (m, 0.5H), 4.44 – 4.26 (m, 1H), 3.63 (s, 1.5H), 3.56 (s, 1.5H), 3.63 – 3.40 (m, 2H), 2.33 – 1.99 (m, 2H); ¹³C

NMR (75 MHz, DMSO-*d*₆) δ 173.07, 172.40, 166.96, 166.75, 166.74, 166.69, 166.63, 166.20, 134.97, 134.78, 134.64, 134.58, 134.11, 133.65, 131.56, 131.36, 131.17, 131.08, 131.00, 128.34, 128.26, 128.20, 128.17, 128.10, 127.57, 127.44, 127.41, 127.38, 127.36, 127.29, 52.01, 51.96, 50.31, 50.08, 47.47, 46.61, 43.37, 42.67, 32.92, 32.17. LRMS, ESI (+) m/z = 474.2.

(2-*S*, 4-*RS*) 2,4,5-Triaminopentanoate (15): A solution of **14** (300 mg, 0.64 mmol) in 6 N HCl (30 mL) was refluxed under Ar for 18 hrs. The reaction was then cooled to 4 °C and washed with Et₂O three times. The aqueous layer was separated and the solvent removed under reduced pressure. The product was not purified further and taken on to the next reaction.

Enduracididine (16): Method A: The solid was dissolved in 100 mM Na₃PO₄ buffer pH 11 (16 mL) was added BrCN (360 mg, 3.4 mmol) dissolved in water (8 mL) in portions over 2.5 hr. The solvent was removed under reduced pressure. The solid was dissolved in 6 N HCl (40 mL) and refluxed for 2 hr. The reaction was allowed to cool to ambient temperature and the solvent removed under reduced pressure. The product was dissolved in minimal water, adjusted to pH 7 and chromatographed on Dowex 50X2 cation exchange resin (H⁺ form) Eluting with water 1 N HCl, 2 N HCl and 4 N HCl affording the product **16** (2 HCl salt form) in the 4 N HCl fractions (47 mg, 0.19 mmol, 30% yield) as a brown solid. ¹H NMR (300 MHz, D₂O) δ 4.39 – 4.27 (m, 1H), 4.26 – 4.09 (m, 1H), 3.82 (td, J = 9.7, 5.6 Hz, 1H), 3.40 (dd, J = 9.9, 6.5 Hz, 1H), 2.26 – 1.95 (m, 2H); ¹³C NMR (75 MHz, D₂O) δ 177.97, 177.70, 159.28, 159.15, 55.96, 55.71, 52.11, 51.92, 48.19, 48.07, 35.45, 35.29; LRMS ESI (+) m/z = 173.1.

Method B: The solid (from 12.2 mmol) was dissolved in water (240 mL) and adjusted to pH 11 with 1 N NaOH. BrCN (5.8 g, 55 mmol) in water (210 mL) was added dropwise over 2.5 hr. The pH was carefully monitored and maintained above pH 10 with 1 N NaOH over the duration of the reaction. After an additional 30 min of

stirring the solvent was removed under reduced pressure. The solid was dissolved in 6 N HCl (600 mL) and refluxed for 2 hr. The reaction was allowed to cool to ambient temperature and the solvent removed under reduced pressure. The product was dissolved in minimal water, adjusted to pH 7 and purified using cation exchange chromatography Dowex 50X2 resin (H⁺ form) Eluting with water, 1 N HCl, 2 N HCl and 4 N HCl affording the product **16** (2 HCl salt form) in the 4 N HCl fractions (2.16 g, 8.79 mmol, 72% yield) as a grey solid. ¹H NMR (300 MHz, D₂O) δ 4.39 – 4.27 (m, 1H), 4.26 – 4.09 (m, 1H), 3.82 (td, *J* = 9.7, 5.6 Hz, 1H), 3.40 (dd, *J* = 9.9, 6.5 Hz, 1H), 2.26 – 1.95 (m, 2H); ¹³C NMR (75 MHz, D₂O) δ 177.97, 177.70, 159.28, 159.15, 55.96, 55.71, 52.11, 51.92, 48.19, 48.07, 35.45, 35.29; LRMS ESI (+) *m/z* = 173.1.

References

1. Izumi, R.; Take, T.; Ando, T.; Noda, T.; Nagata, A., Studies on Tuberactinomycin .3. Isolation and Characterization of 2 Minor Components, Tuberactinomycin-B and Tuberactinomycin-O. *J. Antibiot.* **1972**, *25* (4), 201-207.
2. Noda, T.; Nagata, A.; Take, T.; Wakamiya, T.; Shiba, T., Chemical studies on tuberactinomycin. 3. The chemical structure of viomycin (tuberactinomycin B). *J. Antibiot.* **1972**, *25* (7), 427-428.
3. McDonald, L. A.; Barbieri, L. R.; Carter, G. T.; Lenoy, E.; Lotvin, J.; Petersen, P. J.; Siegel, M. M.; Singh, G.; Williamson, R. T., Structures of the Muraymycins, Novel Peptidoglycan Biosynthesis Inhibitors. *J. Am. Chem. Soc.* **2002**, *124* (35), 10260-10261.
4. (a) Tatsuta, K.; Mikami, N.; Fujimoto, K.; Umezawa, S.; Umezawa, H.; Aoyagi, T., The structure of chymostatin, a chymotrypsin inhibitor. *J. Antibiot.* **1973**, *26* (11), 625-646; (b) Umezawa, H.; Aoyagi, T.; Morishim.H; Kunimoto, S.; Matsuzak.M; Hamada, M.; Takeuchi, T., Chymostatin, a new chymotrypsin inhibitor produced by actinomycetes. *J. Antibiot.* **1970**, *23* (8), 425-427.
5. Bodanszky, M.; Izdebski, J.; Muramatsu, I., Structure of the peptide antibiotic stendomycin. *J. Am. Chem. Soc.* **1969**, *91* (9), 2351-2358.
6. He, H.; Williamson, R. T.; Shen, B.; Graziani, E. I.; Yang, H. Y.; Sakya, S. M.; Petersen, P. J.; Carter, G. T., Mannopectimycins, Novel Antibacterial Glycopeptides from *Streptomyces hygrosopicus*, LL-AC98. *J. Am. Chem. Soc.* **2002**, *124* (33), 9729-9736.

7. Fellows, L. E.; Bell, E. A.; Leet, T. S.; Janzen, D. H., Tetrahydrolathyrine: A new amino acid from seeds of *Lonchocarpus costaricensis*. *Phytochemistry* **1979**, *18* (8), 1333-1335.
8. Bell, E. A.; Foster, R. G., Structure of Lathyrine. *Nature* **1962**, *194* (4823), 91-92.
9. Garcia, A.; Vasquez, M. J.; Quinoa, E.; Riguera, R.; Debitus, C., New Amino Acid Derivatives from the Marine Ascidian *Leptoclinides dubius*. *J. Nat. Prod.* **1996**, *59* (8), 782-785.
10. Fellows, L. E.; Hider, R. C.; Bell, E. A., 3-[2-Amino-2-imidazolin-4(5)-yl]alanine (enduracididine) and 2-[2-amino-2-imidazolin-4(5)-yl] acetic acid in seeds of *Lonchocarpus sericeus*. *Phytochemistry* **1977**, *16* (12), 1957-1959.
11. (a) Hamada, M.; Kondo, S.; Yokoyama, T.; Miura, K.; Iinuma, K., Letter: Minosaminomycin, a new antibiotic containing myo-inosamine. *J. Antibiot.* **1974**, *27* (1), 81-83; (b) Iinuma, K.; Kondo, S.; Maeda, K.; Umezawa, H., Structure of Minosaminomycin. *J. Antibiot.* **1975**, *28* (8), 613-615; (c) Iinuma, K.; Kondo, S.; Maeda, K.; Umezawa, H., Total Synthesis of Minosaminomycin. *Bull. Chem. Soc. Jpn.* **1977**, *50* (7), 1850-1854.
12. (a) Holmes, T. C.; May, A. E.; Zaleta-Rivera, K.; Ruby, J. G.; Skewes-Cox, P.; Fischbach, M. A.; DeRisi, J. L.; Iwatsuki, M.; Omura, S.; Khosla, C., Molecular Insights into the Biosynthesis of Guadinomine: A Type III Secretion System Inhibitor. *J. Am. Chem. Soc.* **2012**; (b) Mihali, T. K.; Kellmann, R.; Muenchhoff, J.; Barrow, K. D.; Neilan, B. A., Characterization of the Gene Cluster Responsible for Cylindrospermopsin Biosynthesis. *Appl. Environ. Microbiol.* **2008**, *74* (3), 716-722.
13. Hatano, K.; Nogami, I.; Higashide, E.; Kishi, T., Biosynthesis of Enduracidin: Origin of Enduracididine and Other Amino Acids. *Agric. Biol. Chem.* **1984**, *48* (6), 1503-08.

14. Yin, X.; Zabriskie, T. M., VioC is a Non-Heme Iron, α -Ketoglutarate-Dependent Oxygenase that Catalyzes the Formation of 3S-Hydroxy-L-Arginine during Viomycin Biosynthesis. *ChemBioChem* **2004**, *5* (9), 1274-1277.
15. Yin, X.; McPhail, K. L.; Kim, K.-j.; Zabriskie, T. M., Formation of the Nonproteinogenic Amino Acid 2S,3R-Capreomycidine by VioD from the Viomycin Biosynthesis Pathway. *ChemBioChem* **2004**, *5* (9), 1278-1281.
16. Yin, X.; Zabriskie, T. M., The enduracidin biosynthetic gene cluster from *Streptomyces fungicidicus*. *Microbiology* **2006**, *152* (10), 2969-83.
17. Magarvey, N. A.; Haltli, B.; He, M.; Greenstein, M.; Hucul, J. A., Biosynthetic Pathway for Mannopeptimycins, Lipoglycopeptide Antibiotics Active against Drug-Resistant Gram-Positive Pathogens. *Antimicrob. Agents Chemother.* **2006**, *50* (6), 2167-2177.
18. Haltli, B.; Tan, Y.; Magarvey, N. A.; Wagenaar, M.; Yin, X.; Greenstein, M.; Hucul, J. A.; Zabriskie, T. M., Investigating β -Hydroxyenduracididine Formation in the Biosynthesis of the Mannopeptimycins. *Chem. Biol.* **2005**, *12* (11), 1163-1168.
19. (a) Iwatsuki, M.; Uchida, R.; Yoshijima, H.; Ui, H.; Shiomi, K.; Kim, Y.-P.; Hirose, T.; Sunazuka, T.; Abe, A.; Tomoda, H.; Omura, S., Guadinomines, Type III Secretion System Inhibitors, Produced by *Streptomyces* sp. K01-0509. *J. Antibiot.* **2008**, *61* (4), 230-236; (b) Iwatsuki, M.; Uchida, R.; Yoshijima, H.; Ui, H.; Shiomi, K.; Matsumoto, A.; Takahashi, Y.; Abe, A.; Tomoda, H.; Omura, S., Guadinomines, Type III Secretion System Inhibitors, Produced by *Streptomyces* sp. K01-0509. *J. Antibiot.* **2008**, *61* (4), 222-229.
20. Highbarger, L. A.; Gerlt, J. A.; Kenyon, G. L., Mechanism of the Reaction Catalyzed by Acetoacetate Decarboxylase. Importance of Lysine 116 in Determining the pKa of Active-Site Lysine 115. *Biochemistry* **1996**, *35* (1), 41-46.

21. Gould, S. J.; Lee, J.; Wityak, J., Biosynthesis of streptothricin F: 7. The fate of the arginine hydrogens. *Bioorg. Chem.* **1991**, *19* (3), 333-350.
22. Overman, L. E.; Wolfe, J. P., Synthesis of Polycyclic Guanidines by Cyclocondensation Reactions of N-Amidinyliminium Ions. *J. Org. Chem.* **2001**, *66* (9), 3167-3175.
23. Yoon, G.; Zabriskie, T. M.; Cheon, S. H., Synthesis of [guanido-¹³C]-gamma-hydroxyarginine. *J. Labelled Compd. Radiopharm.* **2009**, *52* (2), 53-55.
24. Yong, Y. F.; Kowalski, J. A.; Lipton, M. A., Facile and Efficient Guanylation of Amines Using Thioureas and Mukaiyama's Reagent. *J. Org. Chem.* **1997**, *62* (5), 1540-1542.
25. Fotsch, C. H.; Wong, C.-H., Synthesis of a guanidino-sugar as a glycosyl cation mimic. *Tetrahedron Lett.* **1994**, *35* (21), 3481-3484.
26. (a) Feichtinger, K.; Zapf, C.; Sings, H. L.; Goodman, M., Diprotected Triflylguanidines: A New Class of Guanidinylation Reagents. *J. Org. Chem.* **1998**, *63* (12), 3804-3805; (b) Santana, A. G.; Francisco, C. G.; Suárez, E.; González, C. C., Synthesis of Guanidines From Azides: A General and Straightforward Methodology In Carbohydrate Chemistry. *J. Org. Chem.* **2010**, *75* (15), 5371-5374.
27. (a) Saniere, L.; Leman, L.; Bourguignon, J.-J.; Dauban, P.; Dodd, R. H., Iminoiodane mediated aziridination of α -allylglycine: access to a novel rigid arginine derivative and to the natural amino acid enduracididine. *Tetrahedron* **2004**, *60* (28), 5889-5897; (b) Tsuji, S.; Kusumoto, S.; Shiba, T., Synthesis of Enduracididine - Component Amino-Acid of Antibiotic Enduracidin. *Chem. Lett.* **1975**, (12), 1281-1284.
28. (a) Trampota, M. Process for the synthesis of L-(+)-ergothioneine. 2008-240173 2009093642, 20080929., 2009; (b) Altman, J.; Grinberg, M.; Wilchek, M., Approach to chiral vicinal diacylamines by Bamberger ring cleavage of substituted imidazoles.

Liebigs Ann. Chem. **1990**, (4), 339-43; (c) Altman, J.; Shoef, N.; Wilchek, M.; Warshawsky, A., Bifunctional chelating agents. Part 2. Synthesis of 1-(2-carboxyethyl)ethylenediaminetetraacetic acid by ring cleavage of substituted imidazole. *J. Chem. Soc., Perkin Trans. I* **1984**, (1), 59-62.

29. Jackson, M. D.; Gould, S. J.; Zabriskie, T. M., Studies on the Formation and Incorporation of Streptolidine in the Biosynthesis of the Peptidyl Nucleoside Antibiotic Streptothricin F. *J. Org. Chem.* **2002**, 67 (9), 2934-2941.

30. Yin, X.; Chen, Y.; Zhang, L.; Wang, Y.; Zabriskie, T. M., Enduracidin Analogues with Altered Halogenation Patterns Produced by Genetically Engineered Strains of *Streptomyces fungicidicus*. *J. Nat. Prod.* **2010**, 73 (4), 583-589.

31. Nakane, A.; Nakamura, T.; Eguchi, Y., A novel metabolic fate of arginine in *Streptomyces eurocidicus*. Partial resolution of the pathway and identification of an intermediate. *J. Biol. Chem.* **1977**, 252 (15), 5267-5273.

CHAPTER FOUR

SEMISYNTHETIC MODIFICATION OF ENDURACIDIN

Neal Goebel

Introduction

The bioactivity of enduracidin relies on binding as a dimer to the proximal end of Lipid II. The depsipeptide portion of enduracidin forms a binding pocket which coordinates with the sugar diphosphate linkage of Lipid II.¹ The role of the lipid tail of the peptide, however, is less defined. Crystal structures of the related antibiotic ramoplanin suggest the lipid tail associates with the lipid membrane, possibly being responsible for bringing enduracidin in proximity to Lipid II (Fig. 4.1A).² The lipid tail of enduracidin also decreases the solubility of the compound and may be associated with the observed accumulation phenomenon of enduracidin in intramuscular and intravenous injections.³ Our investigations have proceeded in the interest of understanding the biosynthesis of the lipid tail and altering it to improve the physical properties of enduracidin.

The lipid tail is produced through primary metabolic pathways using a valine (for End A) or isoleucine (for End B) derived starter unit followed by the addition, reduction and dehydrogenation of four acetate units forming a saturated lipid chain

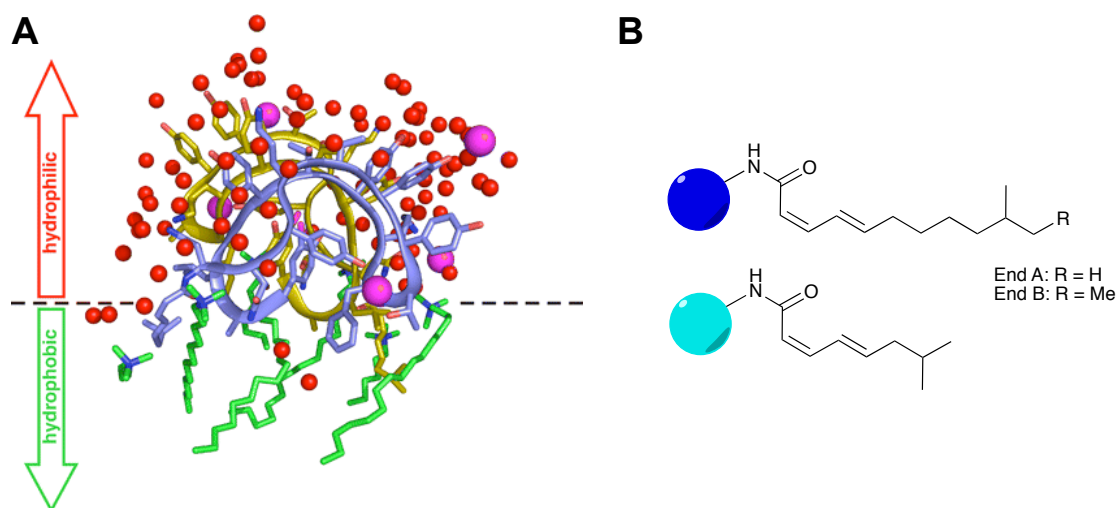


Figure 4.1 A) Crystal structure of a ramoplanin dimer (yellow and purple) interfacing with detergent molecules (green), chloride ions (magenta) and ordered water molecules (red). Figure is from Hamburger *et al.*² B) The lipid tail structures of enduracidin (blue) and ramoplanin (cyan).

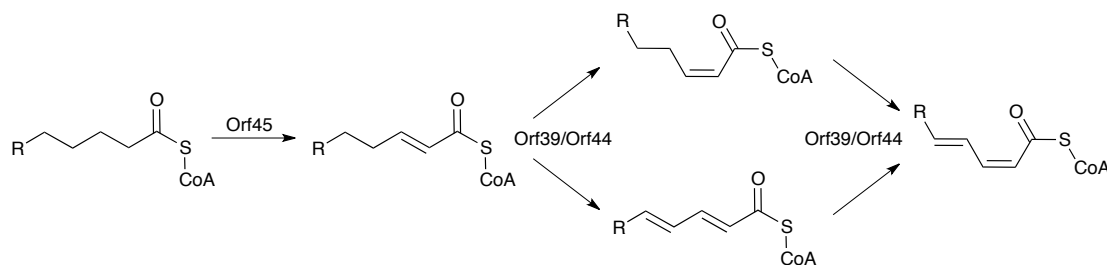


Figure 4.2 Possible routes for the introduction of the C2 and C4 double bonds and isomerization of the C2 alkene.

branched at the 10 carbon (Fig. 4.1B).⁴ Four gene products are predicted to be involved in the activation and tailoring of the 2-*Z*, 4-*E* configured unsaturated lipid tail: Orf35, Orf39, Orf44 and Orf45. Orf35, from bioinformatic analysis, correlates well with the ACP/PCP family proteins and is likely responsible for correlating with the NRPS unit EndA to produce the acyl-Asp starter unit. Bioinformatic analysis predicts that Orf39 and Orf44 are Acyl-CoA dehydrogenases while Orf45 is an Acyl-CoA lygase/hydrogenase fusion protein. Based on the data from friulimicin biosynthesis, it is hypothesized that Orf45 is responsible for the activation of the carboxylic acid as the CoA-thioester and introduction of a double bond.⁵ Orf39 and Orf44 are then predicted to be responsible for the introduction of the second double bond and isomerization of the first to the *Z* configuration (Fig. 4.2). These genes all have homologs in the ramoplanin biosynthetic gene cluster. Ramoplanin contains a shorter lipid tail which shares its double bond pattern with enduracidin (Fig. 4.1B).⁶ For the study of the biosynthetic enzymes, the production of enduracidin analogs having partially reduced and isomerized lipid tails was undertaken.

The planned modification of the enduracidin lipid tail raised further interest in replacing the tail completely. The lipid tail, bound as an amide to the enduracidin depsipeptide ring, has limited synthetic accessibility while incorporated into enduracidin. Hydrolysis via mild acid or base is likely to have no selectivity. Enzymatic deacylation is a known method of deactivating lipopeptide antibiotics in bacteria.⁷ Enzymatic deacylation activity has been found to be linked with ring

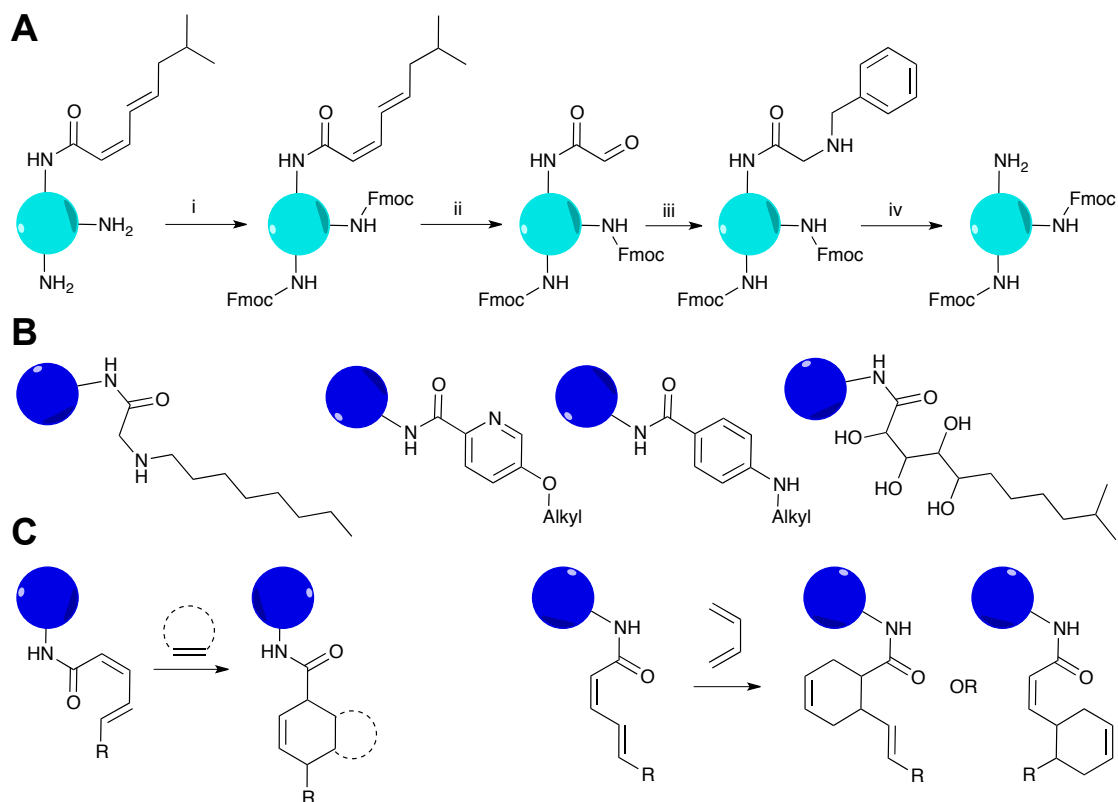


Figure 4.3 A) Removal of the lipid tail of ramoplanin as described by Ciabatti *et al.* starting with i) protection using Fmoc-OSu, ii) Ozonolysis with PPh_3 reductive work up, iii) reductive amination using NaBH_3CN and iv) Edman degradation. B) Proposed lipid tail replacements for enduracidin and tetrahydroxylation of the alkenes. C) Potential Diels-Alder reactions with the lipid tail alkenes.

cleavage reactions particularly at the lactone ester linkage.⁸ The potentially low production yield of deacylated peptide and the time required to isolate the hydrolytic proteins lead to the exploration of an alternative method. After concluding our studies on the deacylation of enduracidin, an enzymatic deacylation method was successfully adapted for ramoplanin.⁹ Unfortunately, there was insufficient time to pursue this method for use with enduracidin.

The presence of the two double bonds in the lipid tail provides a potential chemical handle for the production of altered enduracidins. The semisynthesis of ramoplanin lipid tail analogs by Ciabatti *et al.* demonstrated the use of an ozonolysis reaction to cleave the lipid tail, affording an aldehyde as a synthetic handle on the peptide. The aldehyde was then converted to the benzylamine via reductive amination

and the asparagine-1 α -amine freed via Edman degradation (Fig. 4.3A).¹⁰ In an attempt to improve enduracidin solubility, our investigation focused on the introduction of polar/charged groups into the lipid tail to improve solubility (Fig. 4.3B). As an alternative modification the use of Diels-Alder type reactions for the introduction of new function groups was also explored (Fig. 4.3C). The final lipid tail modification planned was the hydroxylation of the double bonds.

The introduction of nitro groups on the Hpg residues of enduracidin failed during incorporation experiments with 3-nitro-Hpg as described in chapter 2. Therefore, a semisynthetic approach to nitro enduracidin (NO₂-End) was investigated. Several examples in the literature demonstrate the nitration of tyrosine in proteins with peroxyxynitrite¹¹ and tetranitromethane (TNM)¹² and the neutrally buffered conditions are amenable to enduracidin. Nitration reactions on tyrosine using nitrite and nitrate salts under acidic conditions have also been demonstrated on natural products.¹³ The nitration of the β -OH enduracididine-containing antibiotic mannopeptimycin suggests that the enduracididine residues of enduracidin will not be altered under these conditions.¹⁴ Furthermore, the antifungal lipodepsipeptide FR901469 was successfully nitrated, also suggesting that enduracidin would tolerate the reaction conditions. FR901469 required protection of the Orn δ -amine with Boc.¹⁵ As the lipid tail work also required the preparation of protected enduracidin, the production of starting material was simplified. Additionally, personal experience isolating enduracidin by a 1:1:1 MeOH:Acetone:HCl (1 N) extraction indicates that acidic conditions should not interfere in the development of a viable approach to NO₂-End.

Results and Discussion

Biosynthesis of the lipid tail

The disruption of the genes *orf39*, *orf44* and *orf45* had the potential of producing several forms of the lipid tail (Fig. 4.4A). To aid in the identification of analogs produced in low yield, a series of reduced lipid tail enduracidin analogs were produced. Tetrahydro-enduracidin A (H₄-End A) was the initial target for preparation. While enduracidin has poor solubility in ethanol, it has excellent solubility in DMF. Enduracidin A, dissolved in DMF, subjected to hydrogenation with palladium on carbon under a H₂ atmosphere for 30 min, successfully formed three enduracidin compounds (Fig 4.4B). Isolation of the peaks 1-3 and MS analysis revealed that peaks 1 and 3 were both forms of dihydro-enduracidin A (H₂-End A) and peak 2 was H₄-End

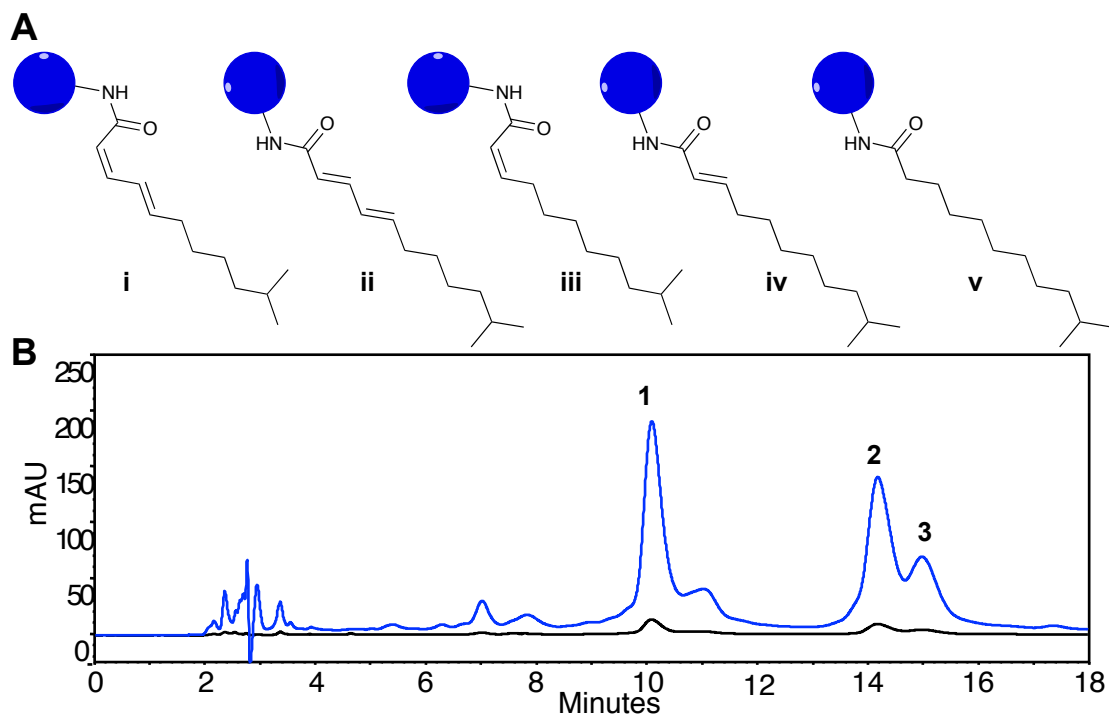


Figure 4.4 A) Possible lipid tail configurations resulting from the disruption of *orf39*, *orf44* and *orf45*. i) enduracidin A, ii) 2-*trans* enduracidin A, iii) 2-*cis*-4,5-H₂-enduracidin A, iv) 2-*trans*-4,5-H₂-enduracidin A and v) H₄-enduracidin A. B) HPLC UV chromatogram (216 nm–blue, 254 nm–black) of the hydrogenation reaction, ambient temperature for 30 min.

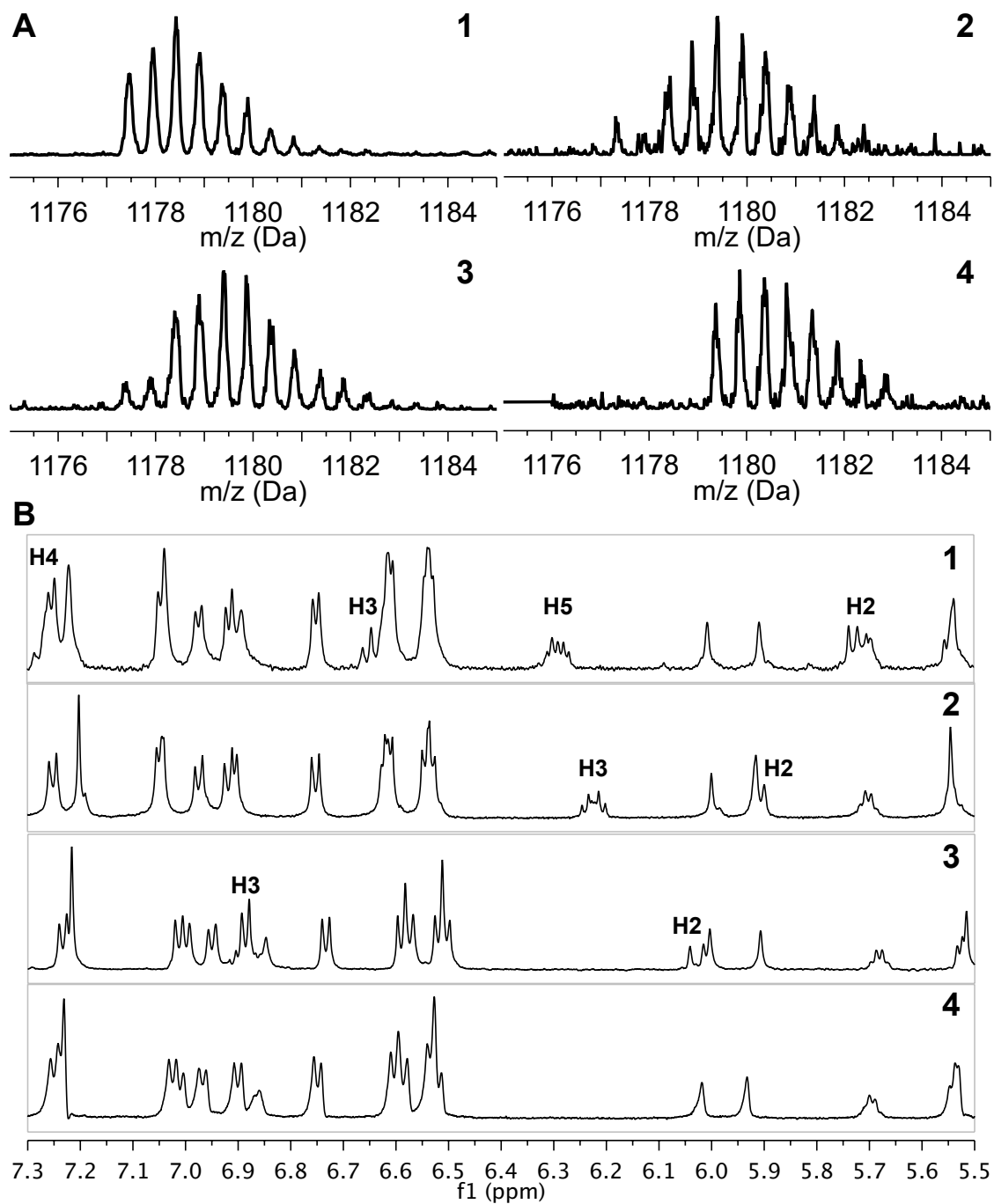


Figure 4.5 A) ESI (+) MS spectra showing the $[M+2H]^{2+}$ ions of 1) Enduracidin A, 2) 2-*cis*-H₂-End A, 3) 2-*trans*-H₂-End A and 4) H₄-End A. B) ¹H NMR spectra for the corresponding compounds. The lipid tail olefin protons are labelled indicating the carbon to which it is bound.

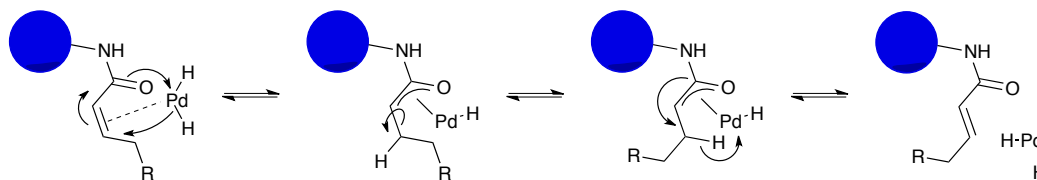


Figure 4.6 Mechanism for the palladium-mediated isomerization of the *cis* olefin to the *trans*. A hydride addition forms the palladium enolate intermediate allowing for rotation around the C2-C3 bond.

A (Fig 4.5A). The different retention times suggested that the two dihydro species have different configurations of a single double bond. NMR analysis of peak 2, H₄-End A, confirmed the reduction of the two olefins (Fig. 4.5B-4). The spectra of peak 1 showed proton shifts consistent with 2-*cis*-H₂ End A (Fig. 4.5B-2). Peak 3 was determined to be 2-*trans*-H₂ End A as the H₂ signal had a coupling constant to H₃ of 15.7 Hz (Fig. 4.5B-3). Upon further experimentation with reaction time and temperature it was discovered that 2-*cis*-H₂-End A was the favored product when the reaction temperature was lowered to 0 °C. Increased yield of H₄-End A was achieved by extending the reaction time to 3 hrs. The production of the *trans* isomer is postulated to result from dihydro-palladium acting as a Lewis acid, catalyzing the

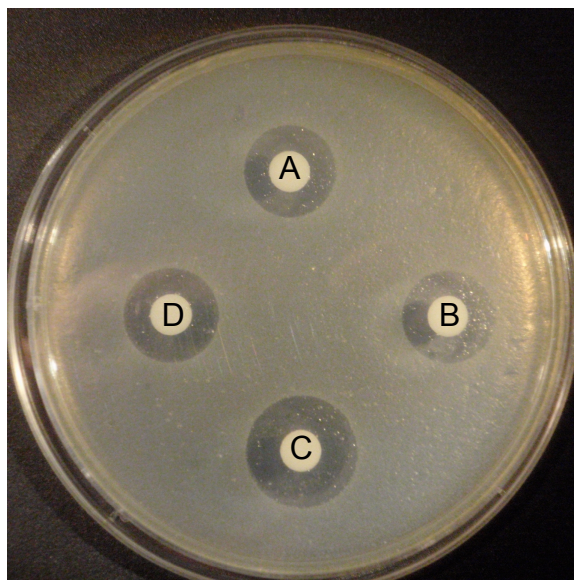


Figure 4.7 Disk diffusion assay of enduracidin lipid tail reduction products against *S. aureus* using 1 mg of A) Enduracidin A, B) H₄-Enduracidin A, C) 2-*trans*-H₂-End A and D) 2-*cis*-H₂-End A.

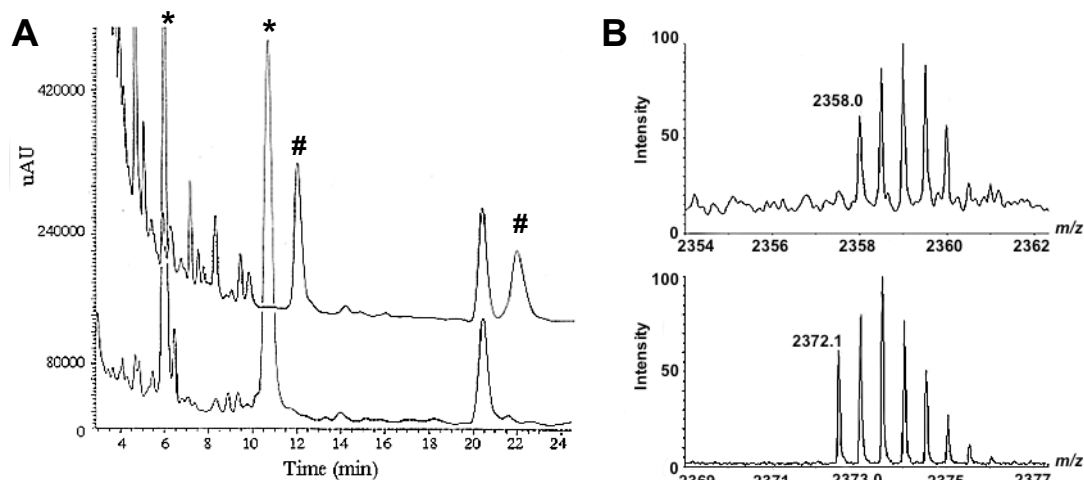


Figure 4.8 A) HPLC chromatogram of extracts from wild-type *S. fungicidicus* (bottom) and *orf45* disruptant Sf45dh::Tn5AT (top). Enduracidin A and B are labelled with asterisks. New enduracidin compounds produced by the mutant strain are labelled with '#'. MALDI-TOF MS analysis of the 12 min peak, H₄-End A (top) and 22 min peak, H₄-End B (Bottom) showing the [M+H]⁺ ion.

isomerization of the double bond (Fig 4.6).¹⁶ The three purified compounds were subjected to a disk-diffusion antibacterial assay. No significant change in bioactivity was observed compared to End A (Fig. 4.7).

With the End A lipid tail analog standards in hand, the analysis of mutants was undertaken. The Acyl-CoA dehydrogenase portion of *orf45* was disrupted by insertion of the apramycin resistance-conferring transposon cassette Tn5AT, producing the mutant Sf45dh::Tn5AT. HPLC analysis of methanolic culture extracts showed two new compounds at 12 and 22 min (Fig. 4.8A). MALDI-TOF MS analysis of the isolated products indicated that the compounds were H₄-End A and B (Fig. 4.8B). The production of H₄-End by Sf45dh::Tn5AT suggests that the hydrogenase of Orf45 is responsible for the introduction of first double bond, because the formation of the second olefin by Orf39/Orf44 would not be possible without the C2-C3 double bond providing conjugation to the carbonyl.

To further study the biosynthetic pathway, the strain Sf44::Tn5AT was produced having an insertional disruption of the putative acyl-CoA dehydrogenase encoding *orf44*. With the aid of the semisynthetic standards it was determined by HPLC and MS that Sf44::Tn5AT also produced H₄-End A (Fig. 4.9). The production of H₄-End by the

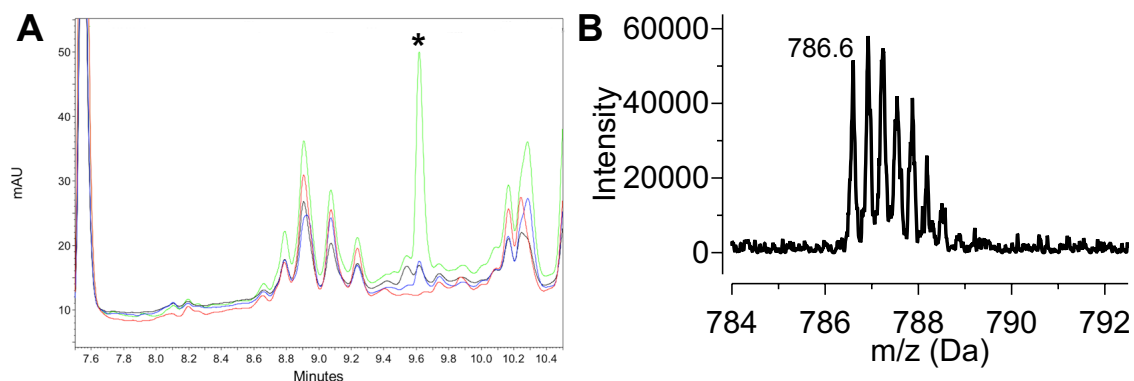


Figure 4.9 A) HPLC chromatogram of the Sf44::Tn5AT culture extract. The new compound is indicated with an asterisk. B) ESI (+) MS spectrum of the 9.6 min. peak showing the $[M+3H]^{3+}$ ion. The neutral mass of 2356.8 Da corresponds with H₄-End A.

orf44 mutant suggests that the dehydrogenase function of Orf45 may rely on interacting with Orf44.

To fully explore this method of examining the lipid tail biosynthetic pathway, the deletion of *orf39* was undertaken. The newly formed deletion mutant Sf Δ 39 was found to have greatly reduced enduracidin production and a product with the same mass as enduracidin that was hypothesized to be 2-*trans*-4-*trans* enduracidin. Since a standard for this isomer had not been produced, the compound was isolated and characterized via NMR to determine the configuration of the C2-C3 olefin. Comparison of the

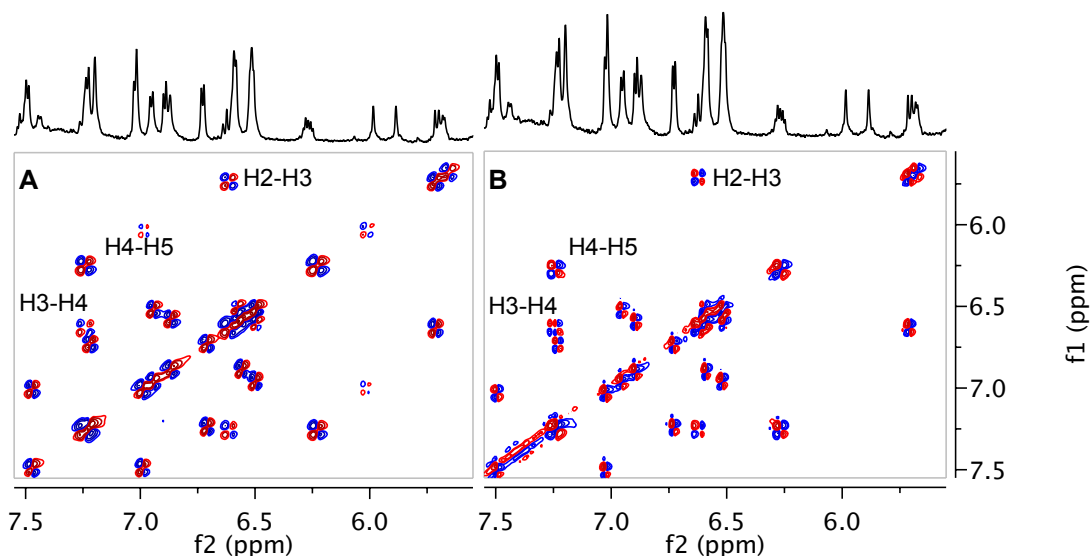


Figure 4.10 Double quantum filtered COSY NMR spectra for A) Enduracidin A and B) the peptide isolated from Sf Δ 39Am^R. The olefinic lipid tail correlations are labeled in each spectrum.

double quantum filtered COSY spectra of enduracidin A and the Sf Δ 39 product showed them to be identical (Fig. 4.10). For further confirmation, the coupling constant for the H₂/H₃ signals, J_{H_2/H_3} , was measured at 11.3 Hz, consistent with the 2-*cis*-4-*trans* configuration of enduracidin. The reduction of enduracidin production suggests that *orf39* is involved in the formation of the lipid tail diene although the role as an isomerase or dehydrogenase is uncertain with the current evidence.

Because H₄-End can be produced in fair quantity by Sf45dh::Tn5AT it may be possible that Orf39, Orf44 and Orf45 do not prevent some altered lipid tails from being incorporated into enduracidin. Based on this assumption, the loading onto Orf35 or the condensation reaction with Asp1 on the NRPS, EndA, are two possible points of inhibition. If Orf39 were responsible for the introduction of the C₄-C₅ double bond the observed results would indicate that another dehydrogenase was capable of complementing the deficiency. Additionally, it would suggest that Orf44, having isomerase functionality, could not function as the production of 2-*cis*-H₂-End was not observed in the *orf39* mutant. The 2-*cis* lipid should be incorporated as readily as the saturated lipid tail as both can take on a similar conformation to the natural 2-*cis*-4-*trans* lipid tail. If Orf39 is responsible for the isomerization of the C₂-C₃ olefin then Orf44, as a dehydrogenase, may have a side reaction isomerizing the C₂-C₃ olefin. The uncatalyzed isomerization of the first double bond or complementation of the mutant by another dehydrogenase/isomerase may explain the lowered production of enduracidin. The production of H₄-End by both *orf44* and *orf45* mutants seems to suggest the two may interact to form a complex, although there is no direct evidence. Disabling Orf44 using point mutations and an in-frame deletion could give further evidence of such an interaction. Ultimately, these hypotheses require significant investigation, likely requiring purified proteins and an NMR or crystal structure to demonstrate the complexing of the two proteins.

From the observed results and the bioinformatic analysis it appears that Orf45 is responsible for the formation of the CoA thioester and the introduction of the first

double bond. The second double bond is then introduced and isomerized by Orf44 and Orf39.

Lipid tail removal with ozone

The semisynthetic approach to modifying enduracidin was predicated heavily on the work done by Ciabatti *et al.* on the antibiotic ramoplanin.¹⁰ Enduracidin and ramoplanin are similar in their structure and even share the same biological target. As semisynthetic work began, however several differences became apparent. The preliminary step in modifying the enduracidin lipid tail was the protection of the δ -amine of Orn4. The protection of ramoplanin's Orn4 and Orn10 was achieved using Fmoc-OSu and TEA in DMF at ambient temperatures. When these conditions were used with enduracidin no reaction was observed. Varying the reaction conditions revealed that the presence of DMF prevented the reaction from occurring. Running the reaction in 50% *aq.* THF with bicarbonate or TEA at ambient temperature produced Fmoc-protected enduracidin (Fmoc-End). However, Boc protection using Boc-anhydride with bicarbonate in 70% MeOH gave excellent yields. Therefore, the higher yield and easy purification of Boc-End led to it being used for most of the reactions.

For the semisynthetic experiments enduracidin extracted from EnradinTM was utilized. It was found that enduracidin from a 1:1:1 MeOH:acetone:HCl (1 N) EnradinTM extract could be bound to activated charcoal. The charcoal was then washed with water, and an aqueous methanol gradient followed by the elution of enduracidin with 70% isopropanol. The dried material was readily prepared at ~70% purity and used as a starting material for the Boc reactions on a gram scale with excellent conversion. The Boc-protected enduracidin was used in the subsequent semisynthetic experiments.

Ozonolysis reactions have been used successfully on peptides previously, including ramoplanin.^{10, 13a, 17} However, the ozonolytic cleavage of the enduracidin lipid tail diene was unsuccessful under numerous conditions. MS analysis of the products of Boc-End using the reaction conditions described by Ciabatti *et al.* with

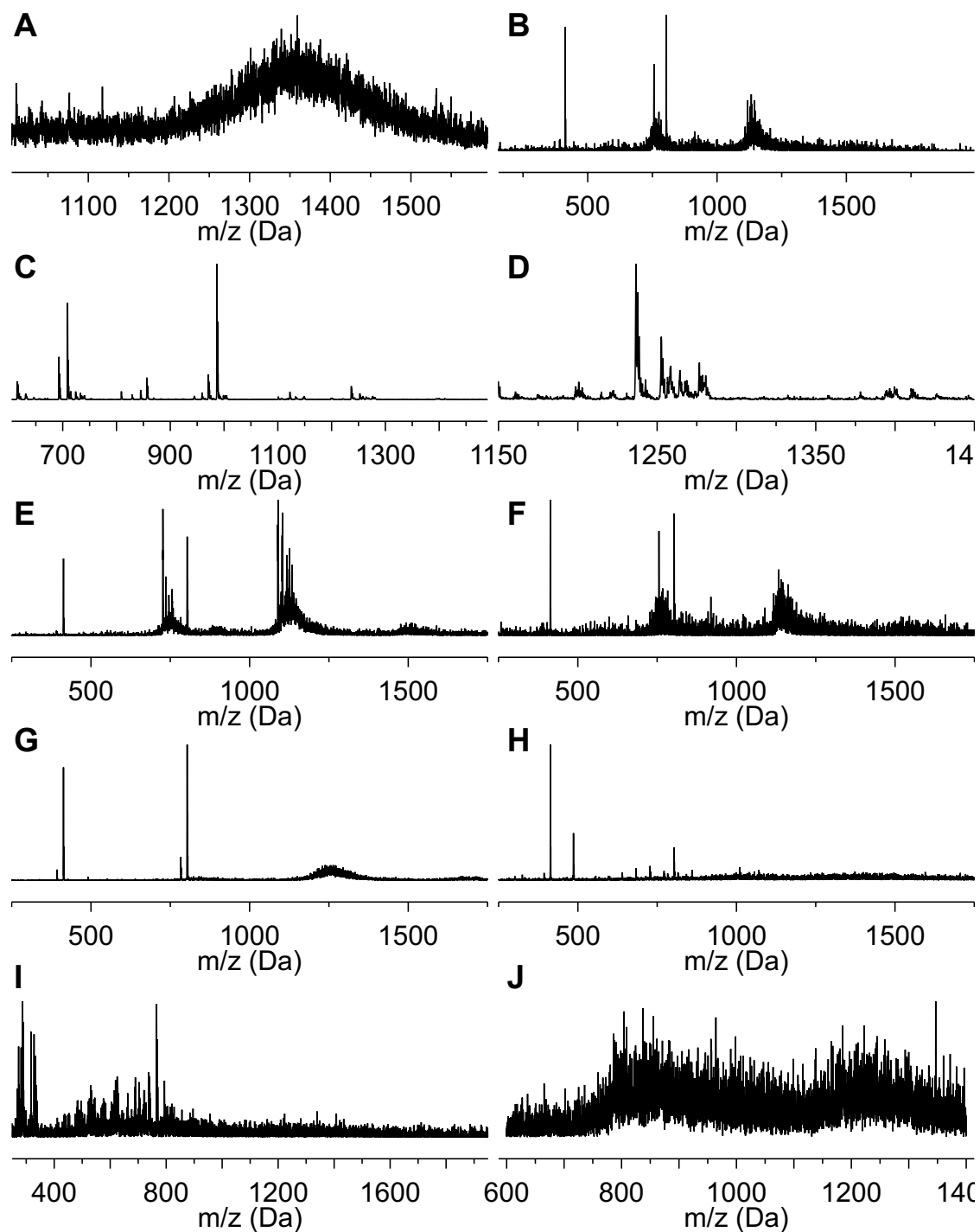


Figure 4.11 Mass spectra of Boc-End ozonolysis products under various conditions. A) 3:1 MeOH:DMF, DMS, 5 min., -78 °C; B) 3 Å MeOH, DMS, 5 min., -78 °C; C) 1:2 DCM:MeOH, DMS, 4 min., -78 °C; D) Close-up of the singly charged degradation products between 1150 and 1400 Da; E) 1:2 DCM:MeOH, DMS, 2 min., -78 °C; F) 1:2 DCM:MeOH, DMS, 1 min., -78 °C; G) 1:2 DCM:MeOH, TPP, 2 min., -78 °C; H) 1:2 DCM:MeOH, Pyr, 2 min., -78 °C; I) 1:2 DCM:MeOH, Zn-AcOH, 2 min., -78 °C; J) Pooled HPLC fractions of reaction I.

dimethylsulfide (DMS) was unsuccessful (Fig. 4.11A). Degradation products are observed as a broad peak in the spectrum. The reaction was run in anhydrous MeOH with DMS as the reducing agent, similar to the conditions used by Black *et al.*^{13a}, except for maintaining the reaction at -78 °C and limiting ozone exposure to five minutes. The result, as observed by ESI MS, was degradation products present in the mass range of double and triple charged enduracidin, however, the major peaks were at m/z 1116.5, 1127.5, 1132.5 and 1144.5 Da, not the expected value of 1159.5 (Fig. 4.11 B). Furthermore, degradation products at m/z 803 and 402 Da were observed. In an attempt to reduce degradation, the solvent was changed to 1:2 DCM:MeOH. When ozone was blown over the reaction until it turned blue (~ 4 min) the MS spectrum still showed a significant amount of degradation (Fig. 4.11C and D). The observed peaks had a charge of +1 indicating that the peptide had been cleaved, but the products could not be readily identified. Reducing the exposure time to ozone reduced the degradation of the compound, however oxidative side reactions were still proceeding (Fig. 4.11E and F). Changing the reducing agent was postulated to improve the reaction. Use of triphenylphosphine and Zn-AcOH were both unsuccessful (Fig. 4.11G and I). The use of pyridine as an additive for ozonolysis reactions has been reported previously.¹⁸ Pyridine is oxidized to its N-oxide form which reacts with the carbonyl peroxide during the rearrangement of the primary ozonide (Figure 4.12). Hence, potential side reactions of the ozonide should be negated and immediate formation of the aldehyde should occur. When run in the presence of pyridine, ozonolysis caused degradation of enduracidin similar to what was observed previously (Fig 4.11H). The Zn-AcOH

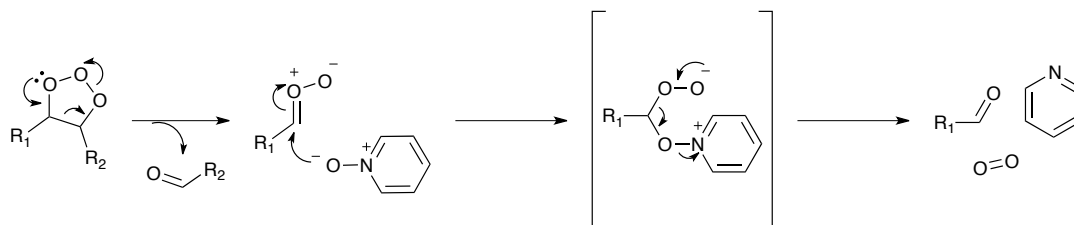


Figure 4.12 Proposed mechanism for the reduction of carbonyl peroxides by pyridine N-oxide after the fragmentation of the primary ozonide.

reactions were observed to produce strange clusters during MS analysis. The product, a five minute wide, polar peak on HPLC, was isolated and analyzed by MS (Fig. 4.11J). Unfortunately the spectrum provided no insight into the structure since the product appears to have further decomposed.

The required isolation of enduracidin from aqueous solvent systems prior to ozonolysis was identified early in the process as a possible source of side reactions forming peroxides and other reactive oxygen species. To reduce water bound to the peptide, the compound was repeatedly dissolved in anhydrous DMF/MeOH and then dried under high vacuum. Further investigation of the degradation focused on the functional group differences between ramoplanin and enduracidin. The presence of the carboxylate of Asp1, dichlorophenol of Dpg-13 and the two guanidines of End-16 and End-11 are the main differences. Dichlorophenol is readily oxidized by ozone under aqueous conditions.¹⁹ Additionally, given the possibility that all water associated with enduracidin may not be eliminated, reactive peroxide species may be contributing to the degradation of enduracidin. Concluding that ozonolysis was not a viable method of removing the lipid tail, alternate approaches to modifying enduracidin's lipid tail were undertaken.

Diels-Alder reaction: maleimides

Diels-Alder type reactions provide a method of selectively reacting with the alkenes of enduracidin. The maleimide and nitroso dienophiles were chosen as they have both been shown to be highly reactive, introduce new functional groups and may be used to form a library of related compounds for analysis. A series of maleimide compounds can be readily produced synthetically from commercially available amines and maleic anhydride. Maleimides have been used as highly reactive dienophiles for the ligation of compounds to DNA.²⁰ The commercially available N-methylmaleimide was examined first. Reactions were performed in a variety of different solvents as observed in the literature (DMF, DMF-water, DMF-NaOAc buffer, MeCN-water, MeOH, MeOH-water and MeOH-NaOAc buffer).²¹ Maleimide reactions have

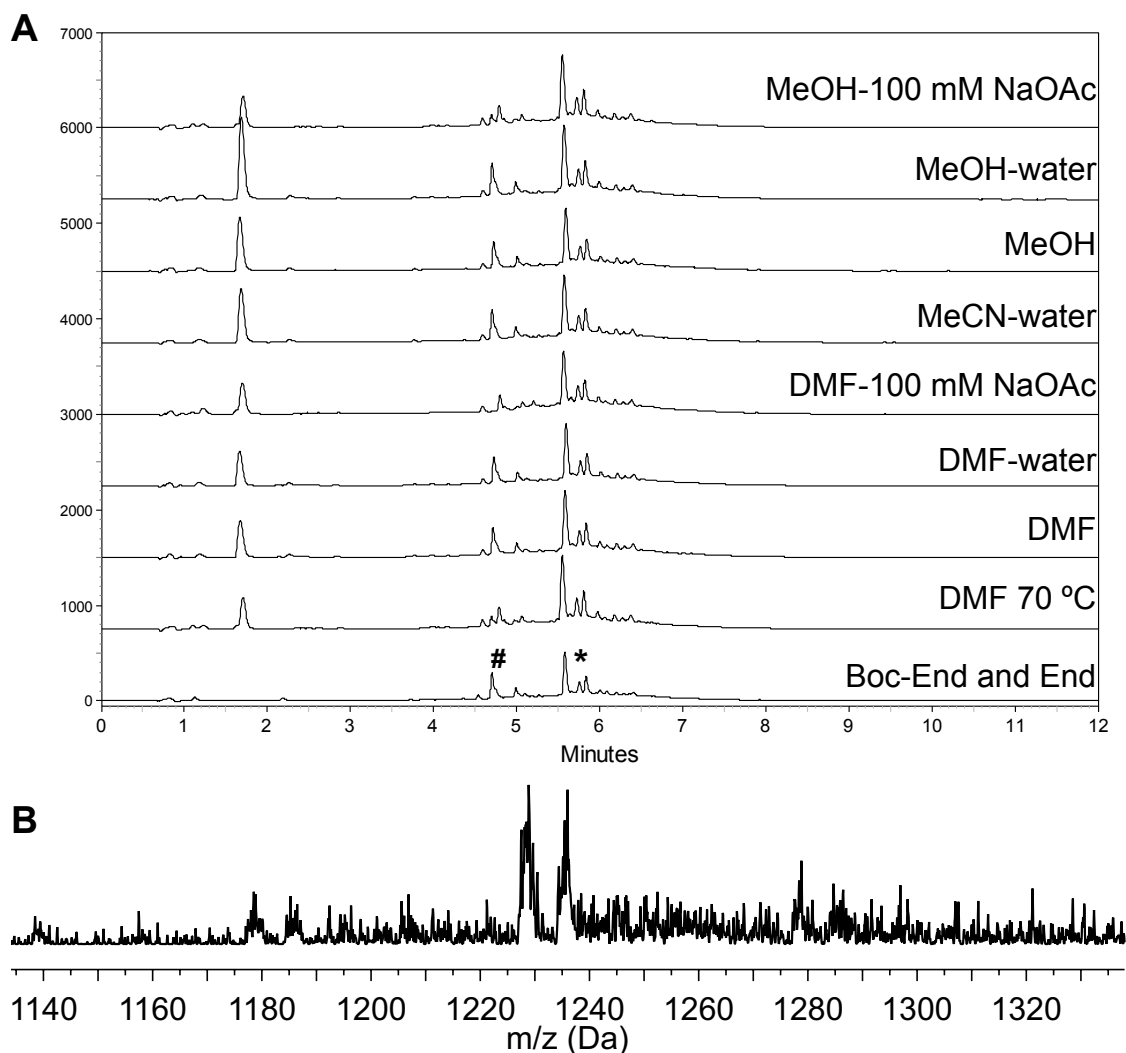


Figure 4.13 A) HPLC chromatograms showing the analysis of the maleimide reaction with Boc-End under various conditions. Boc-End, a set of three peaks, is indicated with an asterisk. Enduracidins A and B are indicated with a '#'. B) ESI (+) MS analysis of representative of the whole reaction series

been used in aqueous, ambient temperature reactions, and thus the reactions with enduracidin were run for 24 hrs at ambient temperature. Only the DMF reaction was heated because the presence of water and protic solvents would potentially hydrolyze enduracidin in the time required for the ambient temperature reaction. HPLC and MS analysis of the products revealed that no reaction took place (Fig. 4.13). The likely limitation for the reaction is the energy required to rotate the diene around the C3-C4 bond achieving the proper configuration for a Diels-Alder reaction. No further

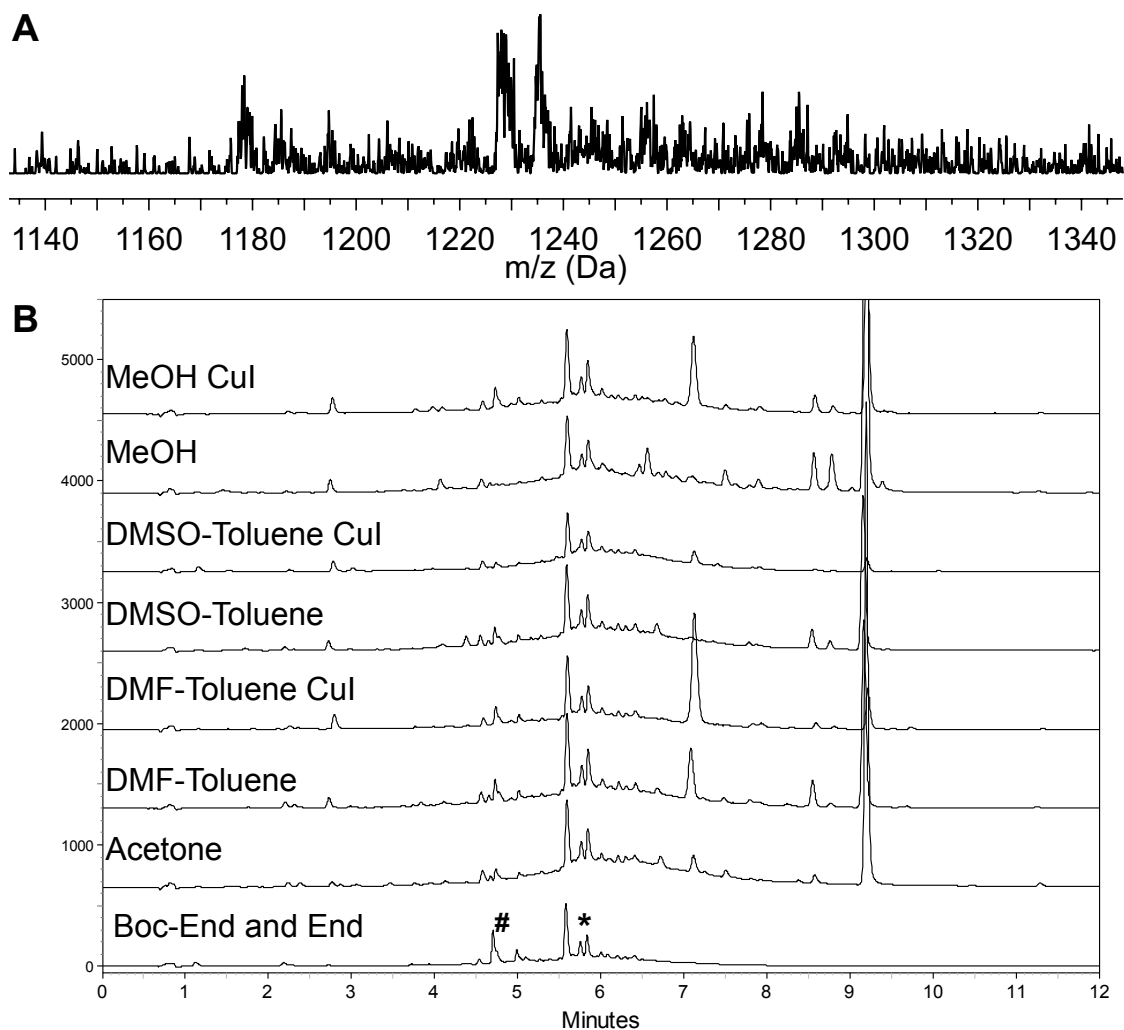


Figure 4.14 A) ESI (+) MS analysis of the NO-Toluene MeOH, CuI reaction representative of the catalyzed reactions. B) HPLC chromatograms showing the analysis of the maleimide reaction with Boc-End under various conditions. Boc-End, a set of three peaks, is indicated with an asterisk. Enduracidins A and B are indicated with a '#'.

maleimide reactions were pursued.

Diels-Alder reaction: nitrosotoluene

Nitroso compounds have been shown to react with dienes in various systems with a variety of substrates.²² Particularly, the reaction of nitroso-benzene with the rapamycin triene suggested that a selective reaction with the enduracidin diene may be possible.²³ For the introduction of polar/charged groups, the oxazine ring formed in the reaction carries a charge under neutral conditions, potentially improving

enduracidin's solubility. For the construction of semisynthetic libraries, nitroso compounds can be prepared from numerous precursors or purchased. Nitroso Diels-Alder reactions require heat for the reaction to proceed. The Lewis acid catalyst copper iodide has previously been used to facilitate Diels-Alder reactions.^{22c, 24} For a dienophile the commercially available 2-nitroso-toluene (NO-toluene) was selected because it is similar to the nitroso-benzene used by Graziani *et al.* on rapamycin.²³ Catalytic reactions were run for 24 hrs at ambient temperature while the uncatalyzed reactions were run at 70 °C. The catalyzed reactions were checked by MS, with the lack of a peak at 1288 Da indicating that no reaction had occurred (Fig. 4.14A). As no product was observed, the reactions were run an additional 18 hrs at 70 °C. The reactions were cooled, dried and redissolved in 70% MeOH. HPLC analysis indicated that all of the conditions failed to produce a new compound (Fig. 4.14B).

The *cis* configuration of the first double bond in the enduracidin diene may be a factor in the dienophile reactions. The *cis* configuration of the C2 olefin sterically restricts rotation to the required planar double bond orientation due to the proximity of H5 and the carbonyl oxygen. As such, the diene likely cannot enter a configuration capable of a Diels-Alder reaction without more energy or the isomerization of the C2 alkene. The failure of the reactions lead to further experimentation using a diene to react with one of the lipid tail double bonds.

Diels-Alder reaction: Danishefsky's diene

To study the Diels-Alder reactions with an olefin from the lipid tail,

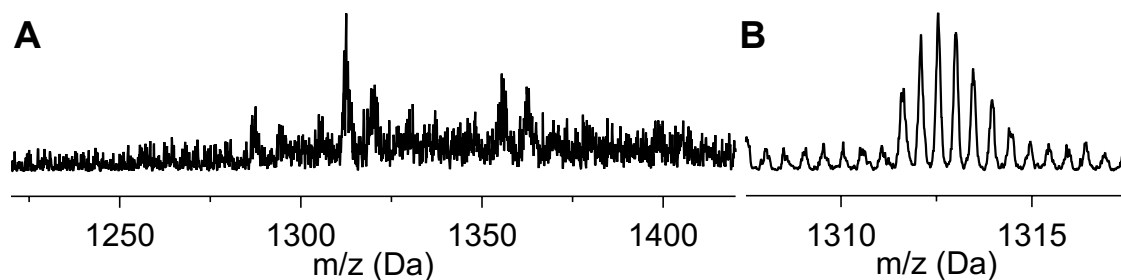


Figure 4.15 ESI (+) MS spectra showing the crude products from the A) first reaction of Boc-End and Danishefsky's Diene. B) A higher resolution spectra of the 1311.5 Da compound from the second reaction with Danishefsky's diene.

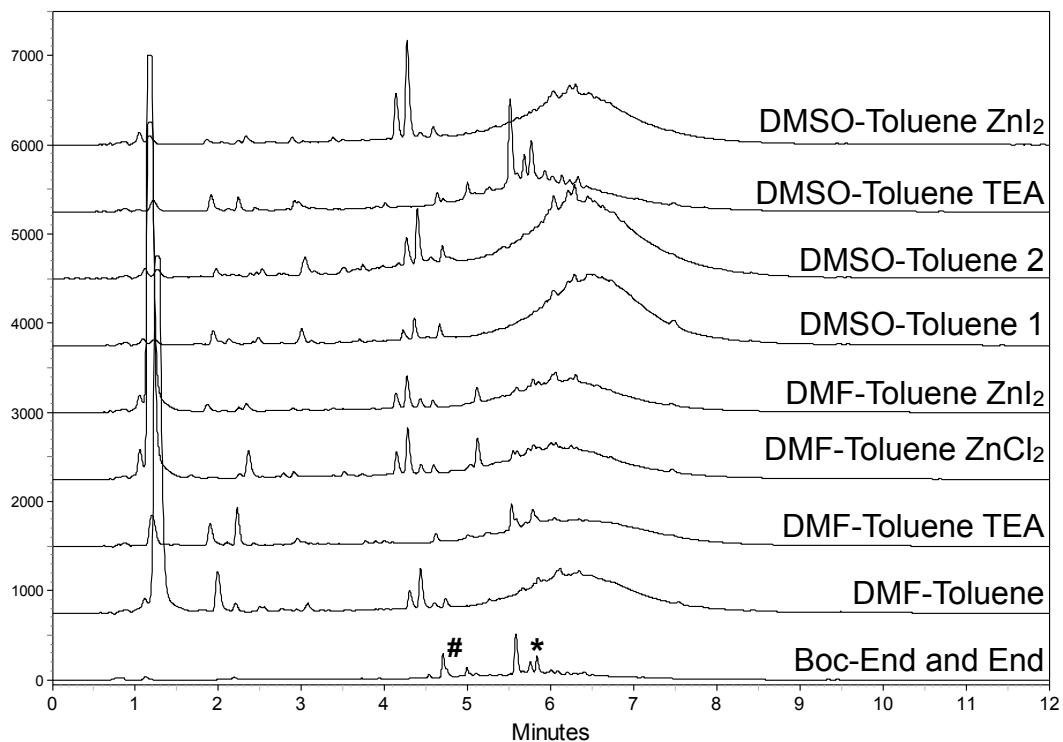


Figure 4.16 HPLC chromatograms showing the Boc-End/Danishefsky's diene reaction products from various conditions. Enduracidin is labelled with an '#' and Boc-End with an asterisk.

Danishefsky's diene (*trans*-1-methoxy-3-trimethylsilyloxy-1,3-butadiene) was selected as it is readily available, is highly reactive and produces a ketone which can serve as a synthetic handle. Using a similar set of reaction conditions to the NO-toluene reactions, Danishefsky's diene was found to react reproducibly with enduracidin in a heated DMSO-toluene solvent system, as observed by MS (Fig. 4.15), however, the observed ion ($m/z=1311.5 [M+2H]^{2+}$) does not correspond with the addition of Danishefsky's diene to enduracidin (expected $m/z=1313.5 [M+2H]^{2+}$). HPLC analysis provided little evidence as to the identity of the new compounds (Fig. 4.16). The reaction was repeated on a larger scale and the product isolated by HPLC. The isolation of the new compound proved to be challenging. HPLC fractionation of the crude product resulted only in the isolation of enduracidin (Fig. 4.17). If a [4+2] cycloaddition occurred it is possible that the product is sufficiently unstable under the acidic conditions required for purification that a retro Diels-Alder reaction is

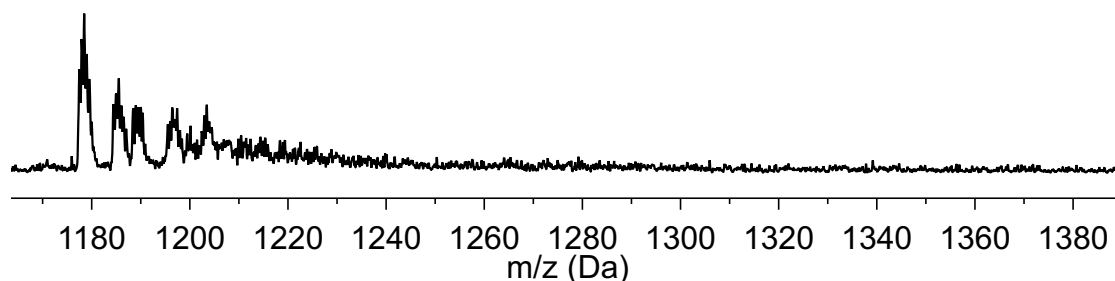


Figure 4.17 ESI (+) MS spectrum of the pooled HPLC fractions from four min. to 8 min. of the spectrum. Enduracidin A and B are present in the $[M+2H]^{2+}$ form at $m/z = 1177.5$ and 1185.5 respectively. The additional peaks are the sodium (+11) and potassium (+18) adducts of enduracidin A and B.

occurring. Further research into this modification should involve the oxidation or hydrogenation of the alkene formed by the Diels-Alder reaction, potentially trapping the product.

Lipid tail modification: alkene dihydroxylation

To further explore the potential for modifying the lipid tail, hydroxylation of the alkenes with osmium tetroxide was examined. Dihydroxylation reactions have proven to be robust reactions tolerated by various functional groups. Notably, OsO_4 catalyzed reactions have been performed on rapamycin and gluconucleosides,²⁵ and the reaction can be run in the presence of water and various protic solvents.²⁶ The dihydroxylation of alkenes conjugated to a carbonyl has been demonstrated previously.²⁷ Interestingly, the selective dihydroxylation of a C4-C5 olefin in a carbonyl conjugated diene suggested that 4,5-dihydroxyenduracidin (4,5-(OH)₂-End) may be produced.²⁸ The reaction proceeded smoothly on unprotected enduracidin using three equivalents of

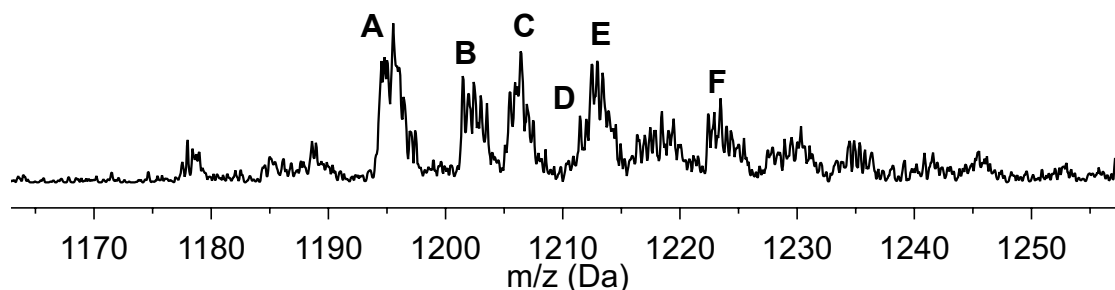


Figure 4.18 ESI (+) MS spectrum of the dihydroxylation reaction of enduracidin. The labeled signals are the +2 ions: A) $m/z=1194.5$, (OH)₂-End A; B) $m/z=1201.5$, (OH)₂-End B; C) $m/z=1205.5$, (OH)₂-End A Na⁺ adduct; D) $m/z=1211.5$, (OH)₄-End A; E) $m/z=1212.5$, (OH)₂-End B Na⁺ adduct; and F) $m/z=1222.5$, (OH)₄-End A Na⁺ adduct.

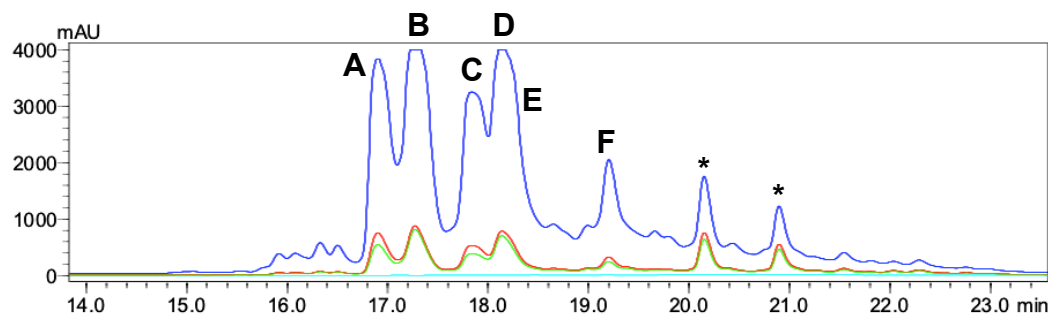


Figure 4.19 HPLC chromatogram showing the separation of hydroxyenduracidin species which were identified by ESI MS as A) $(\text{OH})_4$ -End A, B) $(\text{OH})_2$ -End A, C) $(\text{OH})_4$ -End B, D) $(\text{OH})_2$ -End B E) $(\text{OH})_2$ -End A and F) $(\text{OH})_2$ -End B. Unreacted enduracidin A and B are indicated with asterisks.

NMO and catalytic OsO_4 . MS analysis of the reaction mixture indicated that both dihydroxy and tetrahydroxy species were produced (Fig. 4.18). HPLC and MS analysis indicated that a total of six products were produced; three hydroxylated species for each form of enduracidin (Fig 4.19). Peaks A, B and F were isolated by

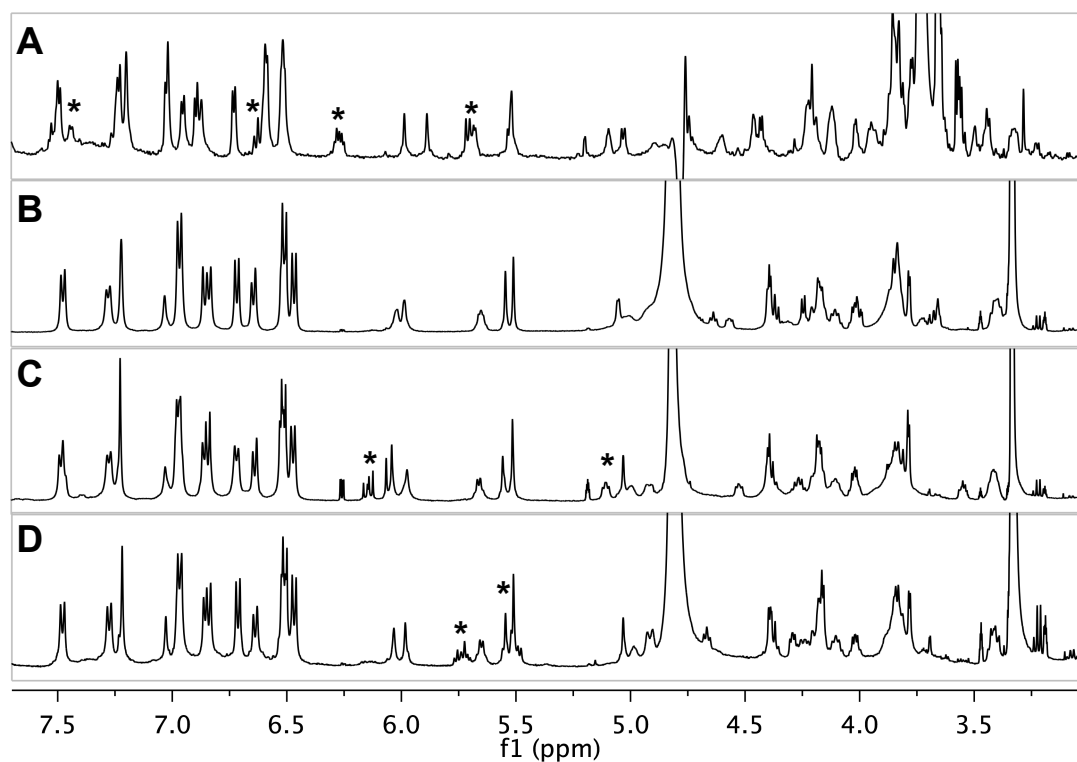


Figure 4.20 Proton NMR spectra comparing the hydroxylated enduracidins with End A. The lipid tail olefinic protons are indicated on each spectra with an asterisk. A) End A; B) Peak A, $(\text{OH})_4$ -End B; C) Peak B, $(\text{OH})_2$ -End A; and D) Peak F, $(\text{OH})_2$ -End A.

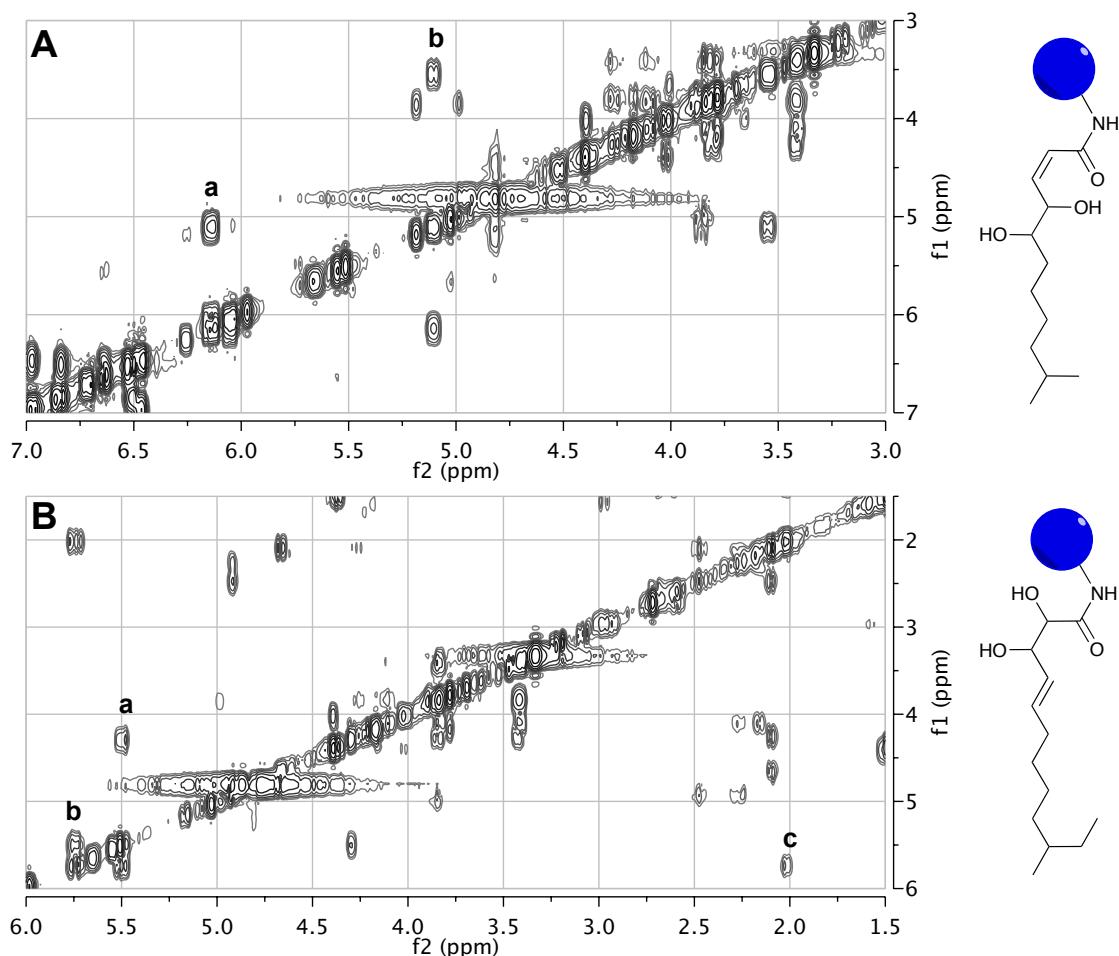


Figure 4.21 A) COSY spectrum of peak B showing the labelled correlations: a) H2-H3; and b) H3-H4. B) COSY spectrum of peak F showing the labelled correlations: a) H3-H4; b) H4-H5; and c) H5-H6. Lipid tail structures of each compound are shown to the right of their corresponding spectra.

HPLC. Analysis by ^1H NMR indicated that the reactions had occurred on the lipid tail alkenes and confirmed that peak A was $(\text{OH})_4$ -End A (Fig 4.20). Further analysis using 2D COSY NMR experiments indicated that peak B was 2,3- $(\text{OH})_2$ -End A and peak F was 4,5- $(\text{OH})_2$ -End B (Fig. 4.21). As the compounds represented each of the hydroxylation patterns, they were analyzed in a bioassay against *S. aureus* to investigate the effects of hydroxylation on bioactivity. End A and ampicillin were used as references in the assay (Fig. 4.22). Compared to End A, 2,3- $(\text{OH})_2$ -End B was four-fold less active, 4,5- $(\text{OH})_2$ End A was 16-fold less active and $(\text{OH})_4$ -End A was over 16-fold less active, showing no bioactivity at 25.6 $\mu\text{g}/\text{mL}$. Ampicillin was found to be

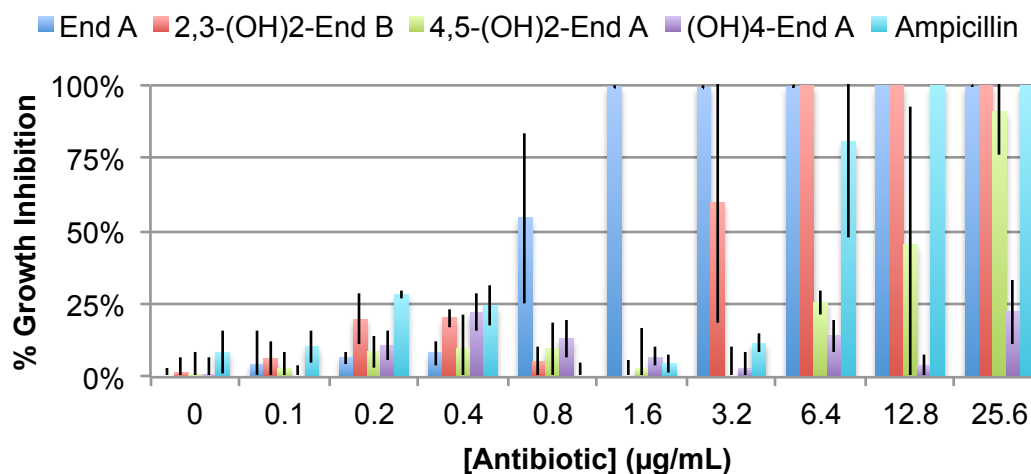


Figure 4.22 Chart showing the percent growth inhibition of *S. aureus* by the various hydroxylated enduracidins compared with End A and ampicillin. Standard of deviation is shown.

8 times less active than End A with a MIC of 12.8 µg/mL in this assay. The enduracidin lipid tail is responsible for coordinating an enduracidin dimer with the lipid membrane, bringing it in proximity to Lipid II. These data suggest that the introduction of polar/hydrogen bond-forming groups on the proximal end of the lipid tail may significantly decrease membrane affinity and coordination, thereby reducing potency. Optimal ramoplanin bioactivity against *S. aureus* is achieved with a C7 to C8 lipid tail (the natural product being 7-Me-octa-2,4-dienoic acid). A decrease to C6 was observed to result in a four-fold loss of activity, consistent with the hydroxylation results.¹⁰ The combined results suggest that further attempts to introduce polar groups onto the lipid tail of enduracidin would not be productive, even if increased solubility was achieved.

Nitration of enduracidin

The synthetic potential for introducing a nitro group into enduracidin holds interest for our semi-synthetic work. As incorporation of NO₂-Hpg directly into enduracidin was unsuccessful, chemical nitration of the natural product was undertaken. Previous work on other lipopeptides suggested several methods for the nitration of enduracidin. Mannopeptimycin, FR901469 and pneumocandin have

successfully undergone aromatic nitration with the use of nitrate/nitrite salts and an organic acid (Fig 4.23).^{13a, 14-15} The literature indicated that neat TFA or AcOH were needed for the reaction. Previous work producing NO₂-Hpg showed that the AcOH-

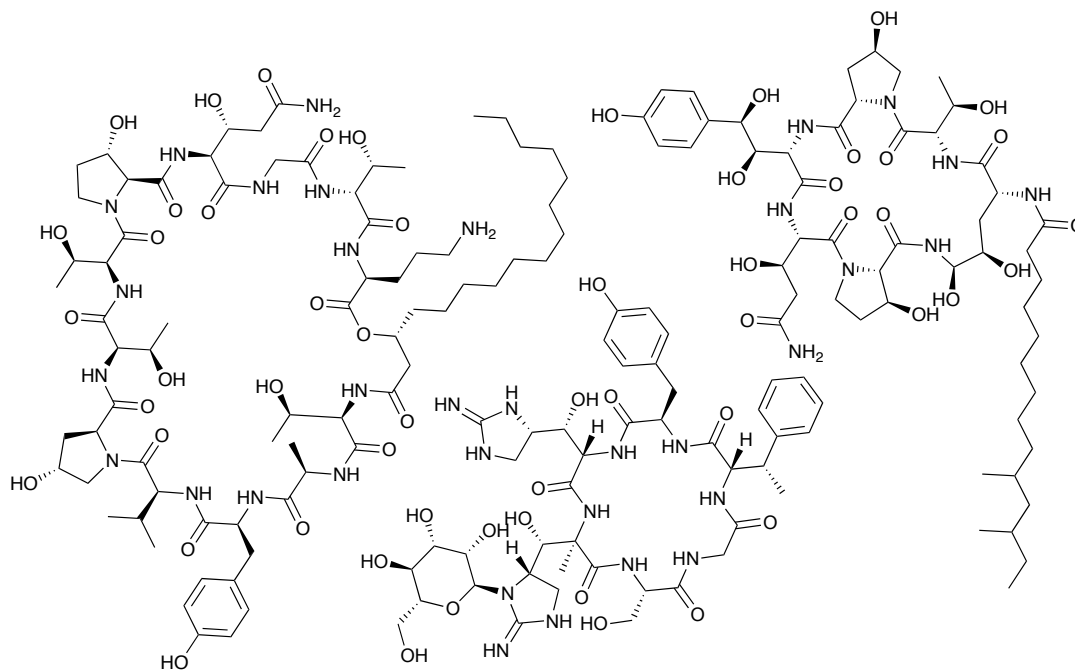


Figure 4.23 Structures of FR901469 (left), mannopeptimycin (center) and Pneumocandin B₀ (right).

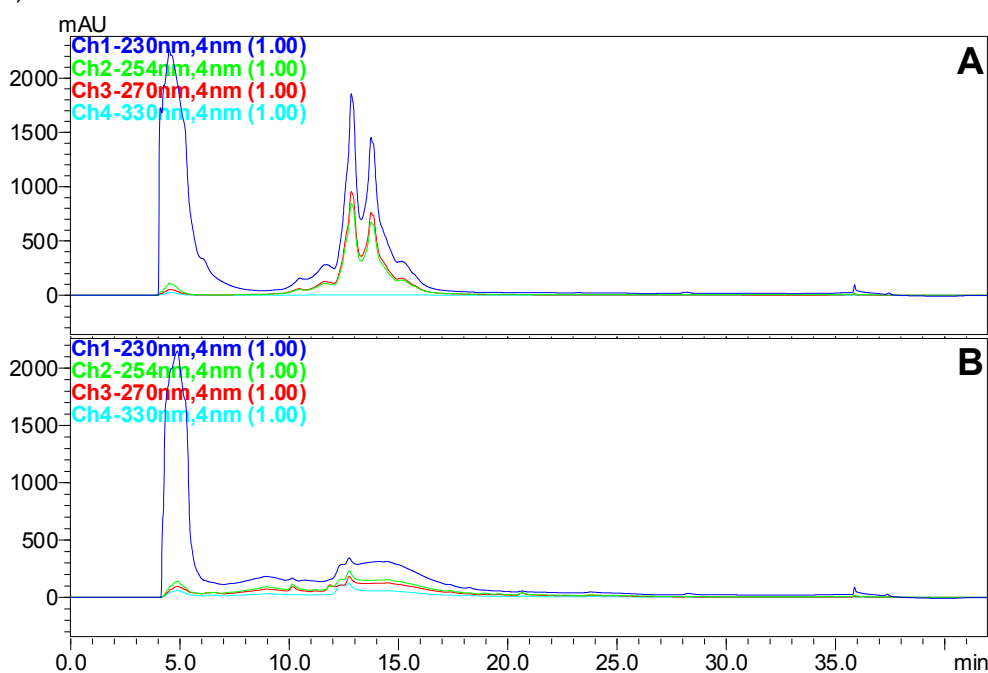


Figure 4.24 HPLC chromatograms showing the A) TFA-KNO₃ and B) AcOH-NaNO₂ reactions.

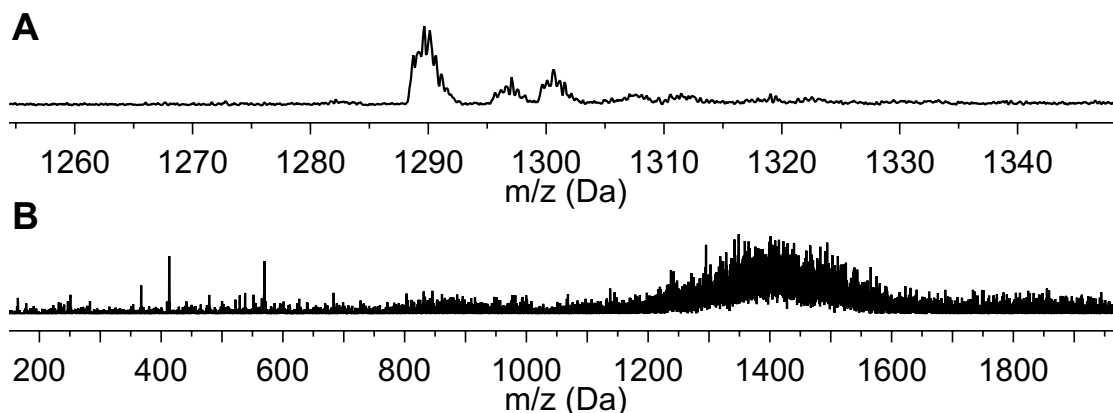


Figure 4.25 ESI (+) MS spectra of pooled HPLC fractions from the A) TFA-KNO₃ and B) AcOH-NaNO₂ reactions.

NaNO₂ was an effective reagent for the nitration of Hpg. Unfortunately, the nitration of enduracidin with NaNO₂ under various conditions proved to be unsuccessful (Figure 4.24B). The use of KNO₃ with both acetic acid and TFA proved to be unsuccessful. No nitrated forms of enduracidin were observed via HPLC (Fig. 4.24A). MS analysis of the isolated peaks indicated that the KNO₃ reaction failed to produce a new compound while the nitrite reaction degraded the enduracidin (Fig. 4.25). As such a new method of nitration was investigated.

The nitration of tyrosine on proteins has been accomplished through several methods. Studies of the cellular response to oxidative stress have focused heavily on peroxynitrite which can be easily produced from nitrite and azide.^{11a, 12e, 29} For the nitration of enduracidin, however, the degradation of unsaturated lipids by

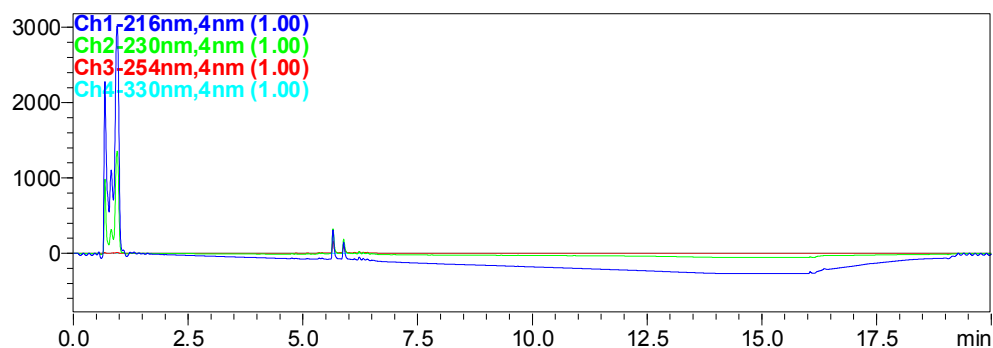


Figure 4.26 HPLC chromatogram showing the product of the TNM-10 mM NH₄OAc buffer reaction. The peaks were identified as starting material.

peroxynitrite negates its use in this synthesis.³⁰ Tetranitromethane (TNM) has been used for the nitration of proteins and peptides, having been used under numerous buffer conditions and in the presence of alcohols. This nitration reaction was performed on enduracidin under numerous conditions using literature methods, but proved to be unsuccessful, as evidenced by the acetate buffer reaction (Fig. 4.26).^{12a, 12d, 31} The overall strategy of introducing nitro groups on the Hpg residues of enduracidin both chemically and through mutasynthesis proved unsuccessful and was abandoned.

Experimental Procedures

Bacterial strains, plasmids, fosmids, media and culture conditions

S. fungicidicus (ATCC21013) and *Escherichia coli* S17-1 (ATCC47055) were purchased from ATCC. *E. coli* DH5 α (Life Technologies, Inc.) and EPI300TM-T1R (Epicentre) were routinely used as hosts for *E. coli* plasmids, fosmids and *E. coli*-*Streptomyces* shuttle vectors. The pGEM-T easy cloning vector was obtained from Promega. Plasmids pSET152 and pIJ773 were provided by Professor Keith Chater (JIC, Norwich, England). ISP2 (DifcoTM ISP Medium 2), ISP4 and TSB (BactoTM Tryptic Soy Broth) were purchased from VWR. Media and culture conditions for *S. fungicidicus* were previously described.³²

DNA isolation and manipulations. Isolation of chromosomal

DNA from *S. fungicidicus* wild-type and the mutant strains, and agarose gel electrophoresis were performed according to Kieser et al.³³ QIAprep Spin Miniprep kits (Qiagen) were used to prepare plasmids and fosmids from *E. coli* strains. Restriction endonucleases, DNA ligase, DNA polymerase, Klenow enzyme and alkaline phosphatase were purchased from Roche and Invitrogen and used according to the manufacturers' recommendations. Primers used for PCR and DNA sequencing were synthesized by Fisher. PCR products and restriction fragments from agarose gels were purified using QIAquick Gel Extraction kits from Qiagen.

Construction of the Tn5AT cassette for in vitro transposon mutation

The Tn5AT cassette was designed to combine three genetic elements: the transposon *Tn5*, *oriT* and *aaC3(IV)*. *Tn5* is specifically and uniquely recognized by Tn5 transposase (Epicentre) and readily inserts into high G + C *Streptomyces* DNA cloned into *E. coli* plasmids and fosmids.³⁴ The gene *oriT* is required for the conjugal transfer of the DNA from *E. coli* S17-1 to *Streptomyces* and *aaC(3)IV* is an *E. coli*-

Streptomyces bifunctional selective marker conferring apramycin resistance.³⁵ Both *oriT* and *aaC3(IV)* were excised from plasmid pIJ773 as a XbaI fragment and then cloned into the transposon donor plasmid pMODTM-2(MCS) (Epicentre), previously linearized with XbaI. The resulting plasmids pXYTn5ATa and pXYTn5ATb only differ by the orientation of XbaI fragment and were used to prepare the Tn5AT cassette by digestion with PvuII according to the manufacturer's specification.

In vitro transposon mutation and selection of targeted fosmids

To generate a library of random mutagenized fosmids for gene replacement experiments, we conducted in vitro transposon insertional mutation of fosmids pXYF305 and pXYF607, carrying segments of the *end* gene cluster.³⁴ The reaction was performed at 37 °C for 2 h after mixing 10 µL (0.5 µg) fosmid template DNA, 2 µL (20 ng) Tn5AT cassette DNA, 2 µL 10 x reaction buffer, 1 µL Tn5 transposase and 5 µL sterile water. Transformation of *E. coli* competent cells EPI300TM-T1R (Epicentre) with the transposon reaction mixture was performed by electroporation. Mutagenized fosmids were selected on LB agar plates supplemented with 100 µg/ml apramycin. Plates were incubated overnight at 37 °C and surviving colonies were randomly picked and grown in LB liquid culture with addition of 100 µg/ml apramycin. The mutagenized fosmid DNA from these colonies and control fosmid pXYF305 were digested with HindIII and analyzed by electrophoresis on 1% agarose gels. The Tn5AT cassette contains a single HindIII site which is useful when screening for single versus multiple disruption events over the fosmid insert. No HindIII sites are present in the fosmids pXYF305 and pXYF607 inserts and only one HindIII site is present in the fosmid vector. Hence, digestion with HindIII readily identifies fosmids with a single insertion of Tn5AT by the presence of two bands in the gel. Colonies carrying mutagenized fosmids with a single transposon insertion were randomly selected and grown in liquid culture to permit fosmid isolation and identification of the disrupted gene. Screening was conducted by sequence analysis using the primer 5'-

AAGGAGAAGAGCCTTCAGAAGGAA-3', which corresponds to a region of the apramycin resistance gene. In this manner, fosmid pXYF305D6 was found to have Tn5AT inserted into orf45 at nucleotide position 111335 and pXYF607D21 had the cassette inserted into orf44 at nucleotide position 109247 (GenBank Accession No. DQ403252).

Disruption of orf44 and the dehydrogenase domain of orf45

The gene replacement fosmids pXYF305D6 and pXYF607D21 were individually transformed into *E. coli* S17-1 by electroporation and then introduced into *S. fungicidicus* by intergeneric conjugation. Exconjugant colonies surviving apramycin selection were passed through two rounds of sporulation without antibiotic selection to create the stable mutant strain via double crossover homologous recombination. The resulting spores were pooled, diluted and plated on ISP2 agar plates supplemented with 50 µg/ml apramycin. The apramycin-resistant colonies were randomly picked and used to inoculate TSB liquid culture for preparation of the genomic DNA for Southern analysis. The confirmed mutant strains were designated as Sf44::Tn5AT for the orf44 disruptant and Sf45dh::Tn5AT for the orf45 disruptant.

Insertional inactivation and in-frame deletion of orf39

Two recombinant plasmids, pXY301Δ39 and pXY301Δ39AmR, were constructed for in-frame deletion and insertional disruption of *orf39*, respectively. To construct pXY301Δ39, two PCR fragments 39Δ1 and 39Δ2, each containing a portion of the in-frame deleted gene and its up or downstream contiguous sequence, were amplified from fosmid pXYF305. HindIII and BamHI restriction sites were designed into PCR primers 39Δ1pf (5'-TATAA**AGCTT**ACGACGGAGGACGGGCCGCT-3', HindIII site is in bold) and 39Δ1pr (5'-TAA**AGGAT**CCGGCCCCGGTGACGATCGCGGT-3', BamHI site is in bold) used to amplify fragment 39Δ1. BamHI and EcoRI restriction sites were introduced into PCR primers 39Δ2pf (5'-AATT**GGATC**CCGGCAGGTCACGGGGTCGGTCATC-3', BamHI site is in bold)

and 39 Δ 2pr (5'-CGTT**GAATT**CCCCGCCGGGTCGAGGATGC-3', EcoRI site is in bold) used to amplify fragment 39 Δ 2. PCR was conducted in a final volume of 100 μ L containing 100 ng of pXYF305 DNA, 150 pmol of each primer, 20 μ L 5 x AccuPrimeTM GC-Rich buffer A (Invitrogen) and 1 μ L polymix (added at 80 °C) from Expand Long Template PCR System (Roche). PCR was performed as follows: 1 cycle at 95 °C for 3 min and at 80 °C for 1 min, 30 cycles at 95 °C for 1 min, at 55 °C for 1 min and at 72 °C for 2 min. The reaction was terminated with one extension cycle at 72 °C for 10 min. PCR products were gel-purified and cloned into the pGEM-T easy vector to afford the plasmids pGEMTE-39 Δ 1 and pGEMTE-39 Δ 2. Error-free inserts of pGEM-T easy derivatives were then confirmed by sequencing. The appropriately restricted and gel-purified fragments 39 Δ 1(949 bp) and 39 Δ 2 (858 bp) were simultaneously ligated with the HindIII- and EcoRI-linearized *E. coli*-*Streptomyces* temperature-sensitive conjugal vector pXY301 to yield pXY301 Δ 39. pXY301 was derived from pXY300 where the BamHI site was eliminated by treating the BamHI digested vector with Klenow enzyme followed by self-ligation.³⁶ After confirming the in-frame deletion assembly by restriction analysis and sequencing, pXY301 Δ 39 was linearized with BamHI and ligated with the apramycin resistance gene-containing fragment (*Am*^R). The resulting plasmid was designated pXY301 Δ 39*Am*^R. The 0.9 kb *Am*^R fragment was amplified from plasmid pSET152 using the primers (*Am*^Rpf: 5'-CACGGATCCGGTTCATGTGCA-3' and *Am*^Rpr: 5'-ATCGGATCCCACGTGTTGC-3'. pXY301 Δ 39*Am*^R was introduced into *S. fungicidicus* by conjugation and the rest of the gene disruption procedures were performed as described previously. The *orf39* disruptant was confirmed by Southern analysis and designated as Sf Δ 39*Am*^R. To generate an *orf39* in-frame deletion mutant strain, pXY301 Δ 39 was introduced into the mutant strain Sf Δ 39*Am*^R by conjugation. Replacement of the apramycin resistance marker with the in-frame deletion copy of the *orf39* gene in mutant Sf Δ 39*Am*^R was confirmed by apramycin-sensitive

phenotype and Southern analysis. The corresponding mutant strain was designated Sf Δ 39.

DNA sequencing and analysis

DNA sequencing was performed at the OSU Center for Genome Research and Biocomputing using the Amplitaq dye-terminator sequencing system (Perkin Elmer) and Applied Biosystems automated DNA sequencers (models 373 and 377). Nucleotide sequences were determined for both strands. Sequence analysis was carried out using the VectorNTI (Invitrogen) software. Nucleotide and amino acid sequence similarity comparisons were carried out in public databases using the BLAST program.³⁷

Sf Δ 39 metabolite analysis and purification

Fermentation conditions for the production of enduracidins from *S. fungicidicus* strains, and the processing of the mycelia to yield an extract containing the peptides, have been previously described.³⁸ The extracts were passed through Varian HF Mega Bond Elut-C18 columns and sequentially eluted with H₂O, 25%, 50%, 100% acetonitrile and 50% acetonitrile in 50 mM phosphate buffer, pH 4.3. Fractions were concentrated and analyzed by HPLC and bioassay. Those containing the desired compounds were combined and further purified by semi-preparative reversed-phase HPLC with a C18 column (Gemini 10 μ M, 250 x 10 mm) from Phenomenex. Solvent A was water with 0.1% TFA, and solvent B was acetonitrile with 0.1% TFA. The flow rate was 5 ml/min starting with 25% B, increasing to 65% B over 30 min, and then held for a further 10 min. Separate 1 min fractions were collected over the entire run. Those containing the pure compounds were pooled for further MS analysis and bioassay.

Southern blot analysis

Genomic DNA from wild type and disruptant strains was prepared as described previously.³⁸ Restricted genomic DNA was separated by electrophoresis in 0.8% agarose gel and transferred onto positively charged nylon membrane (Roche). The DNA probe was prepared using digoxigenin-labeled dUTP and hybridization was revealed using a digoxigenin-DNA detection kit (Roche).

Disk diffusion antibacterial assay

A solution of each antibiotic to be test was prepared in 75% *aq.* methanol (50 mg/mL). Each sterile disk was treated with 20 μ L antibiotic solution and allowed to air dry. The disks were then placed on a TSB agar plate inoculated with *S. aureus* ATCC 29213. The plate was incubated at 37 °C for 16 hr. Diameter of zone of inhibition; The resulting zones of inhibition were measured: Enduracidin A: 14 mm, 2-*trans*-H₂ enduracidin A: 17 mm, 2-*cis*-H₂ enduracidin A: 15 mm, and H₄-enduracidin A: 14 mm.

Microdilution antibacterial assay

A culture of *S. aureus* was grown over night at 37 °C on tryptic soy agar. A single pure colony was used to inoculate a 5 mL TSB culture which was shaken at 150 rpm for 4 hrs at 37 °C. Antibiotic samples were prepared in 50% *aq.* MeOH and 20 μ L of each dilution was loaded into wells on a 96-well Microtest plate (Falcon). To each test well was added 80 μ L of sterile TSB followed by 100 μ L of $\sim 5 \times 10^5$ cells per mL of *S. aureus* in TSB. Each antibiotic was tested concurrently three times at each concentration. Initial absorbance readings at 600 nm were recorded and the plates were then sealed with parafilm and incubated at 37 °C for 16 hrs. Final absorbance readings were taken and percent growth calculated using the untreated well values as the reference. The percent inhibition was then calculated (100% – percent growth), the average was taken and standard deviations were calculated. MICs were determined as the lowest antibiotic concentration that exhibited >95% growth inhibition.

Sf Δ 39 isolate HPLC and mass spectroscopic analysis

HPLC analysis was performed using a Shimadzu CBM-20 instrument equipped with an SPD-20 diode array detector monitoring 230, 254 and 270 nm wavelengths. For general enduracidin analysis a Phenomenex 4.6 x 100 mm Kinetex 2.6 μ m XB-C18 column was used with a linear gradient from 10% MeCN in water + 0.1% TFA to 100% MeCN over 13 min. For the analysis of ozonolysis reactions the method was modified to a gradient from 5% MeCN in water + 0.1% TFA to 50% MeCN over 20 minutes and a five minute gradient to 100% MeCN at 1.5 mL/min. Semisynthetic compounds were purified using a Phenomenex Synergi Polar column (10 x 250 mm, 5 μ m) using a 20 gradient from 15% MeCN in water + 0.1% TFA to 50% MeCN followed by a 10 minute gradient to 100% MeCN at 3 mL/min. Mass spectroscopic analysis was performed using a Thermo-Finnigan LCQ Advantage instrument in ESI (+) mode.

NMR analysis

NMR spectra were recorded using a Bruker 300 MHz instrument for synthetic compounds (^1H -300 MHz, ^{13}C -75 MHz). Proton NMR experiments on enduracidin were performed using a Bruker Avance III 700 MHz instrument (^1H -700 MHz, ^{13}C -175 MHz). NMR experiments on H₂ and H₄-End samples were performed on a Bruker 600 MHz instrument (^1H -600 MHz, ^{13}C -150 MHz) in d₆-DMSO-D₂O (1:4). Enduracidin and fluorinated samples were dissolved in a mixture of 2:5 D₂O: methanol-*d*₄. The proton shifts are referenced to methanol-*d*₄ (3.31 ppm). Fluorine NMR spectra were recorded using a Bruker DPX-400 instrument (376 MHz) and a Bruker AvanceIII 500 instrument (471 MHz). Analysis of spectra was performed using Topspin ver 1.3 and 3.1 (Bruker) and MestReNova ver 8.0.2-11021 (Mestrelab Research).

Solvents and reagents

All solvents and reagents were purchased from Sigma Aldrich or Alpha Aesar and used as received unless stated. All reagents were purchased as ACS reagent grade products. Water was deionized (18 M Ω) using a Barnstead B-Pure filtration system. THF was distilled under Ar from a sodium-benzophenone still using unstabilized anhydrous solvent. Triethylamine was purchased as ACS reagent grade and passed through a column of basic alumina (50-200 μ m) prior to use. DMSO, DMF and MeOH were purchased as anhydrous solvents. MeOH was further dried over 3 Å molecular sieves. Other solvents were purchased and used without further purification.

Lipid tail reduction methods and Sf Δ 39 isolate NMR analysis

Enduracidin A: ^1H NMR (700 MHz, 1:4 d₆-DMSO: D₂O, 25 °C) Alkyl tail shifts: δ 2.23 (m, 2H, H-6), 5.71 (d, $J=11.3$, 1H, H-2), 6.27 (dt, $J = 14.7, 7.2$ Hz, 1H, H-5), 6.63 (m, 1H, H-3), 7.24 (m, 1H, H-4); LRMS ESI (+) m/z 1177.4 [M+2H]²⁺.

2-*cis*-H₂ enduracidin A: A mixture of enduracidin A (4 mg, 1.7 μ mol) and 5% Pd/C (0.36 mg, 0.17 μ mol) in DMF (3 mL) was stirred under hydrogen atmosphere (1 atm) at 0 °C for 30 min. The reaction was filtered through a plug of celite and a syringe filter (0.2 μ m). The filtrate solvent was evaporated under reduced pressure and the residue purified by HPLC, retention time 10 min. ^1H NMR (600 MHz, 1:4 d₆-DMSO: D₂O, 35 °C) Alkyl tail shifts: δ 2.61 (m, 2H, H-4), 5.91 (d, $J=11.5$ Hz, 1H, H-2), 6.22 (dt $J=11.5, 7.5$ Hz, 1H, H-3); LRMS ESI (+) m/z 1178.5 [M+2H]²⁺.

2-*trans*-H₂ enduracidin A: A mixture of enduracidin A (4 mg, 1.7 μ mol) and 5% Pd/C (0.36 mg, 0.17 μ mol) in DMF (3 mL) was stirred under hydrogen atmosphere (1 atm) at ambient temperature for 60 min. The reaction was filtered through a plug of celite and a syringe filter (0.2 μ m). The filtrate solvent was evaporated under reduced pressure and the residue purified by RP-HPLC, retention time 15.1 min. ^1H NMR (600 MHz, 1:4 d₆-DMSO: D₂O, 35 °C) Alkyl tail shifts: δ 2.25 (m 2H, H-4), 6.03 (d, $J=15.5$ Hz, 1H, H-2), 6.89 (m, 1H, H-3); LRMS ESI (+) m/z 1178.4 [M+2H]²⁺.

H₄ enduracidin A: A mixture of enduracidin A (4 mg, 1.7 μ mol) and 5% Pd/C (0.36 mg, 0.17 μ mol) in DMF (3 mL) was stirred under hydrogen atmosphere (1 atm) at ambient temperature for 3 hrs. The reaction was filtered through a plug of celite and a syringe filter (0.2 μ m). The filtrate solvent was evaporated under reduced pressure and the residue purified by RP-HPLC, retention time 14.2 min. ¹H NMR (600 MHz, 1:4 d₆-DMSO: D₂O, 35 °C) Alkyl tail shifts were not determined; LRMS ESI (+) *m/z* 1179.5 [M+2H]²⁺.

Sf Δ 39 enduracidin A isolate: ¹H NMR (700 MHz, 1:4 d₆-DMSO: D₂O, 25 °C) Alkyl tail shifts: δ 2.23 (m, 2H, H-6), 5.71 (d, *J*=11.3, 1H, H-2), 6.27 (dt, *J* = 14.7, 7.2 Hz, 1H, H-5), 6.63 (m, 1H, H-3), 7.24 (m, 1H, H-4); LRMS ESI (+) *m/z* 1177.4 [M+2H]²⁺.

Lipid tail ozonolysis methods

Orn4-N-Boc-enduracidin: To a solution of enduracidin (3.0 g, 1.3 mmol) in 70% *aqueous* MeOH (100 mL) was added NaHCO₃ (2.2 g, 25.5 mmol) followed by Boc₂O (2.84 g, 12.7 mmol) at ambient temperature. The reaction was stirred for 24 hrs. under Ar and monitored by HPLC (Kinetex column method). After conversion of the starting material (rt = 4.7 and 4.9 min) to product (rt = 5.7 and 5.9 min) was observed the reaction was cooled in an ice bath and acidified with AcOH (15 mL). After the solvent was removed under reduced pressure the crude product was dissolved in DMF and precipitated with EtOAc. The solid is collected by filtration and washed with ether then water. The product is then dissolved in 2:2:1 anhydrous methanol:EtOAc:toluene and the solvent removed yielding Boc-End (2.3 g, 0.94 mmol, 74%) as a white powder. LRMS ESI (+) *m/z* = 1227.5 (Boc-End A) and 1234.5 (Boc-End B) [M+2H]²⁺.

Orn4-N-Fmoc-enduracidin To a solution of enduracidin (200 mg, 0.085 mmol) in 50% *aqueous* THF (10 mL) was added NaHCO₃ (440 mg, 5.1 mmol) followed by Fmoc-ONSu (440 mg, 1.3 mmol) at ambient temperature. The reaction was stirred for

18 hrs. under Ar and monitored by HPLC (Kinetex column method). After conversion of the starting material (rt = 4.7 and 4.9 min) to product (rt = 5.8 and 6.0 min) was observed the reaction was acidified with AcOH (3 mL). After the solvent was removed under reduced pressure the crude product was dissolved in DMF and precipitated with EtOAc. The solid is collected by filtration and washed with EtOAc and water. The product is then dissolved in 2:2:1 anhydrous methanol:EtOAc:toluene and the solvent removed yielding Fmoc-End (100 mg, 0.039 mmol, 46%) as a white powder. LRMS ESI (+) m/z = 1288.5 (Boc-End A) and 1295.5 (Boc-End B) $[M+2H]^{2+}$.

Ozonolysis general method Ozone was bubbled into a solution of protected enduracidin (10 mg, 4 μ mol) in solvent (5 mL) with stirring in a flame dried flask under Ar at -78 °C. After the specified time, Ar was bubbled through the solvent for 10 min, and then the reducing agent was added. The reaction was then allowed to warm to ambient temperature over 5 hrs. The solvent was removed and the crude product dissolved in 70% *aqueous* MeOH for analysis. Only degraded product was observed in the reaction mixtures. Starting material: Boc-End was used for the examination of reaction conditions. Solvents: MeOH, 2:1 MeOH:DCM, 1:1 MeOH:DCM, 2:1 MeOH:DMF, 2:1 DCM:DMF, and 4:1 DCM:DMF. Reducing reagent: DMS, TPP and Zn-AcOH were used in each of the solvent systems while Pyr was only used in MeOH-DCM solvents as prescribed in literature.^{18a}

Lipid tail Diels-Alder reactions

N-Me-Maleimide/Enduracidin reaction A solution of Boc-End (10 mg, 4 μ mol) in solvent (300 μ L) with N-methylmaleimide (1 mg, 8 μ mol) in a 4 mL vial was stirred under Ar for 48 hrs. The reaction was monitored by MS. The solvent was removed under reduced pressure. The crude product was dissolved in 70% *aqueous* MeOH and filtered, yielding only starting material. LRMS ESI (+) m/z = 1227.5 (Boc-End A) and 1234.5 (Boc-End B). Solvents: 2:1 DMF:water, 2:1 MeOH:water, 2:1 DMF:100 mM NaAcOH, 2:1 MeOH:100 mM NaAcOH, 2:1 MeCN:water, DMF and MeOH.

2-nitroso-toluene/Enduracidin reaction A solution of Boc-End (10 mg, 4 μmol) in solvent (500 μL) with 2-nitroso-toluene (5 mg, 40 μmol) in a 4 mL vial was heated at 70 $^{\circ}\text{C}$ under Ar for 24 hrs. To a set of reactions was added a CuI catalyst (0.8 mg, 4 μmol). Catalyzed reactions were run for 24 hrs. at ambient temperature then check by MS prior to heating for 24 hrs at 70 $^{\circ}\text{C}$. The solvent was then removed under reduced pressure. The crude product was dissolved in 70% *aqueous* MeOH and filtered. HPLC and MS analysis indicated no new enduracidin compounds were produced. LRMS ESI (+) m/z = 1227.5 (Boc-End A) and 1234.5 (Boc-End B). Solvents: 1:4 DMSO:toluene, MeOH, 1:4 DMF:toluene and Acetone. The solvent systems 1:4 DMSO:toluene, MeOH and 1:4 DMF:toluene were used for the catalyzed series of experiments.

Danishefsky's diene/Enduracidin reaction A solution of Boc-End (10 mg, 4 μmol) in solvent (500 μL , 1:4 DMSO:toluene or 1:4 DMF:toluene) with Danishefsky's diene (8 μL , 40 μmol) in a 4 mL vial was heated at 70 $^{\circ}\text{C}$ under Ar for 24 hrs. A set of reactions were run with TEA (6 eq.) as an additive. To an additional set of reactions was added ZnI_2 (1.4 mg, 4 μmol) or ZnCl_2 (0.6 mg, 4 μmol) as catalysts. Catalyzed reactions were run for 24 hrs. at ambient temperature then check by MS prior to heating for 24 hrs at 70 $^{\circ}\text{C}$. To end the reaction the solvent was removed under reduced pressure. The crude product was then dissolved in 70% *aqueous* MeOH and filtered. HPLC and MS analysis indicated no new enduracidin compounds were produced. The reactions containing zinc were found to have deprotected Boc-End. LRMS ESI (+) m/z = 1177.5 and 1184.5. The reactions containing TEA were found to return starting material. LRMS ESI (+) m/z = 1227.5 (Boc-End A) and 1234.5 (Boc-End B). The other solvent systems with no additive were found to degrade the compound. The DMSO-toluene reaction was found to produce a new compound which could not be identified. LRMS ESI (+) m/z = 1311.5.

Lipid tail dihydroxylation

General method To a stirred solution of enduracidin (30 mg, 13 μmol) in 70% aqueous IPA (500 μL) was added a 2.5% solution of OsO_4 in *t*-BuOH (13 μL , 1 μmol) followed by a 50% solution of NMO in water (10 μL , 38 μmol). The reaction was monitored by MS and stopped after 30 min by the addition of saturated Na_2SO_3 (100 μL). The solvent was then removed and the crude product dissolved in 70% MeOH, syringe filtered (2 μm) and purified by HPLC using the Polar column method. Six products were formed. Three representative compounds were isolated and characterized.

2,3,4,5-(OH)₄-enduracidin A ^1H NMR (500 MHz, 2:1 d_4 -methanol: D_2O , 25 $^\circ\text{C}$) Alkyl tail shifts could not be identified; LRMS ESI (+) m/z 1211.5 $[\text{M}+2\text{H}]^{2+}$.

2,3-(OH)₄-enduracidin B ^1H NMR (500 MHz, 2:1 d_4 -methanol: D_2O , 25 $^\circ\text{C}$) Alkyl tail shifts: δ 5.75 (m, 1H, H-5), 5.51 (m, 1H, H-4), 4.29 (m 1H, H-3), 2.02 (m, 2H, H-6); LRMS ESI (+) m/z 1201.5 $[\text{M}+2\text{H}]^{2+}$.

4,5-(OH)₄-enduracidin A: ^1H NMR (500 MHz, 2:1 d_4 -methanol: D_2O , 25 $^\circ\text{C}$) Alkyl tail shifts: δ 6.14 (m, 1H, H-2), 5.11 (m, 1H, H-3), 3.53 (m 1H, H-4), 1.51 (m, 1H, H-5); LRMS ESI (+) m/z 1194.5 $[\text{M}+2\text{H}]^{2+}$.

Enduracidin nitration

Sodium nitrite general method: To a stirred solution of Fmoc-End (6 mg, 2 μmol) in AcOH (1 mL) under Ar was added NaNO_2 (1.5 mg, 16 μmol). The reaction was stirred for 3 hrs. The solvent was removed under reduced pressure and the crude product was dissolved in 70% MeOH and syringe filtered. The reaction was analyzed by HPLC and MS indicating the degradation of the compound. Solvent conditions were altered to 1:2 water:AcOH to aid in solubility yielding on degraded product. The reaction conditions were altered with the water-AcOH reactions cooling the reaction in an ice bath. Reaction times were reduced to 30 minutes in an attempt to prevent degradation. All reaction conditions resulted in product degradation.

Potassium nitrate general method: To a stirred solution of Fmoc-End (6 mg, 2 μ mol) in TFA (1 mL) under Ar was added KNO₃ (12 mg, 0.12 mmol). The reaction was stirred for 2 hrs. The solvent was removed under reduced pressure and the crude product was dissolved in 70% MeOH and syringe filtered. The reaction was analyzed by HPLC (Polar column isolation method) and MS indicating that no reaction had occurred. LRMS ESI (+) m/z = 1288.5 (Fmoc-End A) and 1295.5 (Fmoc-End B). Solvent conditions were altered to 1:2 water:TFA and 100% AcOH to aid in solubility. The altered reaction conditions resulted in only starting material.

Tetranitromethane general method: To a solution of Fmoc-End (10 mg, 4 μ mol) was dissolved in 2 mL of (1:1) MeOH:10 mM ammoniumacetate pH 7 and stirred at room temperature. Tetranitromethane (17 mg, 85 μ mol) in 2.7 mL of MeOH was added slowly over 30 min and stirred for 5 h. The reaction was halted by the addition of AcOH (0.5 mL) and the solvent was removed under reduced pressure. The crude product was dissolved in 70% *aqueous* MeOH and analyzed by HPLC (Kinetex analysis method) and MS. Only starting material was observed. HPLC, retention time 5.7 and 6.0 min; LRMS ESI (+) m/z = 1288.5 (Fmoc-End A) and 1295.5 (Fmoc-End B).

References

1. Fang, X.; Tiyanont, K.; Zhang, Y.; Wanner, J.; Boger, D.; Walker, S., The Mechanism of Action of Ramoplanin and Enduracidin. *Mol. BioSyst.* **2006**, *2*, 69-76.
2. Hamburger, J. B.; Hoertz, A. J.; Lee, A.; Senturia, R. J.; McCafferty, D. G.; Loll, P. J., A crystal structure of a dimer of the antibiotic ramoplanin illustrates membrane positioning and a potential lipid II docking interface. *Proc. Natl. Acad. Sci. U. S. A.* **2009**, *106* (33), 13759-13764.
3. (a) Matsuzawa, T.; Fujisawa, H.; Aoki, K.; Mima, H., Effect of Some Non-ionic Surfactants on the Absorption of Enduracidin From the Muscles. *Chem. Pharm. Bull. (Tokyo)* **1969**, *17* (5), 999-1004; (b) Peromet, M.; Schoutens, E.; Yourassowsky, E., Clinical and Microbiological Study of Enduracidin in Infections Due to Methicillin-resistant Strains of *Staphylococcus aureus*. *Chemotherapy* **1973**, *19* (1), 53-61; (c) Yourassowsky, E.; Monsieur, R., *In vitro* and *in vivo* Activity of Enduracidin on *Staphylococcus aureus*. *Chemotherapy* **1972**, *17*, 182-187.
4. Heinzelmann, E.; Berger, S.; Muller, C.; Hartner, T.; Poralla, K.; Wohlleben, W.; Schwartz, D., An acyl-CoA dehydrogenase is involved in the formation of the delta-cis3 double bond in the acyl residue of the lipopeptide antibiotic friulimicin in *Actinoplanes friuliensis*. *Microbiology* **2005**, *151* (6), 1963-1974.
5. Heinzelmann, E.; Berger, S.; Müller, C.; Härtner, T.; Poralla, K.; Wohlleben, W.; Schwartz, D., An acyl-CoA dehydrogenase is involved in the formation of the Δ cis3 double bond in the acyl residue of the lipopeptide antibiotic friulimicin in *Actinoplanes friuliensis*. *Microbiology* **2005**, *151* (6), 1963-1974.
6. Hoertz, A. J.; Hamburger, J. B.; Gooden, D. M.; Bednar, M. M.; McCafferty, D. G., Studies on the biosynthesis of the lipodepsipeptide antibiotic Ramoplanin A2. *Biorg. Med. Chem.* **2012**, *20* (2), 859-865.

7. D'Costa, V. M.; McGrann, K. M.; Hughes, D. W.; Wright, G. D., Sampling the Antibiotic Resistome. *Science* **2006**, *311* (5759), 374-377.
8. D'Costa, V. M.; Mukhtar, T. A.; Patel, T.; Koteva, K.; Waglechner, N.; Hughes, D. W.; Wright, G. D.; De Pascale, G., Inactivation of the Lipopeptide Antibiotic Daptomycin by Hydrolytic Mechanisms. *Antimicrob. Agents Chemother.* **2012**, *56* (2), 757-764.
9. (a) Gandolfi, R.; Marinelli, F.; Ragg, E.; Romano, D.; Molinari, F., Chemoenzymatic deacylation of ramoplanin. *Bioorg. Med. Chem. Lett.* **2012**, *22* (16), 5283-5287; (b) Kreuzman, A. J.; Hodges, R. L.; Swartling, J. R.; Pohl, T. E.; Ghag, S. K.; Baker, P. J.; McGilvray, D.; Yeh, W. K., Membrane-associated echinocandin B deacylase of *Actinoplanes utahensis* : purification, characterization, heterologous cloning and enzymatic deacylation reaction. *J. Ind. Microbiol. Biotechnol.* **2000**, *24* (3), 173-180.
10. Ciabatti, R.; Maffioli, S. I.; Panzone, G.; Canavesi, A.; Michelucci, E.; Tiseni, P. S.; Marzorati, E.; Checchia, A.; Giannone, M.; Jabes, D.; Romano, G.; Brunati, C.; Candiani, G.; Castiglione, F., Synthesis and Preliminary Biological Characterization of New Semisynthetic Derivatives of Ramoplanin. *J. Med. Chem.* **2007**, *50* (13), 3077-3085.
11. (a) Bartesaghi, S.; Peluffo, G.; Zhang, H.; Joseph, J.; Kalyanaraman, B.; Radi, R., Chapter 12 Tyrosine Nitration, Dimerization, and Hydroxylation by Peroxynitrite in Membranes as Studied by the Hydrophobic Probe N-t-BOC-L-tyrosine tert-Butyl Ester. In *Methods Enzymol.*, Enrique, C.; Lester, P., Eds. Academic Press: 2008; Vol. Volume 441, pp 217-236; (b) Bhuyan, B. J.; Mugesh, G., Effect of peptide-based captopril analogues on angiotensin converting enzyme activity and peroxynitrite-mediated tyrosine nitration. *Org. Biomol. Chem.* **2011**, *9* (14), 5185-5192; (c) Nakagawa, H.; Takusagawa, M.; Arima, H.; Furukawa, K.; Kinoshita, T.; Ozawa, T.;

Ikota, N., Selective Scavenging Property of the Indole Moiety for the Nitrating Species of Peroxynitrite. *Chem. Pharm. Bull.* **2004**, *52* (1), 146-149.

12. (a) Choi, S. K.; Goodnow, R. A.; Kalivretenos, A.; Chiles, G. W.; Fushiya, S.; Nakanishi, K., Synthesis of novel and photolabile philanthotoxin analogs: Glutamate receptor antagonists. *Tetrahedron* **1992**, *48* (23), 4793-4822; (b) Cook, S.; Jackson, G., Characterization of Tyrosine Nitration and Cysteine Nitrosylation Modifications by Metastable Atom-Activation Dissociation Mass Spectrometry. *J. Am. Soc. Mass. Spectrom.* **2011**, *22* (2), 221-232; (c) Guillemette, G.; Bernier, M.; Parent, P.; Leduc, R.; Escher, E., Angiotensin II: dependence of hormone affinity on the electronegativity of a single side chain. *J. Med. Chem.* **1984**, *27* (3), 315-320; (d) Leite, J. F.; Cascio, M., Probing the Topology of the Glycine Receptor by Chemical Modification Coupled to Mass Spectrometry. *Biochemistry* **2002**, *41* (19), 6140-6148; (e) Petersson, A.-S.; Steen, H.; Kalume, D. E.; Caidahl, K.; Roepstorff, P., Investigation of tyrosine nitration in proteins by mass spectrometry. *J. Mass Spectrom.* **2001**, *36* (6), 616-625.

13. (a) Black, R. M.; Balkovec, J. M.; Nollstadt, K. M.; Dreikorn, S.; Bartizal, K. F.; Abruzzo, G. K., Synthesis and structure-activity relationships of novel 3'-Hty-substituted pneumocandins. *Bioorg. Med. Chem. Lett.* **1997**, *7* (22), 2879-2884; (b) Bonnett, R.; Nicolaidou, P., Nitrosation and nitrosylation of haemoproteins and related compounds. Part 2. The reaction of nitrous acid with the side chains of alpha-acylamino-acid esters. *J. Chem. Soc., Perkin Trans. 1* **1979**, 1969-1974; (c) Wright, J. B., The synthesis of benzoxazole-5-acetic acid derivatives. *J. Heterocycl. Chem.* **1972**, *9* (3), 681-682.

14. Sum, P.-E.; How, D.; Torres, N.; Newman, H.; Petersen, P. J.; Mansour, T. S., Synthesis and activity of novel benzoxazole derivatives of mannopeptimycin glycopeptide antibiotics. *Bioorg. Med. Chem. Lett.* **2003**, *13* (15), 2607-2610.

15. Barrett, D.; Tanaka, A.; Harada, K.; Ohki, H.; Watabe, E.; Maki, K.; Ikeda, F., Synthesis and biological activity of novel macrocyclic antifungals: acylated conjugates

of the ornithine moiety of the lipopeptidolactone FR901469. *Bioorg. Med. Chem. Lett.* **2001**, *11* (4), 479-482.

16. Keinan, E.; Greenspoon, N., Highly chemoselective palladium-catalyzed conjugate reduction of α,β -unsaturated carbonyl compounds with silicon hydrides and zinc chloride cocatalyst. *J. Am. Chem. Soc.* **1986**, *108* (23), 7314-7325.

17. Alligood, K. J.; Charifson, P. S.; Crosby, R.; Consler, T. G.; Feldman, P. L.; Gampe Jr, R. T.; Gilmer, T. M.; Jordan, S. R.; Milstead, M. W.; Mohr, C.; Peel, M. R.; Rocque, W.; Rodriguez, M.; Rusnak, D. W.; Shewchuk, L. M.; Sternbach, D. D., The formation of a covalent complex between a dipeptide ligand and the src SH2 domain. *Bioorg. Med. Chem. Lett.* **1998**, *8* (10), 1189-1194.

18. (a) Semenov, V. V.; Kiselyov, A. S.; Titov, I. Y.; Sagamanova, I. K.; Ikizalp, N. N.; Chernysheva, N. B.; Tsyganov, D. V.; Konyushkin, L. D.; Firgang, S. I.; Semenov, R. V.; Karmanova, I. B.; Raihstat, M. M.; Semenova, M. N., Synthesis of Antimitotic Polyalkoxyphenyl Derivatives of Combretastatin Using Plant Allylpolyalkoxybenzenes. *J. Nat. Prod.* **2010**, *73* (11), 1796-1802; (b) Schwartz, C.; Raible, J.; Mott, K.; Dussault, P. H., Fragmentation of Carbonyl Oxides by *N*-Oxides: An Improved Approach to Alkene Ozonolysis. *Org. Lett.* **2006**, *8* (15), 3199-3201.

19. Qiu, Y.; Kuo, C.-H.; Zappi, M. E., Ozonation Kinetics of Six Dichlorophenol Isomers. *Ozone: Science & Engineering* **2002**, *24* (2), 123-131.

20. Buller, F.; Mannocci, L.; Zhang, Y.; Dumelin, C. E.; Scheuermann, J.; Neri, D., Design and synthesis of a novel DNA-encoded chemical library using Diels-Alder cycloadditions. *Bioorg. Med. Chem. Lett.* **2008**, *18* (22), 5926-5931.

21. (a) Goh, Y. W.; Pool, B. R.; White, J. M., Structural Studies on Cycloadducts of Furan, 2-Methoxyfuran, and 5-Trimethylsilylcyclopentadiene with Maleic Anhydride and *N*-Methylmaleimide. *J. Org. Chem.* **2007**, *73* (1), 151-156; (b) Iosif, F.; Parvulescu, V. I.; Perez-Bernal, M. E.; Ruano-Casero, R. J.; Rives, V.; Kranjc, K.;

Polanc, S.; Kocevar, M.; Genin, E.; Genet, J.-P.; Michelet, V., Heterogeneous hydrogenation of bicyclo[2.2.2]octenes on Rh/TPPTS/LDH catalysts. *J. Mol. Catal. A: Chem.* **2007**, *276* (1-2), 34-40.

22. (a) Krchnak, V.; Waring, K. R.; Noll, B. C.; Moellmann, U.; Dahse, H.-M.; Miller, M. J., Evolution of Natural Product Scaffolds by Acyl- and Arylnitroso Hetero-Diels-Alder Reactions: New Chemistry on Piperine. *J. Org. Chem.* **2008**, *73* (12), 4559-4567; (b) Monbaliu, J.-C. M. R.; Cukalovic, A.; Marchand-Brynaert, J.; Stevens, C. V., Straightforward hetero Diels-Alder reactions of nitroso dienophiles by microreactor technology. *Tetrahedron Lett.* **2010**, *51* (44), 5830-5833; (c) Yamamoto, Y.; Yamamoto, H., Catalytic Asymmetric Nitroso-Diels-Alder Reaction with Acyclic Dienes. *Angew. Chem. Int. Ed.* **2005**, *44* (43), 7082-7085.

23. (a) Graziani, E. I.; Ruan, B.; Pong, K.; Bowlby, M. R. Immunophilin Ligands and Methods for Modulating Immunophilin and Calcium Channel Activity. WO2008/94147, 2010-08-05, 2008; (b) Ruan, B.; Pong, K.; Jow, F.; Bowlby, M.; Crozier, R. A.; Liu, D.; Liang, S.; Chen, Y.; Mercado, M. L.; Feng, X.; Bennett, F.; von Schack, D.; McDonald, L.; Zaleska, M. M.; Wood, A.; Reinhart, P. H.; Magolda, R. L.; Skotnicki, J.; Pangalos, M. N.; Koehn, F. E.; Carter, G. T.; Abou-Gharbia, M.; Graziani, E. I., Binding of rapamycin analogs to calcium channels and FKBP52 contributes to their neuroprotective activities. *Proc. Natl. Acad. Sci. U. S. A.* **2008**, *105* (1), 33-38.

24. Alcaide, B.; Almendros, P.; Alonso, J. M.; Aly, M. F., Useful Dual Diels-Alder Behavior of 2-Azetidinone-Tethered Aryl Imines as Azadienophiles or Azadienes: A β -Lactam-Based Stereocontrolled Access to Optically Pure Highly Functionalized Indolizidine Systems. *Chem. Eur. J.* **2003**, *9* (14), 3415-3426.

25. (a) Grugier, J.; Xie, J.; Duarte, I.; Valéry, J.-M., Synthesis of 2-(N-Acetylamino)-2-deoxy-C-glucopyranosyl Nucleosides as Potential Inhibitors of Chitin Synthases. *J. Org. Chem.* **2000**, *65* (4), 979-984; (b) Sedrani, R.; Thai, B.; France, J.;

Cottens, S., Dihydroxylation of the Triene Subunit of Rapamycin. *J. Org. Chem.* **1998**, *63* (26), 10069-10073.

26. (a) Izquierdo, I.; Plaza, M. T.; Tamayo, J. A., Polyhydroxylated pyrrolizidines. Part 5: Stereoselective synthesis of 1,2-dihydroxypyrrolizidines as a model for the preparation of densely polyhydroxylated pyrrolizidines. *Tetrahedron: Asymmetry* **2004**, *15* (22), 3635-3642; (b) Ward, R. A.; Procter, G., A Total Synthesis of the Natural Enantiomer of the Gastroprotective Natural Products AI-77-B and Amicoumacin C Hydrochloride. *Tetrahedron* **1995**, *51* (45), 12301-12318.

27. Amat, M.; Llor, N.; Huguet, M.; Molins, E.; Espinosa, E.; Bosch, J., Unprecedented Oxidation of a Phenylglycinol-Derived 2-Pyridone: Enantioselective Synthesis of Polyhydroxypiperidines. *Org. Lett.* **2001**, *3* (21), 3257-3260.

28. Hunter, T. J.; O'Doherty, G. A., An Enantioselective Synthesis of Benzylidene-Protected syn-3,5-Dihydroxy Carboxylate Esters via Osmium, Palladium, and Base Catalysis. *Org. Lett.* **2001**, *3* (7), 1049-1052.

29. (a) Manuszak, M.; Koppenol, W. H., The enthalpy of isomerization of peroxyxynitrite to nitrate. *Thermochim. Acta* **1996**, *273* (0), 11-15; (b) Nonoyama, N.; Oshima, H.; Shoda, C.; Suzuki, H., The Reaction of Peroxyxynitrite with Organic Molecules Bearing a Biologically Important Functionality. The Multiplicity of Reaction Modes as Exemplified by Hydroxylation, Nitration, Nitrosation, Dealkylation, Oxygenation, and Oxidative Dimerization and Cleavage. *Bull. Chem. Soc. Jpn.* **2001**, *74* (12), 2385-2395; (c) Uppu, R. M.; Squadrito, G. L.; Cueto, R.; Pryor, W. A., Synthesis of peroxyxynitrite by azide-ozone reaction. In *Methods Enzymol.*, Lester, P., Ed. Academic Press: 1996; Vol. Volume 269, pp 311-321.

30. Rubbo, H.; Trostchansky, A.; O'Donnell, V. B., Peroxyxynitrite-mediated lipid oxidation and nitration: Mechanisms and consequences. *Arch. Biochem. Biophys.* **2009**, *484* (2), 167-172.

31. Toth, G.; Russell, K. C.; Landis, G.; Kramer, T. H.; Fang, L.; Knapp, R.; Davis, P.; Burks, T. F.; Yamamura, H. I.; Hruby, V. J., Ring substituted and other conformationally constrained tyrosine analogs of [D-Pen²,D-Pen⁵]enkephalin with δ opioid receptor selectivity. *J. Med. Chem.* **1992**, *35* (13), 2384-2391.
32. Higashide, E.; Hatano, K.; Shibata, M.; Nakazawa, K., Enduracidin, a new antibiotic. I. *Streptomyces fungicidicus* No. B5477, an enduracidin producing organism. *J. Antibiot.* **1968**, *21* (2), 126-37.
33. Kieser, T.; Bibb, M. J.; Chater, K. F.; Hopwood, D. A., *Practical Streptomyces Genetics*. John Innes Foundation: Norwich Research Park: Colney, Norwich, 2000.
34. Yin, X.; Zabriskie, T. M., The enduracidin biosynthetic gene cluster from *Streptomyces fungicidicus*. *Microbiology* **2006**, *152* (10), 2969-83.
35. Mazodier, P.; Petter, R.; Thompson, C., Intergeneric conjugation between *Escherichia coli* and *Streptomyces* species. *J. Bacteriol.* **1989**, *171* (6), 3583-3585.
36. Yin, X.; O'Hare, T.; Gould, S. J.; Zabriskie, T. M., Identification and cloning of genes encoding viomycin biosynthesis from *Streptomyces vinaceus* and evidence for involvement of a rare oxygenase. *Gene* **2003**, *312* (0), 215-224.
37. Altschul, S. F.; Gish, W.; Miller, W.; Myers, E. W.; Lipman, D. J., Basic local alignment search tool. *J. Mol. Biol.* **1990**, *215* (3), 403-410.
38. Yin, X.; Chen, Y.; Zhang, L.; Wang, Y.; Zabriskie, T. M., Enduracidin Analogues with Altered Halogenation Patterns Produced by Genetically Engineered Strains of *Streptomyces fungicidicus*. *J. Nat. Prod.* **2010**, *73* (4), 583-589.

CHAPTER FIVE

GENERAL CONCLUSIONS

Neal Goebel

Biosynthetic Studies

The understanding of the biosynthetic pathways involved in producing enduracidin precursors, and tailoring enduracidin lays a foundation for the modification of enduracidin through genetic manipulation. Additionally, large-scale production of enduracididine through biochemical methods would aid in research into new mannopeptimycin analogs. Presently much of the enduracididine biosynthetic pathway remains unknown. The bioassay results, while not clearly elucidating enzyme function, indicated that 4-hydroxyarginine (4-OH-Arg) or a variant serves as an intermediate in the pathway. Our collaborative work has shown that EndR/MppR is responsible for the cyclization reaction forming the aminoimidazoline ring. It is evident from the complementation experiments that EndQ can act as a transaminase using 4-OH Arg and 2-ketoenduracididine as substrates. EndP and EndQ are predicted to function as transaminases. The timing of the introduction of the 4-hydroxyl group on arginine is still unknown. Because the biosyntheses of related compounds, like capreomycin, rely on monooxygenases for similar reactions it seems likely that the *S. fungicidicus* and *Amycolatopsis hygroscopicus* genomes may contain a monooxygenase for the biosynthesis of 4-OH Arg. Additional research sequencing the genome, bioinformatic analysis and genetic disruption experiments should provide further insight into the production of 4-OH Arg. The continued work of our collaborator (Dr. Nicholas Silvaggi, University of Wisconsin-Milwaukee) into the structure and function of MppP and MppQ should provide insight into each enzyme's function in enduracididine biosynthesis.

The biosynthetic work on the lipid tail provides limited information on the roles of each enzyme proposed to introduce the diene. Bioinformatic data and the production of H₄-enduracidin in *orf45* disruptants suggest that Orf45 is responsible for the formation of the lipid-CoA thioester and the introduction of the C2 double bond.

The proposed function of Orf44 and Orf39 are the isomerization of the C2 alkene and introduction of the C4 olefin. The clarification of each individual enzyme's role will require a more direct approach and will likely involve purified protein assays, NMR or crystallization for the determination of the structure of the proteins bound to possible substrates. The possibility of protein-protein interactions and the potential that a mutant-produced lipid tail with alternate stereochemistry is not being incorporated into enduracidin due to enzyme stereoselectivity prevents the mutagenic approach from revealing the exact details of the biosynthetic pathway.

The biosynthetic function of the halogenase, Orf30, was probed during the incorporation experiments using 2-F and 3-F-Hpg. The production of deschloro enduracidin by *S. fungicidicus* supplemented with 3-F-Hpg indicates that Orf30 may be inhibited by 3-F-Hpg. This fact appears to be confirmed as both the mono and deschloro species of 3'-F₆-enduracidin are produced. Interestingly, the presence of fluorine in the 2' position of Hpg-13 also inhibited halogenation, yielding the monochloro species. The halogenation appears to occur at the 5' position according to NMR analysis. The production of dichloro-3'-F₆-enduracidin and the ¹⁹F-NMR data of dichloro-2'-F₆-enduracidin suggest that the halogenase can act on an alternate Hpg residue. The confirmation of this data will hopefully be resolved by MS/MS analysis, which has to this point failed. The production of more compound is possible and would allow the determination to be made by NMR spectroscopy.

Semisynthetic Studies

The semisynthetic studies with enduracidin have indicated that few of the modification routes attempted are viable. Enduracidin's apparent sensitivity to oxidation, as observed in the ozonolysis and nitration reactions, limits the semisynthetic methods possible. Interestingly, hydroxylation of the enduracidin lipid diene proved to be a feasible approach. The production of three dihydroxylation

products using OsO₄ and NMO provided valuable information concerning the introduction of polar groups on the lipid tail. C2 and C3 dihydroxylated enduracidin proved to have with the best bioactivity though it was significantly reduced compared to the parent antibiotic. The introduction of more hydroxyl groups, further down the lipid tail, decreased bioactivity further, providing useful data for minimal length of alternate lipid tails. Exploration of modifications to the dihydroxyl groups should be approached next. The reduction of the lipid tail double bonds appears to have little effect on the bioactivity. The structures did prove useful in the analysis of the lipid tail biosynthesis. Future work in this area should involve the use of an enzymatic deacylation reaction and subsequent alkylation to access new enduracidin analogs.

The use of the lipid tail diene in a variety of Diels-Alder reactions was unsuccessful. The natural configuration appears to prevent the proper alignment for the diene to react in a [4+2] reaction. Use of a lipid tail olefin as a dienophile similarly proved unsuccessful. Using Danishefsky's diene, one product was observed by MS but could not be isolated and did not correspond to a predicted product.

Mutasynthetic Modification of Enduracidin

By utilizing the data known about hydroxyphenylglycine (Hpg) biosynthesis the incorporation of fluorine, through F-Hpg, into enduracidin was achieved. Two F-Hpg isomers (2-F-Hpg and 3-F-Hpg) were found to incorporate into enduracidin. The incorporation of a difluoro-Hpg or nitro-Hpg was unsuccessful. The minimal loss of bioactivity for both 2'-F₆ and 3'-F₆-enduracidin indicated that the Hpg residues are viable targets for modification. Low production of 2'-F₆-enduracidin limits its viability for larger scale production. Presently the specificity of wild-type biosynthetic enzymes limit the number of compounds capable of being produced. Future work to modify the adenylation domains may increase production of F₆-enduracidin and allow for the incorporation of nitro-Hpg and other Hpg variants. Further analysis of this method for

modifying the physical properties of enduracidin is needed. While lab-scale methods are inefficient at producing the large quantities of compound, larger scale cultures using a bioreactor could provide sufficient compound for the evaluation of the physical properties of each of the F₆-enduracidins. These general methods should be applicable to other organisms producing Hpg-containing natural products.

Potential of Enduracidin

Though failing to be developed for clinical use during its initial evaluation, enduracidin still holds high potential for use as a clinical antibiotic. The continued battle against drug resistant bacterial strains necessitates the development of new and potent antibiotics. The work presented here has demonstrated a preliminary proof of concept for the mutasynthetic modification of enduracidin and some semisynthetic modifications. Further exploration of new analogs and their production is needed before extensive biological evaluations can begin. The methods of production, particularly by mutasynthesis, can be refined and improved. Additionally, the use of enduracidin and related peptides as feed additives needs to be reexamined. The potential for developing resistance remains and minimization of antibiotic use at sub-therapeutic levels is needed in order to preserve human clinical efficacy. The study of enduracidin, its mechanism of action and biosynthesis demonstrates its rarity as an antibiotic.